



NTNU – Trondheim
Norwegian University of
Science and Technology

Mucus barrier components, challenges for nanoscale drug delivery

Hamid Jalalian Javadpour

Medical Technology

Submission date: June 2013

Supervisor: Kurt Ingar Draget, IBT

Norwegian University of Science and Technology
Department of Biotechnology



Acknowledgements

This master thesis is conducted at Norwegian University of Science and Technology-NTNU, Biotechnology department, The Norwegian Biopolymer Laboratory-NOBIPOL, January 2013-June 2013.

The author gratefully acknowledges Professor Kurt I Draget and Dr. Catherine Taylor Nordgård for their supervision and motivation toward his master thesis. I am particularly grateful for the assistance given by Astrid Bjørkøy on Matlab script and for teaching confocal microscopy technique. I also wish to acknowledge the help provided by Morten Johnsen Dille on Matlab and Sigmaplot software's.

A special thank goes to my parent for their support and encouragement throughout my study.

Hamid J. J
25.06.2013



Abstract

In this present study changes in nanoparticles motion were explored in the presence and the absence of G-blocks in mucus matrices such as; porcine gastric mucus (45 mg/ml), and a mixture of porcine gastric mucus + polymeric mucus (non-degraded mucin from porcine stomach (45 mg/ml) respectively.

These mucus types were tested to determine nanoparticle motion in their mesh networks, in order to deepen the understanding of nanoparticle motion behaviors in these complex biological environments, clarify the involvement of mucus components as motion barrier to nanoparticle diffusion, as well as identify the exciting challenges for nanoscale drug delivery.

Multiple particle tracking technique was used to image movements of amine and carboxylate modified nanoparticles in mucus samples precisely by a series of experimental design.

Nanoparticles exhibited sub diffusive motion in mucus samples, which is a common behavior of nanoparticle in mucus matrix, however, there were other types of nanoparticle motion modes seen in samples; diffusive (nanoparticle display increased motion with time scale), immobile (nanoparticle could not move with increasing time scale), and hindered motion (nanoparticle could not move further in mucus with increasing time scale and show vibrating motion).

It was found that, nanoparticle motion is dependent on mucus components presented in mucus mesh. A significant increased on nanoparticle motion was identified in porcine gastric mucus mixed with polymeric mucus (45 mg/ml) compared to nanoparticle motion in sigma porcine mucus which not subjected to mixture with polymeric mucus (45 mg/ml).

It was stated that, polymeric mucus makes more pores or either provides a scaffold in mucus network which results in increased nanoparticle motion.

A shift toward greater nanoparticle motion at longer time scales confirmed the ability of G-blocks to improve nanoparticle diffusion. It is apparent that high levels of G-blocks may collapse all the structure and increase the mucus barrier. In addition, nanoparticle motion is dependent on the surface chemistry which determines the degree of interaction with the mucus components and mucus barrier disruption.



Mucus barrier components, challenges for nanoscale drug delivery

The apparent barriers to particle motion vary with time scale. At short timescales movements on short distance are shown.

Trajectory patterns at short time scales could reflect particle interaction with the matrix architecture or moving within network pores but are unlikely to show particles crossing matrix pore elements.

A key success in nanoparticle transport is to avoid adhesive interaction within mucus components. Results of this study indicate that, G-blocks have enough potential to engineer nanoparticle in order to traverse mucus matrix and reach targeted sites in the body.

Reduction of barrier properties of the mucus layer would be associated to G-blocks ability to alter mucus rheology in a favorable manner to uptake nanoparticle.

Whether the barrier is decreased or increased by G-blocks depends on amount of G-blocks, Nanoparticle surface, addition of G-blocks in mucus matrix, as well as time scale.

Such an improvement in nanoparticle transport through mucus blanket can lead to innovative drug delivery system for site specific target drug release, in order to combat against respiratory disease in particular cystic fibrosis disorder.

The data presented here may be consistent with a model where G-blocks alter the mucus barrier architecture. This study must be repeated in ex vivo native matrices because it has been clearly shown here that the matrix components is critical to the barrier properties.

*SPM= Sigma pig mucus, *PM= Polymeric mucus



Contents

Abstract.....	ii
Chapter 1.....	1
Introduction.....	1
Aim of thesis-Motivation.....	1
1.1 Mucus.....	2
1.1.1 Physiology.....	2
1.1.1.1 Mucus function in mucociliary clearance system	5
1.1.2 Mucus biochemistry and structure	6
1.1.2.1 Mucin	6
1.1.3 Mucus rheology	8
Unstirred layer	9
1.1.4 Mucus dynamics	11
1.1.5 Mucus barrier.....	12
1.1.5.2 Mucus barrier to pathogens in gut epithelium.....	12
1.1.5.1 Mucus epithelial barrier to nanoparticle diffusion	13
1.2 Nanoparticle.....	15
1.3 Nanomedicine and its application in penetrating of drug and gene delivery to mucus.....	15
1.3 Alginate and G-blocks	17
1.4.1 G-blocks ability to form a bio-gel in the presence of calcium	18
1.5 Cystic fibrosis	19
1.5.1 G-blocks in cystic fibrosis.....	20
1.6 G-block and enabling technology for nanomedicine applications	21
1.7 Multiple Particle Tracking	22
1.7.2 Mean square displacement analysis	23
1.7.2.1 Time scale	23
1.7.1 Nanoparticle trajectories classification	25
1.7.3 Effective diffusivity analysis	26
1.7.3.1 Diffusivities.....	27
1.7.4 Beads on string.....	28
Chapter 2.....	29
Material and methods.....	29



Mucus barrier components, challenges for nanoscale drug delivery

2.1 Nanoparticles	29
2.2 Porcine gastric mucin.....	29
2.3 Polymeric mucin	29
2.4 G-blocks dried powder.....	30
2.5 MES sodium salt	30
2.6 Cover glass slide chamber.....	30
2.7 Phase 1 of experiments	31
2.7.1 Preparation of mucus matrixes.....	31
2.7.2 Nanoparticle treatment with G-blocks to apply in mucus.....	31
2.7.3 Preparation of mucus matrixes.....	31
2.7.4 Nanoparticle treatment with G-blocks to apply in mucus.....	31
2.8 Phase 2 of experiments	32
2.8.1 Sample preparation	32
2.8.2 Mucus treatment with G-blocks.....	32
2.8.3 Nanoparticle treatment with G-blocks	32
2.8.4 Sample preparation	32
2.8.5 Mucus treatment with G-blocks.....	33
2.8.6 Nanoparticle treatment with G-blocks	33
2.9 Confocal Laser Scanning Microscopy	33
2.9.1 Sample visualization	34
2.10 Data analysis	34
Chapter 3.....	35
Results and Discussion	35
3.1 The motion of carboxylate nanoparticles in sigma pig mucus.....	35
3.2 Exclusion criteria	38
3.3 The comparison between triplicates maximum and minimum MSD and Deff values for carboxylate nanoparticles.....	39
3.3.1 Discussion	40
3.4 Study to investigate the effect of G-blocks on nanoparticle mobility in sigma pig mucus.....	41
3.4.1 Discussion	42
3.5 Study to determine the influence of G-blocks on nanoparticle mobility in sigma pig mucus + polymeric mucus	43
3.5.1 Discussion	44
3.6 Study to compare nanoparticle mobility in mucus types A and B	45

*SPM= Sigma pig mucus, *PM= Polymeric mucus



Mucus barrier components, challenges for nanoscale drug delivery

3.6.1 Discussion	46
3.7 Study to compare nanoparticle motion in mucus matrix A and mucus matrix B in the presence of G-blocks.....	47
3.7.1 Discussion	48
3.8 Study to quantify the method of bead addition on nanoparticle mobility in sigma pig mucus...	49
3.8.1 Study to verify the effect of bead addition on nanoparticle mobility in sigma pig mucus + polymeric mucus	51
3.8.2 Discussion	53
3.9 Alteration mechanisms to mucus barrier function and enhancing uptake of therapeutic in drug delivery system	54
3.10 Transport of carboxylate-modified nanoparticles in sigma pig mucus mixed with G-blocks ..	56
3.10.1 Transport of carboxylate-modified nanoparticles treated with G-blocks in sigma pig mucus	58
3.10.1.2 Discussion	59
3.11 Transport of amine-modified nanoparticles in sigma pig mucus mixed with G-blocks	61
3.11.1 Discussion	63
3.11.2 Transport of amine-modified nanoparticles treated with G-blocks in sigma pig mucus ...	64
3.11.3 Discussion	65
3.12 The transport of amine nanoparticle vs. carboxylate nanoparticles in sigma pig mucus	67
3.12.1 Discussion	68
3.13 Trajectory patterns of nanoparticle over time scales.....	70
Chapter 4.....	71
Conclusion	71
Chapter 5.....	72
Data analysis	72
5.1 The motion of carboxylate-modified nanoparticles in sigma pig mucus	72
5.2 The effect of G-blocks treatment on carboxylate nanoparticles motion in sigma pig mucus by MPT	76
5.3 The comparison between triplicate maximum and minimum MSD and Deff values for 150 COOH-modified nanoparticles treated with G-blocks.....	79
5.4 The transport of carboxylate nanoparticles in the presence of G-blocks in sigma pig mucus	80
5.5 The motion of carboxylate nanoparticles in sigma pig mucus + polymeric mucus by MPT	84
5.6 The transport of carboxylate nanoparticles in sigma pig mucus + polymeric mucus	88
5.7 The motion of carboxylate nanoparticle treated with G-blocks in sigma pig mucus + polymeric mucus	92



Mucus barrier components, challenges for nanoscale drug delivery

5.8 Real-time dynamic motion of carboxylate-modified nanoparticles in sigma pig mucus contains G-blocks	99
5.9 Real-time dynamic motion of carboxylate nanoparticle treated with G-blocks in sigma pig mucus	101
5.10 The movement of amine nanoparticles in sigma pig mucus contains G-blocks	103
5.11 The movement of amine nanoparticle treated with G-blocks in sigma pig mucus	105
Bibliography	107
Appendixes	111
Appendix A: Nanoparticles showed active motion.....	111
Appendix B: Experimental design and protocols	113
Appendix C: Confocal microscope setting	118
Appendix D: Matlab pre difiend script	119



Table of Figures

Figure 1.1: General characteristics of the mucus gel on epithelial surfaces.	3
Figure 1.2: Mucus layer in different epithelial surfaces based on its anatomical location.	4
Figure 1.3: Schematic representation of mucus structure by gel-on-brush model.	5
Figure 1.4: Schematic structure of the mucin polymer.	6
Figure 1.5: SEM pictures of different mucus layers.	7
Figure 1.6: Structural features of cervical mucus.	7
Figure 1.7: Summary of mucus viscosity as a function of shear rate for mucus obtained from many sources and observed by various methods.	9
Figure 1.8: Mucus as a lubricant gel on epithelial surface.	10
Figure 1.9: Dynamic properties of mucus.	11
Figure 1.10: The mucus layer as barrier to pathogens in the gut.	12
Figure 1.11: Mucus barrier components.	13
Figure 1.12: Two main mechanisms employed to prevent nanoparticle diffusion in mucus gel.	14
Figure 1.13: Schematic presentation of systematic drug delivery versus targeted drug delivery through human body.	16
Figure 1.14: The schematic structure of alginate.	17
Figure 1.15: Gel formation between G-blocks and calcium (Ca^{2+}) based on “egg box model”.	18
Figure 1.16: Strategy targets of cystic fibrosis respiratory therapies.	19
Figure 1.17: Rheological disruption of CF sputum in the presence of G-blocks.	20
Figure 1.18: Mucus network alteration with G-blocks treatment.	21
Figure 1.19: Procedure for Multiple particle tracking technique.	22
Figure 1.20: Illustration of time scale for 30 frame wise images obtained from a movie over 20 second.	23
Figure 1.21: Transport mode categorization by MSD plots.	24
Figure 1.22: Nanoparticle trajectories based on their transport mode in mucus matrix.	25
Figure 1.23: Transport mode categorization by MSD plots.	26
Figure 1.24: Three models of nanoparticle diffusion in biological environmet	27
Figure 1.25: Mucus matrix as barrier to nanoparticle transport.	28
Figure 3.1: The motion of carboxylate nanoparticle in sigma pig mucus.	36



Mucus barrier components, challenges for nanoscale drug delivery

Figure 3.2: Triplicate combined MSD and Deff plots in sigma pig mucus.	37
Figure 3.3: Maximum and minimum MSD and Deff values of triplicate experiments for stirred carboxylate nanoparticles in sigma pig mucus.	39
Figure 3.4: Graphical presentation of combined MSD and Deff values from triplicate results as a single data set.	40
Figure 3.5: The effect of G-blocks on stirred carboxylate nanoparticles motion in sigma pig mucus.	42
Figure 3.6: The effect of G-blocks on stirred carboxylate nanoparticles motion in sigma pig mucus + polymeric mucus.	44
Figure 3.7: Carboxylate nanoparticles motion in mucus matrix A and matrix B.	45
Figure 3.8: Schematic representation of mucus matrix A (sigma pig mucus) and mucus matrix B (sigma pig mucus + polymeric mucus).	46
Figure 3.9: Carboxylate nanoparticles motion in the presence of G-blocks in mucus matrix A and matrix B.	48
Figure 3.10: Study the method of beads addition on carboxylate nanoparticle mobility in sigma pig mucus.	50
Figure 3.11: Study the method of beads addition on carboxylate nanoparticle mobility in sigma pig mucus + polymeric mucus.	52
Figure 3.12 : Schematic illustration of nanoparticles interaction in mucus network.	54
Figure 3.13: Transport of carboxylate nanoparticle in sigma pig mucus contains G-blocks. .	57
Figure 3.14: Transport of carboxylate nanoparticles treated with G-blocks in sigma pig mucus.	59
Figure 3.15: Transport of amine nanoparticle in sigma pig mucus contains G-blocks.	62
Figure 3.16: Transport of amine nanoparticles treated with G-blocks in sigma pig mucus. ...	65
Figure 3.17: Transport of amine nanoparticle versus carboxylate particle in sigma pig mucus.	68
Figure 3.18: Schematic illustration of nanoparticle induced disruption of mucus.	69
Figure 3.19: Representative trajectories of nanoparticles in mucus over time scale.	70
Figure 5.1: The motion of unstirred carboxylate nanoparticle in sigma pig mucus.	73
Figure 5.2: Duplicate combined MSD and Deff plots for unstirred carboxylate nanoparticle in sigma pig mucus.	74
Figure 5.3 : Maximum and minimum MSD and Deff values from duplicate experiments for unstirred carboxylate nanoparticle in sigma pig mucus.	75

*SPM= Sigma pig mucus, *PM= Polymeric mucus



Mucus barrier components, challenges for nanoscale drug delivery

Figure 5.4: The motion of stirred carboxylate nanoparticle treated with G-blocks in sigma pig mucus	77
Figure 5.5 : Triplicate combined MSD and Deff plots for stirred carboxylate nanoparticle treated with G-blocks in sigma pig mucus.....	78
Figure 5.6 : Maximum and minimum MSD and Deff values from triplicate experiments for stirred carboxylate nanoparticle treated with G-blocks in sigma pig mucus.	79
Figure 5.7: The motion of unstirred carboxylate nanoparticle treated with G-blocks in sigma pig mucus.	81
Figure 5.8: Triplicate combined MSD and Deff plots for unstirred carboxylate nanoparticle treated with G-blocks in sigma pig mucus.....	82
Figure 5.9: Maximum and minimum MSD and Deff values from triplicate experiments for unstirred carboxylate nanoparticle treated with G-blocks in sigma pig mucus.	83
Figure 5.10: The motion of stirred carboxylate nanoparticle in sigma pig mucus + polymeric mucus.	85
Figure 5.11: Duplicate combined MSD and Deff plots for stirred carboxylate nanoparticle in sigma pig mucus.	86
Figure 5.12: Maximum and minimum MSD and Deff values from duplicate experiments for stirred carboxylate in sigma pig mucus..	87
Figure 5.13: The motion of unstirred carboxylate nanoparticle in sigma pig mucus + polymeric mucus.....	89
Figure 5.14: Duplicate combined MSD and Deff plots for unstirred carboxylate nanoparticle in sigma pig mucus + polymeric mucus.	90
Figure 5.15 : Maximum and minimum MSD and Deff values from duplicate experiments for unstirred carboxylate nanoparticle in sigma pig mucus + polymeric mucus.....	91
Figure 5.16: The motion of stirred carboxylate nanoparticle treated with G-blocks in sigma pig mucus + polymeric mucus.	93
Figure 5.17: Duplicate combined MSD and Deff plots for stirred carboxylate nanoparticle treated with G-blocks in sigma pig mucus + polymeric mucus.....	94
Figure 5.18: Maximum and minimum MSD and Deff values from duplicate experiments for stirred carboxylate treated with G-blocks in sigma pig mucus + polymeric mucus.....	95
Figure 5.19: The motion of unstirred carboxylate nanoparticle treated with G-blocks in sigma pig mucus + polymeric mucus	96



Mucus barrier components, challenges for nanoscale drug delivery

Figure 5.20: Duplicate combined MSD and Deff plots for unstirred carboxylate nanoparticle treated with G-blocks in sigma pig mucus + polymeric mucus.....	97
Figure 5.21: Maximum and minimum MSD and Deff values from duplicate experiments for unstirred carboxylate nanoparticle treated with G-blocks in sigma pig mucus + polymeric mucus.	98
Figure 5.22: Real-time dynamic motion of carboxylate nanoparticle in sigma pig mucus contains G-blocks.....	100
Figure 5.23: Real-time dynamic motion of carboxylate nanoparticle treated with G-blocks in sigma pig mucus.	102
Figure 5.24 : The movement of amine nanoparticle in sigma pig mucus contains G-blocks.	104
Figure 5.25: The movement of amine nanoparticle treated with G-blocks in sigma pig mucus.	106
Figure A.1: Shows active mobility of carboxylate nanoparticles in 45 mg/ml sigma pig mucus + polymeric mucus.....	111
Figure A.2 : Shows active mobility of carboxylate nanoparticles in 45 mg/ml sigma pig mucus + polymeric mucus.	111
Figure A.3: Shows active mobility of carboxylate nanoparticles in 45 mg/ml sigma pig mucus + polymeric mucus.....	112
Figure A.4: Shows active mobility of carboxylate nanoparticles in 45 mg/ml sigma pig mucus + polymeric mucus.....	112

*SPM= Sigma pig mucus, *PM= Polymeric mucus



Chapter 1

Introduction

Aim of thesis-Motivation

The aim of this master thesis was to investigate barrier properties of mucus to nanoparticle movement and the way in which G-blocks alter these barrier properties. The mucosal surfaces of the gastrointestinal, respiratory and genitourinary tracts are major targets for drug delivery and effective drug delivery at these sites involves drug transport across secreted mucus.

Mucus is a highly hydrated network of polymeric mucin molecules where the pores in the network additionally contain other biopolymers, which may or may not form non covalent associations with the mucin matrix. Traditionally mucus has not been considered a major barrier to drug delivery, and it does not generally present a significant hindrance to the passage of small drug molecules. However, new trends in drug development have led to increasing interest in the use of biological macromolecules, such as proteins, and polymeric or colloidal carrier systems, such as in gene delivery, and for these classes of pharmaceuticals mucus can present a significant barrier to uptake.



1.1 Mucus

1.1.1 Physiology

Mucus is a viscoelastic bio-gel that provides a semipermeable protective coverage to surfaces of the body tissues not supported by skin, such as those respiratory, gastrointestinal (GI), female reproductive tract, and the surface of the eye [1].

The semipermeable property of mucus network allows the exchange of nutrients, water, gases, odorants, hormones, and gametes, while being impermeable to most foreign particles, bacteria and pathogens [2, 3].

Mucus is one of the body's first defenses against infection by preventing pathogen access the epithelial surface [4].

Mucus provides a wet layer over epithelium tissue to minimize the friction between organs, and lubricate the surfaces [5, 6]. Importantly, mucus secretion protects the stomach from the chemical action of its own gastric juice [7].

Mucus gel is secreted and transported continually before being digested or shed in epithelial surface. The body produces nearly 10 l (2.5 gal) of mucus gel each day which is digested and recycled or released in feces, sputum, saliva, and nasal secretions, reproductive tract secretion, and tears (Figure 1.1) [2].

In human GI tract, the mucus layer is thickest in the stomach (180 μm ; range 50-450 μm) and colon (110-160 μm). In the small intestine, the mucus thickness can change greatly based on digestive activity stimulated by diet (Figure 1.1) [2].

The thickness of mucus gel is dominated by the balance between the rate of secretion and rate of degradation and shedding. Toxic and irritating substances can greatly stimulate mucus secretion, increasing the thickness of mucus blanket and facilitating irritants removal from epithelial surface [2].

In respiratory tract, mucus performs its regulatory functions by continuously moving, and trapping particulates on airways surfaces. Mucus function is supported by ciliated epithelial cells, which form the mucociliary escalator alongside cough, in order to maintain sterile



Mucus barrier components, challenges for nanoscale drug delivery

airways system. The mucus layer is much thinner (averaged 15 μm) in respiratory tract than GI tract and cilia motion removes particles by mucus clearance (Figure 1.1) [2, 5].

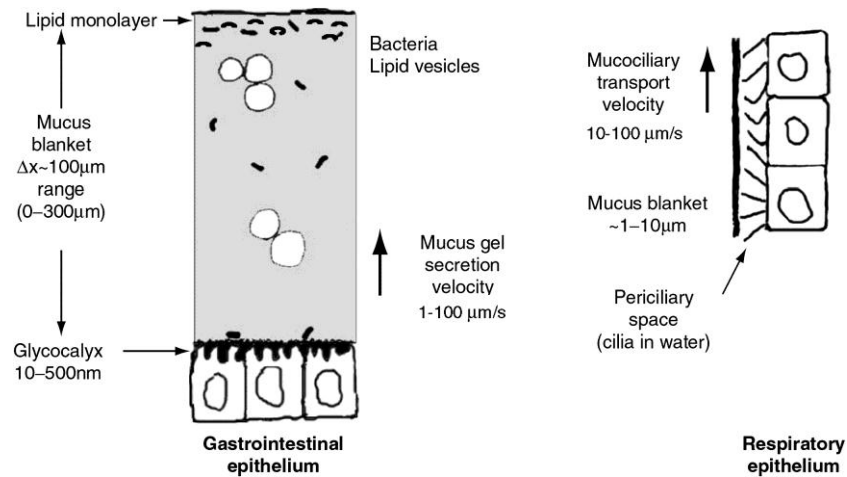


Figure 1.1: General characteristics of the mucus gel on epithelial surfaces [2].

*SPM= Sigma pig mucus, *PM= Polymeric mucus



Mucus barrier components, challenges for nanoscale drug delivery

Mucus clearance time, blanket thickness, and pH can differ based on its anatomical location on epithelial surfaces (Figure 1.2) [8].

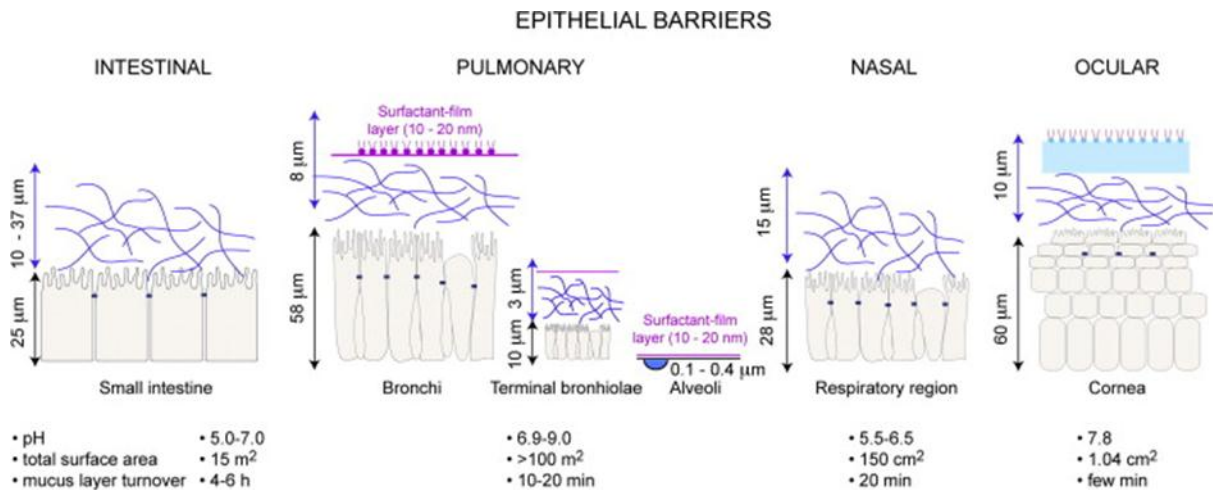


Figure 1.2: Mucus layer in different epithelial surfaces based on its anatomical location. Epithelial cells from different anatomical locations are drawn here in the same size. Mucin polymers coated all wet epithelia which serve as protective gel (shown in blue). Mucus features such as thickness, clearance time and pH, as well as total surface area of epithelial surfaces are present in figure [8].



1.1.1.1 Mucus function in mucociliary clearance system

In the mammalian lung, mucus performs its protective function by trapping and removing a wide variety of toxic substances and invading pathogens from the airways surfaces. Mucus layer and a periciliary layer (PCL) are two components of the clearance system that has recently described as gel-on-brush model (Figure 1.3) [9, 10].

The mucus gel layer traps particles and is propelled out of the lung by cilia beat which generating the required forces for particle removal. The periciliary layer (a liquid-filled domain) is occupied by membrane-spanning mucins and large mucopolysaccharides that cooperating with cilia, microvilli, and epithelial surface, in order to maintain a favorable environment for cilia beating and cell surface lubrication (Figure 1.3) [9].

Failure in this system causes mucus build up and breathing problems which appear for example in patients with chronic obstructive pulmonary disease (COPD) and cystic fibrosis (CF). Both diseases are accrued by dehydrated airways mucus with mucin and globular protein concentrations several times higher than in normal mucus, while in healthy individuals without lungs disease the inhaled particles are transport out by sticky mucus and cilia propulsion [9].

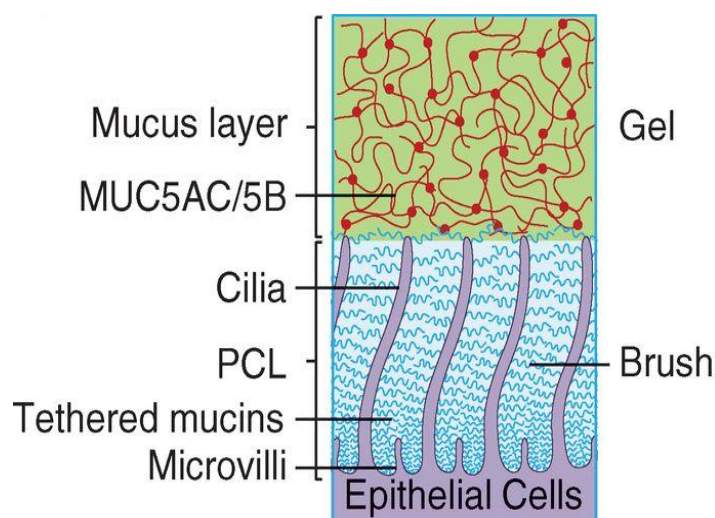


Figure 1.3: Schematic representation of mucus structure by gel-on-brush model [10].



1.1.2 Mucus biochemistry and structure

1.1.2.1 Mucin

Mucin polymer is the main gel-forming molecule of mucus. Mucins are high molecular weight glycoprotein (10^6 - 10^7 Da) that contains protein backbone which are highly O-glycosylated. Thus, mucin polymer composition is dominated by carbohydrates, which making up to 80 % of the dry weight of the molecule (Figure 1.4) [11].

Mucin polymers are enriched in the amino acids serine and threonine, which form the protein backbone with sugars linkages including; N-acetylgalactosamine, galactose, and fucose. In addition, mucin polymer contains sialic acids and sulfates, making mucins negatively charged at physiological pH (Figure 1.4) [11, 12].

As shown in Figure 1.4, mucin subunit is a rod-shaped molecule which composed of a linear polypeptide core of $100,000 < M_w < 250,000$ g mol⁻¹ in center with o-linked chains of 2 to 12 monosaccharide residues. Mucin are polymerized N-N, C-C, to form mucin polymers [11].

Mucin polymers are relatively resistant to proteases due to high degree of glycosylation, making the protein backbone less accessible to enzymatic hydrolysis and resulting in a more robust mucus layer in mammalian organs [11].

Hydrated mucin polymers associate non-covalently form a gel matrix that is around 95 % water. The negative charges on mucins mean the fibers in the mucus matrix repel each other and prevent mucin aggregate and gel collapse.

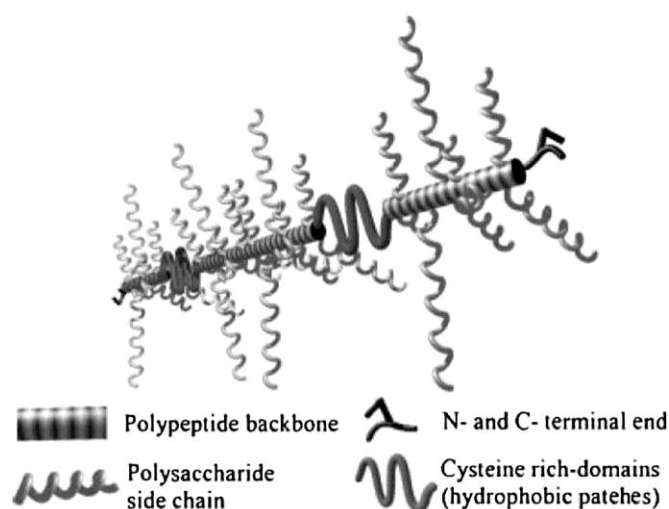


Figure 1.4: Schematic structure of the mucin polymer [11].



Mucus barrier components, challenges for nanoscale drug delivery

The multifunctional glycoproteins in mucus prevent barrier dehydration and are the major determinant of proper functionality. The condensed and complex microstructure of the mucus network gives rise to a heterogeneous bio-gel [13].

Mucus structure can be investigated by scanning electron microscopy (SEM) technique, to image the mucus network. SEM images show 3 dimensional networks of mucin fibers with varying pore sizes and pore size distributions. Images from various mucus preparation show broad similarities (Figure 1.5) [14].

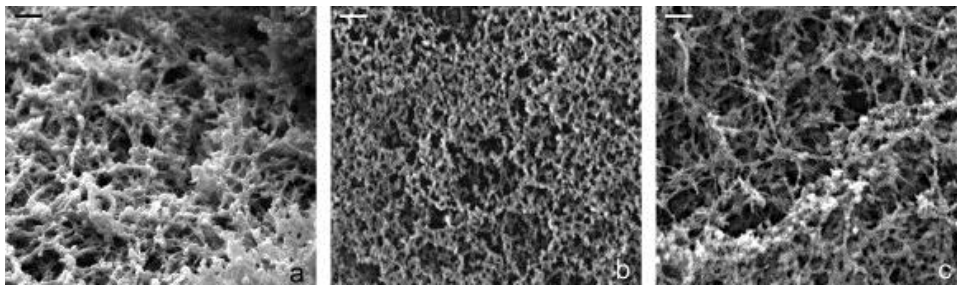


Figure 1.5: SEM pictures of different mucus layers. Scanning electron microscope (SEM) images of the mucus matrix formed by different type of mucins. (a) Presents porcine stomach mucus layer with porous mesh up to 0.9 μm in diameter, (b) the matrix of the bovine sub maxillary layer formed of porous network up to 0.4 μm , (c) Human salivary mucin with mesh size of 0.8 μm in diameter [14].

M-C Lavaud and co-workers have also shown varying thicknesses of mucin filaments within the matrix. Thinner filaments linked together thicker filaments measuring between 300 and 400nm. The intermediate filaments varied between 100 and 200nm. Very thin and sparse filaments crossed the meshes, measuring between 10 to 100nm. They also saw Spermatozoa, bacteria and unspecified round cells were enmeshed in the mucus (Figure 1.6) [15].

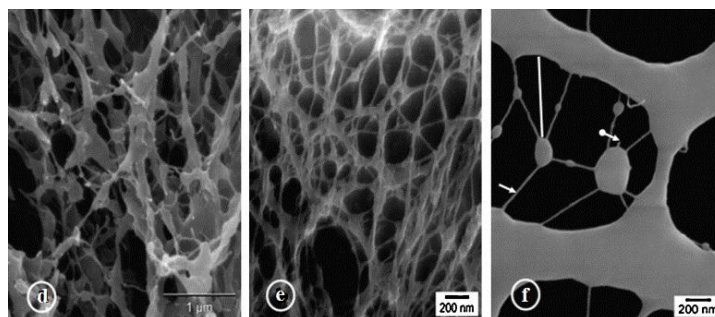


Figure 1.6: Structural features of cervical mucus (d), and nasal (e) mucus. The filaments measuring 20 nm (arrow), often broken and crossing meshes measuring 650 nm (f) [15].

*SPM= Sigma pig mucus, *PM= Polymeric mucus



1.1.3 Mucus rheology

Mucus is characterized as rheological reversible gel and has the rheological potential of conversion from gelled form to liquid form or vice versa. This reversibility property of mucus is due to its mucin mesh and other constituents which are non-covalently cross-linked together [16]. And therefore, bonds have the abilities to break and reform.

The rheological properties of mucus can change as a function of stress, time scale (rate) of shearing as well as length scale. Changes in rheological properties of mucus may alter its ability to function as a lubricant, exchange nutrients, and its barrier properties against environmental threats (e.g. invasive pathogens) [5, 8].

Rheological measurements, including viscosity (resistance to flow) and elasticity (stiffness), are important behavior of all mucus secretions and all secretions broadly conform to the same pattern. However, the absolute moduli and flow stress values vary significantly depending on the source of mucus and physiological or pathological statuses of the specimen [16, 17].

For instance, mucus blanket becomes too thick in cystic fibrosis patients where the sputum viscosity can be more than 100,000 times that of water, patients experience difficulties to breathe due to reduction on mucus clearance capacity and bacterial overgrowth. The bulk rheology of mucus is non-Newtonian that is not linear with shear rate. Mucus has a strong resistance to deformation at low shear rates and weak resistance at high shear rates. Thus, bulk rheology is critical for proper clearance and lubrication function of mucus secretion [16].

The abnormal mucus secretion with altered rheology properties can result in morbidity and mortality in chronic airways diseases (e.g. asthma, cystic fibrosis (CF), and chronic obstructive pulmonary disease (COPD)). Thus, normal mucus secretion is vital for maintaining human health [1, 10].

The shear-thinning (non-Newtonian) property of mucus gel is shown in Figure 1.7 by plotting the viscosity of mucus gel as a function of shear rate. As can be seen in the log-log plot, the viscosity of a mucus gel decreases as shear rate increases, whereas, the viscosity of water (a Newtonian fluid) does not change with shear rate as shown by the horizontal line (Figure 1.7) [2].



Mucus barrier components, challenges for nanoscale drug delivery

It is apparent from Figure 1.7, that mucus behaviour is dependent on shear rate and that presumably results in decreasing adhesive interaction between mucus components (e.g. fibers) as the shear rate increases. At maximum physiological shear rate the viscosity of mucus gel approaches that of water mucus and, making mucus gel an excellent viscous lubricant [2].

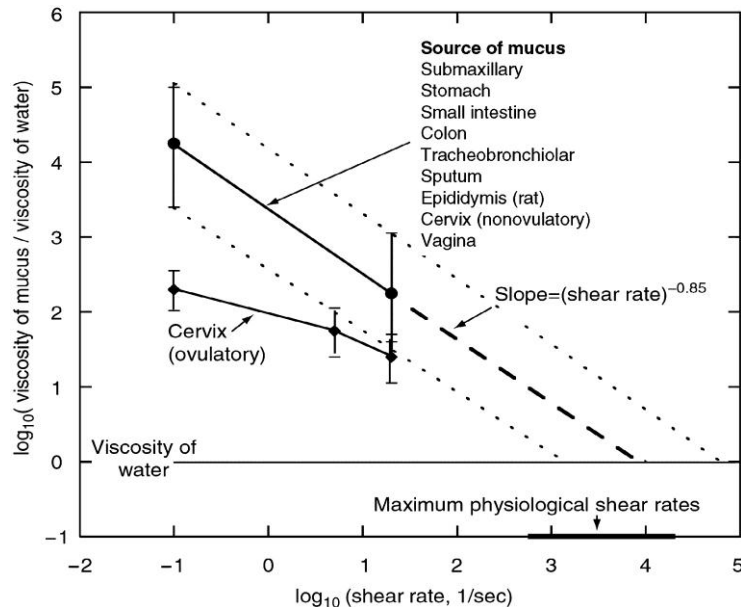


Figure 1.7: Summary of mucus viscosity as a function of shear rate for mucus obtained from many sources and observed by various methods.

Note that viscosity decreases markedly as the shear rate increases (shear thinning), that most mucus secretions are rather comparable, and that all approach the viscosity of water at maximum physiological shear rates [18].

Unstirred layer

The gel nature of mucus provides an unstirred layer at the mucosal surfaces. Mucus does this by being shear-thinning gel which capable to form a lubrication slippage field between sliding surfaces as indicated in Figure 1.8 [2].

As mucus begins to supply between two epithelial surfaces the adhesive interactions within mucus fibers reduces, promoting mucus fibers to drawn apart and to create a slippage plain. As that happen, the viscosity of mucus gel reduces dramatically between the surfaces and causing gel layers remain unstirred (Figure 1.8) [1, 2].

*SPM= Sigma pig mucus, *PM= Polymeric mucus



Mucus barrier components, challenges for nanoscale drug delivery

In the GI tract, mucus has important lubricant function. Bilayer sloppy lubricant mucus protects the underlying firmer gel and hence unstirred layer. In addition to the GI tract, mucus gel maintains this bilayer (a cell-adherent layer and non-adherent, luminal sloppy layer) in the female tract which is essential for mucus to perform lubricant task (Figure 1.8).

The formation of slippage plane during copulation, swallowing, or peristalsis stimulated can be controlled by excess in mucus secretion between the cell-associated, unstirred and the non-adherent layers. This causes the viscosity remain low between slippage planes as long as mucus is secreted. Indeed, slippage plane protect unstirred layer from breakage (Figure 1.8). Therefore, any object that needs to penetrate mucus must go up stream through mucus [18].

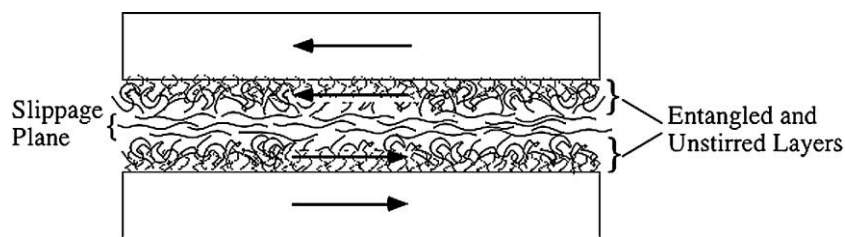


Figure 1.8 Mucus as a lubricant gel on epithelial surface.

Shearing action between two surfaces forms a slippage plane due to the non-Newtonian, shear-thinning property of mucus. Note each surface remains coated by an unstirred adherent layer of mucus [18].



1.1.4 Mucus dynamics

The dynamic viscoelastic properties of mucus secretions are integral to their physical function, in order to protect mucosal surfaces, maintain shear stress dependent lubrication, and to move over lung epithelial by mucociliary transport systems [17].

Mucus is continuously secreted and recycled to prevent pathogens or ultra-fine particulates from reaching the epithelial cells. Mucus lifetime is short from minutes to hours. Mucus turnover rate depends on its epithelial surface and the fastest mucus turn over being observed in thinnest mucus layer. Mucus facilitates the removal of particles in a matter of minutes to hours by its turnover, and can be replaced with new layer with approximately twenty minutes. Thus, this bio-gel is not only critical for human health maintenance, but it also significantly limits the potential for localized and sustained drug and gene delivery to mucosal surfaces (Figure 1.9) [1, 19].

Mucus turnover results in removal of toxic and foreign substance. Thus, pathogens and therapeutic nanoparticles must be able to diffuse upstream through mucus to reach underlying epithelium [18].

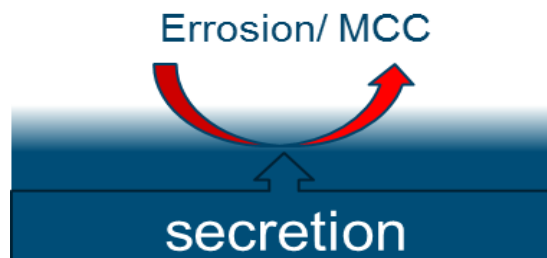


Figure 1.9: Dynamic properties of mucus (Taken from Nordgård).

*SPM= Sigma pig mucus, *PM= Polymeric mucus



1.1.5 Mucus barrier

Mucosal tissues are preferential for therapeutic pharmaceuticals administration, due to accessibility to targeted sites (e.g. GI and respiratory tracts) and minimum patient compliance. However, mucus presents a critical barrier for nanoscale drug delivery systems such as liposomes, polypeptides, and gene delivery, [8, 20].

1.1.5.2 Mucus barrier to pathogens in gut epithelium

Mucus lines the gut epithelium with thick gel layer and that is considered as a major protective barrier for pathogenic bacteria and particles. However, pathogenic bacteria employed mechanisms to pass this mucus barrier and reach the epithelial surface (Figure 1.10) [4].

In addition, epithelial and paneth cells themselves secrete antimicrobial peptides to prevent bacterial penetration into the inner mucus layer. Thus, mucus layer function as protective layer against bacterial colonization, in order to maintain a sterile environment over epithelial surfaces (Figure 1.10) [4].

Effective prophylactic and therapeutic based treatment could be possible by enhancing transport of medicine through mucus mesh without modifying its protective properties. This can be used for treating diseases such as cystic fibrosis (CF), sexually transmitted infections (STI), degenerative eye diseases, lung cancer, and irritable bowel disease [21].

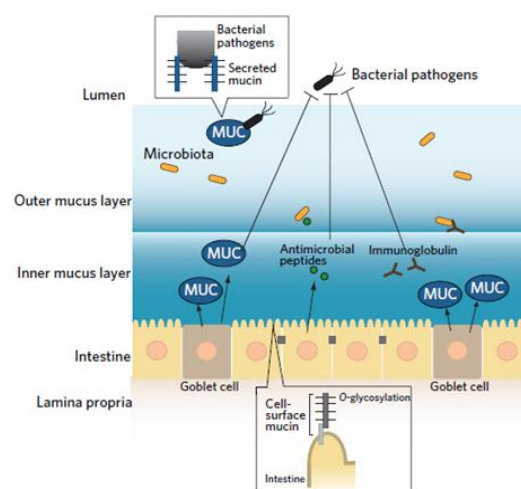


Figure 1.10: The mucus layer as barrier to pathogens in the gut [4].



1.1.5.1 Mucus epithelial barrier to nanoparticle diffusion

Mucus components can potentially stick to nanoparticle surfaces and may result in aggregation, destabilization, charge neutralization, and displacement of their cargoes to the unstirred layer discussed previously. In addition, mucus gel can limit free nanoparticle mobility by its adhesiveness. Therefore, nanoparticles do not freely diffuse in mucus and that is known as hindered nanoparticle motion. Mucus gel forms adhesive interactions with particulates upon their attachment via hydrophobic, electrostatic, and hydrogen bonding interactions (Figure 1.11) [1].

In contrast, steric barrier depends on particle size, and that limits particle diffusion in the mucus. Wang et al. have studied the influence of particle size in mucus and have found that, particles with $1\mu\text{m}$ size or larger are significantly hindered in the mucus, whereas particle with smaller size for example 500nm able to diffuse in the mucus mesh in the absence of adherent interactions (Figure 1.11) [3].

Hydrophobic, electrostatic, and hydrogen bond are forms of attraction that are present in mucus and can overlap particles. A dense porous structure is formed by mucus gel. Therefore, nanoparticle must have small neutral surfaces to avoid adhesion, in order to cross barrier [21].

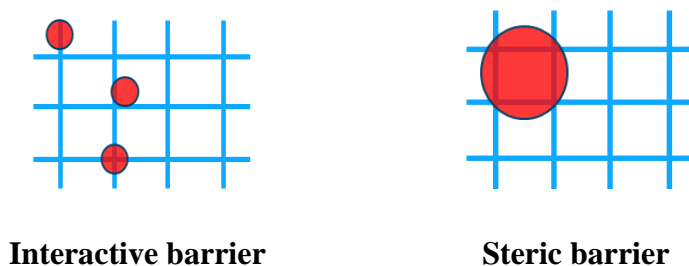


Figure 1.11 : Mucus barrier components (Taken form Nordgård).



Mucus barrier components, challenges for nanoscale drug delivery

Nevertheless, mucus layers contain a large number of pores and low-viscosity channels that can allow nanoparticle to penetrate into underlying tissues.

Electrostatic interactions mainly arise from the presence of carboxyl or sulfate groups on mucin- sugar bonds, and the strength of the electrostatic interactions and thus filtrating mechanism is regulated by both mucin charge states and particle surface chemistry [8].

Hydrophobic interactions arise from highly density of hydrophobic protein residues belong to mucin fibers, which creates various low-affinity adhesive interactions with hydrophobic surface of nanoparticle, result in immobilization of nanoparticle in mucus network [8].

Interactive and steric barriers can also be referred to interaction filtering and size filtering mechanisms which recently described by Sigurdsson and et al [7].

Size filtering mechanism allows nanoparticles that are smaller than mucus mesh's pores to pass, whereas larger nanoparticles are rejected regardless of surface charge (green nanoparticles) (Figure 1.12 (a))

In contrast, Electrostatic, and/or hydrophobic forces and/or hydrogen bonds or specific banding interaction are involved in interaction filtering mechanism to prevent nanoparticles from crossing the mucus elements. Thus, surface chemistry of nanoparticle is a key player in this mechanism to enhance or to prevent particle diffusion in mucus blanket (orange nanoparticles) (Figure 1.12 (b)) [7].

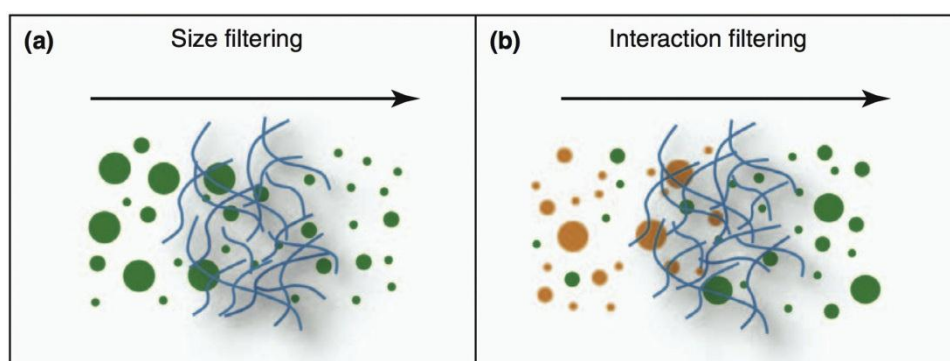


Figure 1.12: Two main mechanisms employed to prevent nanoparticle diffusion in mucus gel. (a) Size filtering mechanism and (b) Interaction filtering [7].

Therefore, the effective transport of nanoparticles through mucus layer required to consider the barrier properties of mucus critically, in order to improve nanoparticle transport through mucus matrix, and to achieve desired therapeutic and diagnosis goals [8].



1.2 Nanoparticle

Nanoparticles can be defined as ultra fine particle with size ranges between 1 nm to 500 nm in at least two dimensions. Nanoparticles have a wide potential usage in the area of, engineering, food industry, cosmetics and medicine. For instance, nanoparticles are used for drug delivery purposes due to their size and compatibility in biological environment [22].

Synthetic nanoparticles typically feature hydrophobic, charged or hydrogen bonding surfaces, and these make them able to interact with mucus as biological environment. For example, Polystyrene nanoparticles are widely used as a model to study interactions between NPs and biological environments like mucus matrix, cells due to various practical reasons including their commercial availability, high quality and wide variety of size and surface chemistry. Nanoparticles also can be used as sophisticated probe to discover the barrier properties of mucus surface to improve epithelial uptake of therapeutic agents [3, 22].

1.3 Nanomedicine and its application in penetrating of drug and gene delivery to mucus

Nanomedicine is broad combination of multiple fields including, nanotechnology, biomolecular engineering, biology and medicine. Nanomedicine provides novel strategies in treatment of diseases, and overcome challenges faced by conventional therapies [23].

Nanotechnology provides new design of diagnostics or therapeutics on the nanoscale with many potential applications in clinical medicine and research. Due to their unique size dependent properties nanomaterial such as nanoparticles offer the possibility to navigate within the biological environment for the treatment, and prevention of disease.

Thus, nanomedicine can be considered as applied-nanotechnology to medical problems. Nanomedicine approaches offer many applications in diagnosis and treatment of disease such as; nanoparticle-based molecular imaging probes for biological studies, nano-carriers for targeted drug and gene delivery, and regenerative medicine [24].

For example, in regard of drug delivery, nanomedicine tools have great potential to manage drug pharmacokinetics, non-specific toxicity, and immunogenicity for improved efficiency [24].

Delivery of genetic material and medicines via nanoparticle system may be a good strategy to combat a variety of disease affecting epithelial surfaces, including genetic disorders like cystic fibrosis, infectious diseases and cancers [21].

*SPM= Sigma pig mucus, *PM= Polymeric mucus



Mucus barrier components, challenges for nanoscale drug delivery

Medical nanoparticles with the same size as biological entities can also interact in biological barriers like mucus. Therefore, understanding mucosal barriers and their interaction with foreign fine particles, can result in design of nanoparticles that are able to overcome this barrier and deliver its therapeutic agents into the targeted cells or tissue [23-25].

The resulting progress should open the way to more innovative and powerful in vivo diagnosis tools and treatment.

In systematic drug delivery, drug transfers with either oral intake or intravenous injection which results in medicine distribution throughout the body regardless of specific binding to target site, whereas, in targeted nano-drug delivery, nanomedicine can localize and banded to desire targeted site in the body [26].

Thus , targeted drug delivery strategy (nano-drug delivery) can potentially reduce side effects of medicine due to a low drug dose, and more efficient way to administrate drugs as well as less costly (Figure 1.13) [26].

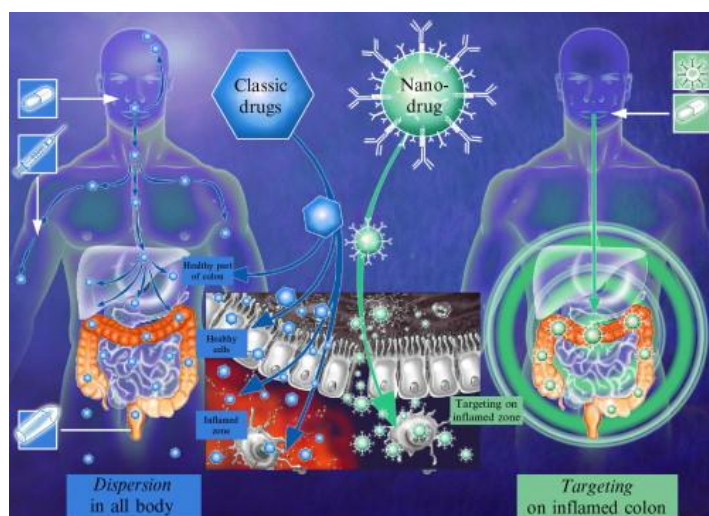


Figure 1.13: Schematic presentation of systematic drug delivery versus targeted drug delivery through human body [27].



1.3 Alginate and G-blocks

Alginate is a natural occurring family of polysaccharides produced by marine brown algae and bacteria, consisting of (1 → 4) linked β -D-mannuronic acid (M) and α -L-guluronic acid (G) residues. Alginate polymer is arranged by homopolymeric regions of M residue, G residue and alternating MG residue (mixture sequence) in blockwise patterns (Figure 1.14) [28, 29].

The alginate polymer is commonly used in food industry due to gel forming ability, as well as viscosifying and stabilizing properties. Indeed, the application of alginate polymer within biotechnology and medicine can provide a novel pharmaceutical delivery to the target sites in the body. In addition, alginate polymer can form a hydrogel with multivalent cations (e.g. Ca^{2+}) due to electrolyte nature and its physical properties [28].

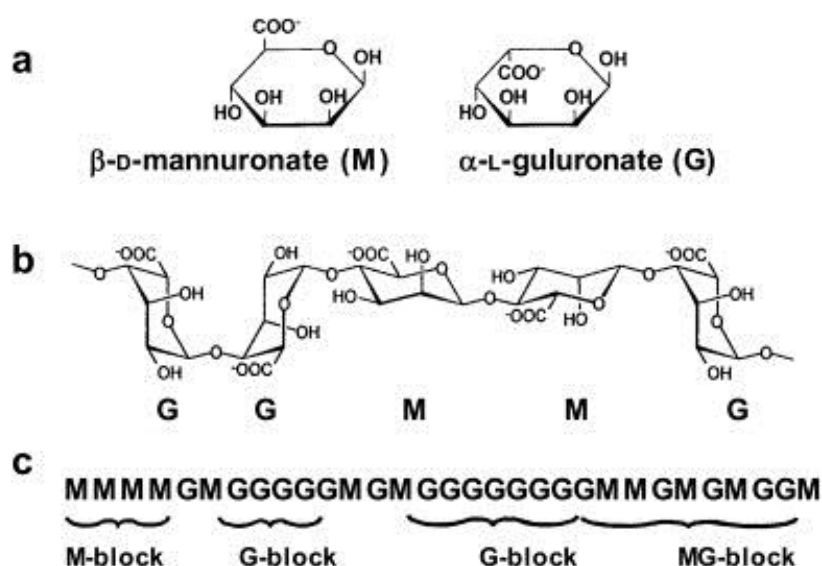


Figure 1.14: The schematic structure of alginate: a) Alginate monomer, b) Chain conformation, c) Block distribution [28].



1.4.1 G-blocks ability to form a bio-gel in the presence of calcium

Alginate biopolymer can produce a three dimensional (3D) hydrogel structure in solution contains divalent Ca^{2+} due to form a bond with ionic interaction between G-blocks and cations. The 3D gel structure is known as “egg-box model” and shown in Figure 1.15 [29].

G-blocks polysaccharide is negatively charged due to the presence of functional groups including oxygen, carboxylate oxygen as well as hydroxyl oxygen. These negatively charged residues over contribute to chelating aqueous cations such as Ca^{+2} and Mg^{+2} . As shown in Figure 1.15- a and b, Ca^{+2} trapped inside and formed the junction zone with alginate polymer [30].

The ability of alginate to form a bio-gel is a key factor for its biological function and its application for drug delivery system. The G-blocks used in this study are extracted from high G alginate by acid hydrolysis preparation, and have an average DP of around 10.

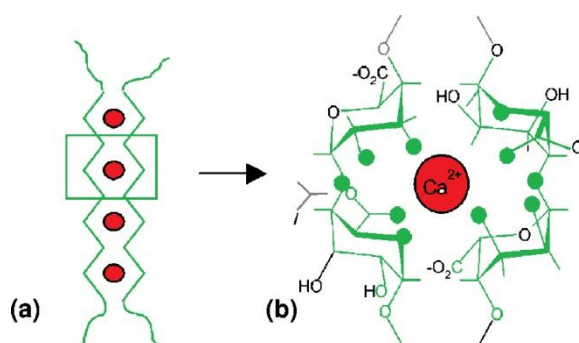


Figure 1.15: Gel formation between G-blocks and calcium (Ca^{2+}) based on “egg box model”[31].



1.5 Cystic fibrosis

Cystic fibrosis (CF) is a monogenetic (Mutation on one gene) disorder, is caused by mutation on CFTR gene (Cystic fibrosis transmembrane regulator). This gene is responsible for chloride channel, and defective gene resulted in abnormally thick, sticky mucus that affects the lungs, the digestive system and respiratory system. There are complications in multiple organs but most significantly in lung and pancreas (Figure 1.16) [32].

As mucus becomes too thick, patients face great difficulty in mucus clearance, resulting in bacterial overgrowth. It also causes breathing problems, by clogging lung air ways. In addition, patient faces chronic infection specifically by bacterium named pseudomonas aeruginosa which secretes alginate, leading to declining lung function and ultimately respiratory failure [32].

Cystic fibrosis is associated with considerable disability and early death, even though there have been improvements in patient's survival and health situation in last two decades. Various medications comprehensive care plans, results in life expectancy life of 40 years for patients with cystic fibrosis [32].

Figure 1.16 shows a summary of the pathophysiology in the lung. Physiological changes of reduced CFTR activity in the lungs of patients with cystic fibrosis are highlighted by large gray arrows. Therapeutic classes that have been investigated for treatment of cystic fibrosis are shown in light gray boxes [32].

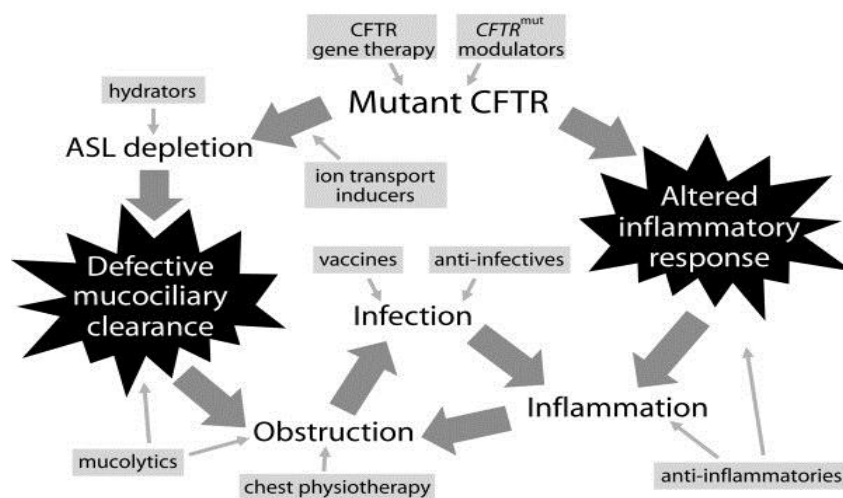


Figure 1.16: Strategy targets of cystic fibrosis respiratory therapies [32].

*SPM= Sigma pig mucus, *PM= Polymeric mucus



1.5.1 G-blocks in cystic fibrosis

CF patients suffer from secretion of thick gelid mucus layer in their lung. The normal mucus removal system is unable to clear the mucus, resulting in mucus build and to respiratory failure. G-blocks are able to modify CF mucus and make it more mobile [17].

Nordgård and Draget have showed that, applying G-block into the CF mucus reduces mucus resistance to deformation (Figure 1.17) [17].

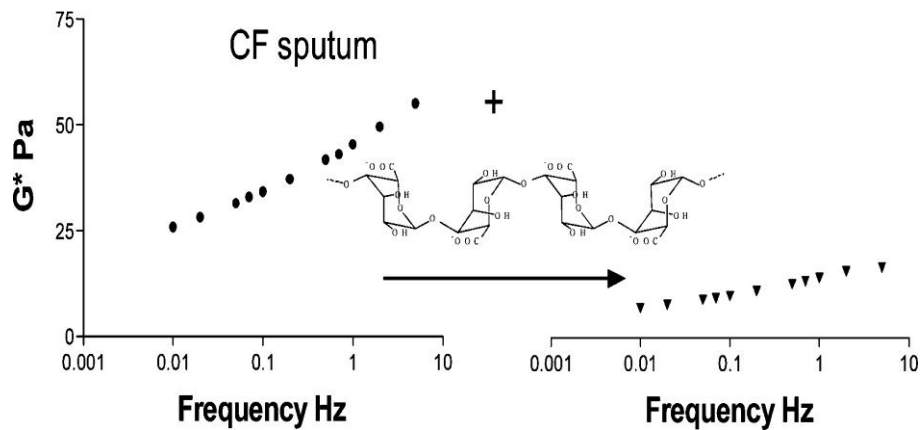


Figure 1.17: Rheological disruption of CF sputum in the presence of G-blocks [17].



1.6 G-block and enabling technology for nanomedicine applications

It has been shown that G-blocks alter the mucin matrix architecture (personal communications with Nordgård/Draget) [17].

As shown in Figure 1.18 B G-blocks increased pore size of mucus mesh into more open network to diffuse in. These changes raise the possibility that G-blocks also alter mucus barrier properties.

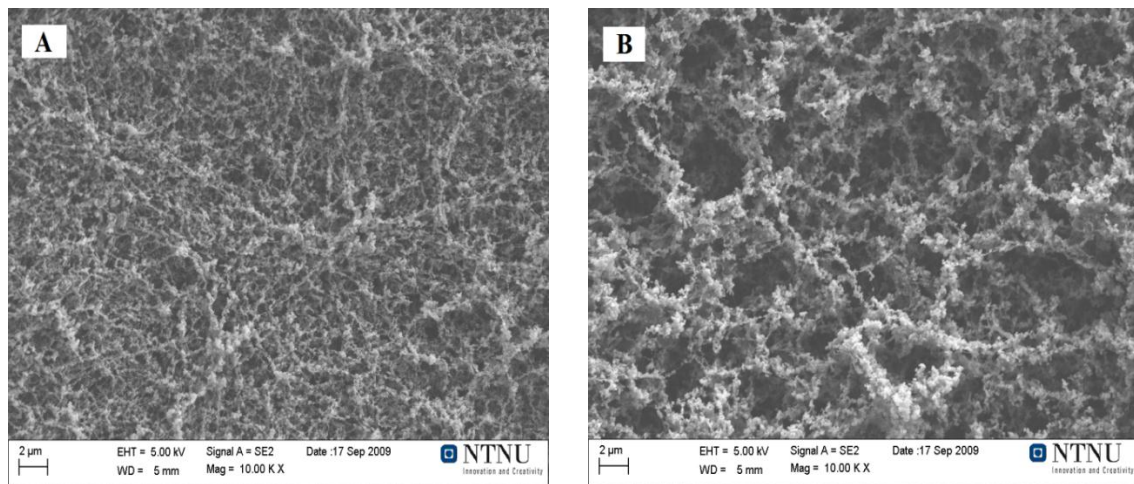


Figure 1.18: Mucus network alteration with G-blocks treatment (A) Mucus matrix without G-blocks treatment, (B) mucus matrix after G-blocks treatment (Unpublished work from Draget and Taylor).



1.7 Multiple Particle Tracking

Multiple particles tracking (MPT) is a powerful method for tracking the motion pattern of single particles. This method takes advantage of fluorescence video microscopy to detect and track the movements of individual fluorescence particles in a matrix (for example mucus). Referring to the diagram, the movements of particle in the matrix (in our case mucus) are observed through a confocal microscope and captured frame-wise as a film. The film is analyzed using the Image J plugin software, which selectively tracks single particles and relays each particle's x and y position. Using Matlab predefined script gives mean square displacement (MSD) parameter and effective diffusivities (D_{eff}) ($MSD/4 \cdot T$) further. Graphical representation of the obtained data can then be made by plotting the MSD and D_{eff} values against time scale using the Sigma Plot software (Figure 1.19) [20].

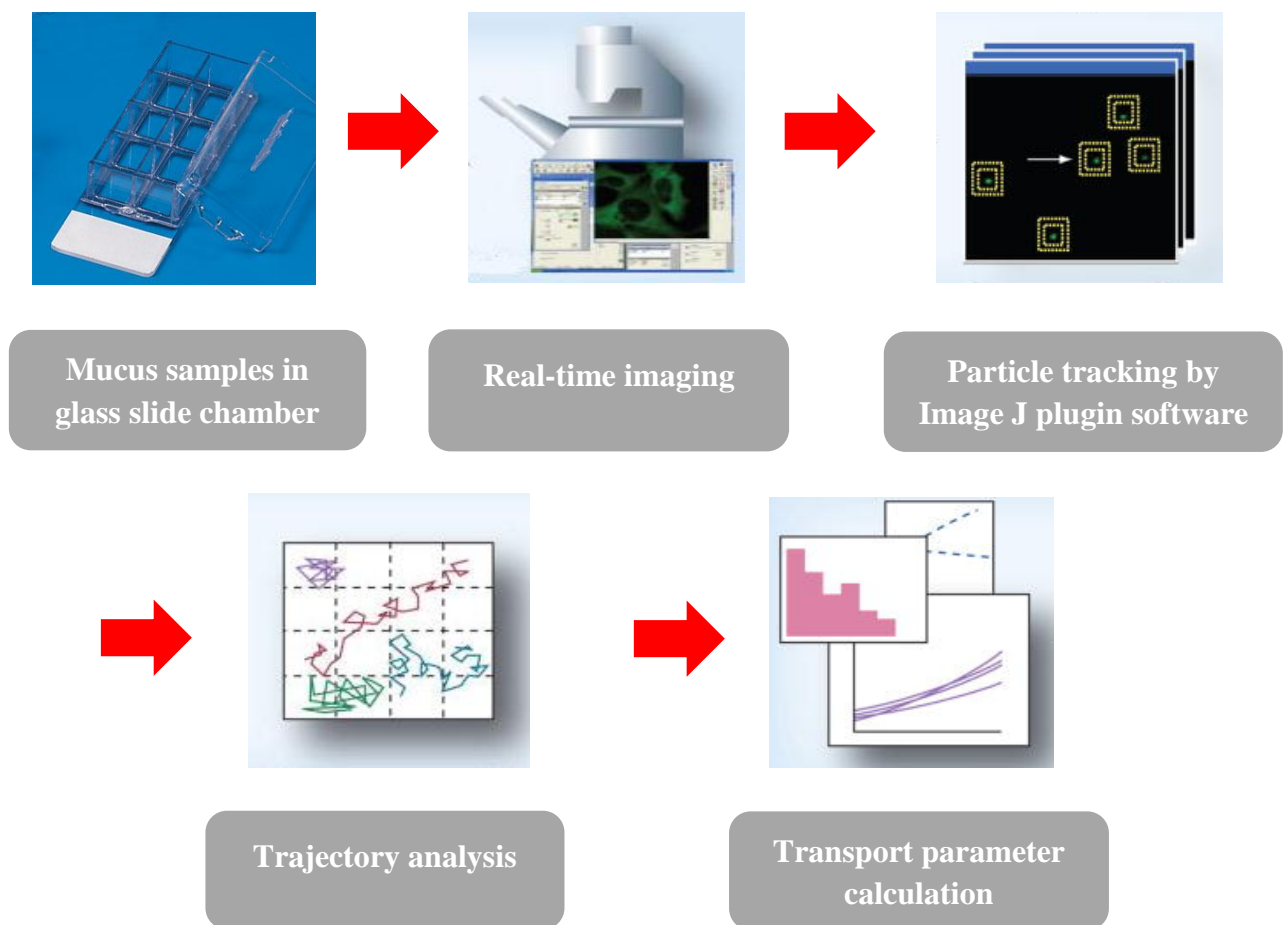


Figure 1.19: multiple particle tracking technique by procedure [20].



1.7.2 Mean square displacement analysis

A single trajectory of the each nanoparticle has x and y positional data over time. The obtained 2-dimensional position (x, y) can be used to calculate the mean square displacement (MSD) or $\langle \Delta r^2(\tau) \rangle$ over time scale and is given as [1]:

$$\langle \Delta r^2(\tau) \rangle = \langle \Delta x^2 \rangle + \langle \Delta y^2 \rangle \quad (1)$$

In this equation, τ is time scale or time lag, $\langle \Delta x^2 \rangle = [x(t + \tau) - x(t)]^2$, and $\langle \Delta y^2 \rangle = [y(t + \tau) - y(t)]^2$ (t indicates time in seconds) [33, 34].

1.7.2.1 Time scale

Assume a camera is able to capture 30 frames of images from a 20 second long movie. In total, there will be 600 recorded frames of particle. The time interval between each frame is 33 ms, meaning that particle mobility can be calculated only frame-wise giving the shortest time scale of 33-ms (Figure 1.20) [35].

In this case, the 600 framed movies results in 599 displacement values. The next shortest time scale is 66ms which gives 598 displacement values. Thus, time scale can be defined as the time a particle is allowed to move around before its displacement value is determined based on the distance travelled from an initial point (Figure 1.20) [35].

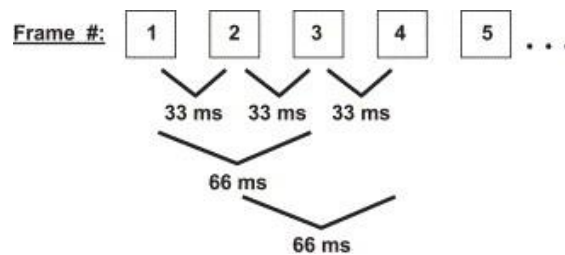


Figure 1.20: Illustration of time scale for 30 frame wise images obtained from a movie over 20 second [35].

*SPM= Sigma pig mucus, *PM= Polymeric mucus



Mucus barrier components, challenges for nanoscale drug delivery

The mode of transport of each individual particle can be identified by the slope of the MSD versus time on a log-log scale. Three theoretical MSD plots based on differences in particle diffusivity are given in Figure 1.20. Each line represents the MSD of an individual particle which can be found by ascertaining mean the change in x and y position over time scale. Particle selection takes place randomly and analysis is done using the Image J plugin software. If a particle's x and y position does not change over time scale the particle is classified as being immobile (Figure 1.21 A, red line), while limited changes in x and y position (particle mobility) over time scale is known as a sub-diffusive particle (Figure 1.21 B, blue line). On the other hand, if the particle show significant changes in x and y position over time scale it is known as a mobile particle (Figure 1.21 C, green line) (Note that the number of tracked particles result variations in particle trajectories, and therefore MSD plot) (Figure 1.21) [36].

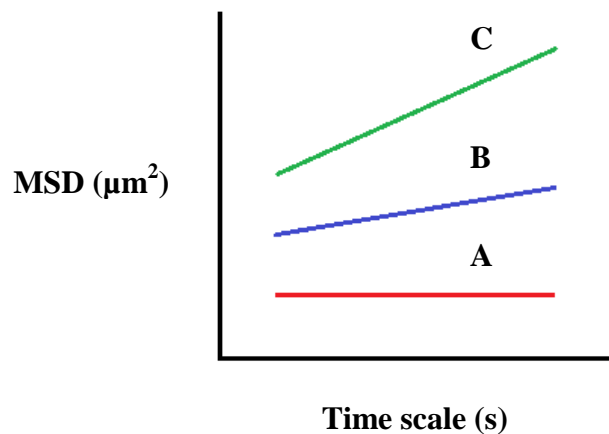


Figure 1.21: Transport mode categorization by MSD plots, (A) an immobile particle (red plot), (B) a sub-diffusive particle (blue plot), and (C) a mobile particle (green).



1.7.1 Nanoparticle trajectories classification

The particle trajectory shows the pattern movement by the particle during the observation. The form of the trajectory can give some information about the barriers to motion that particle experiences.

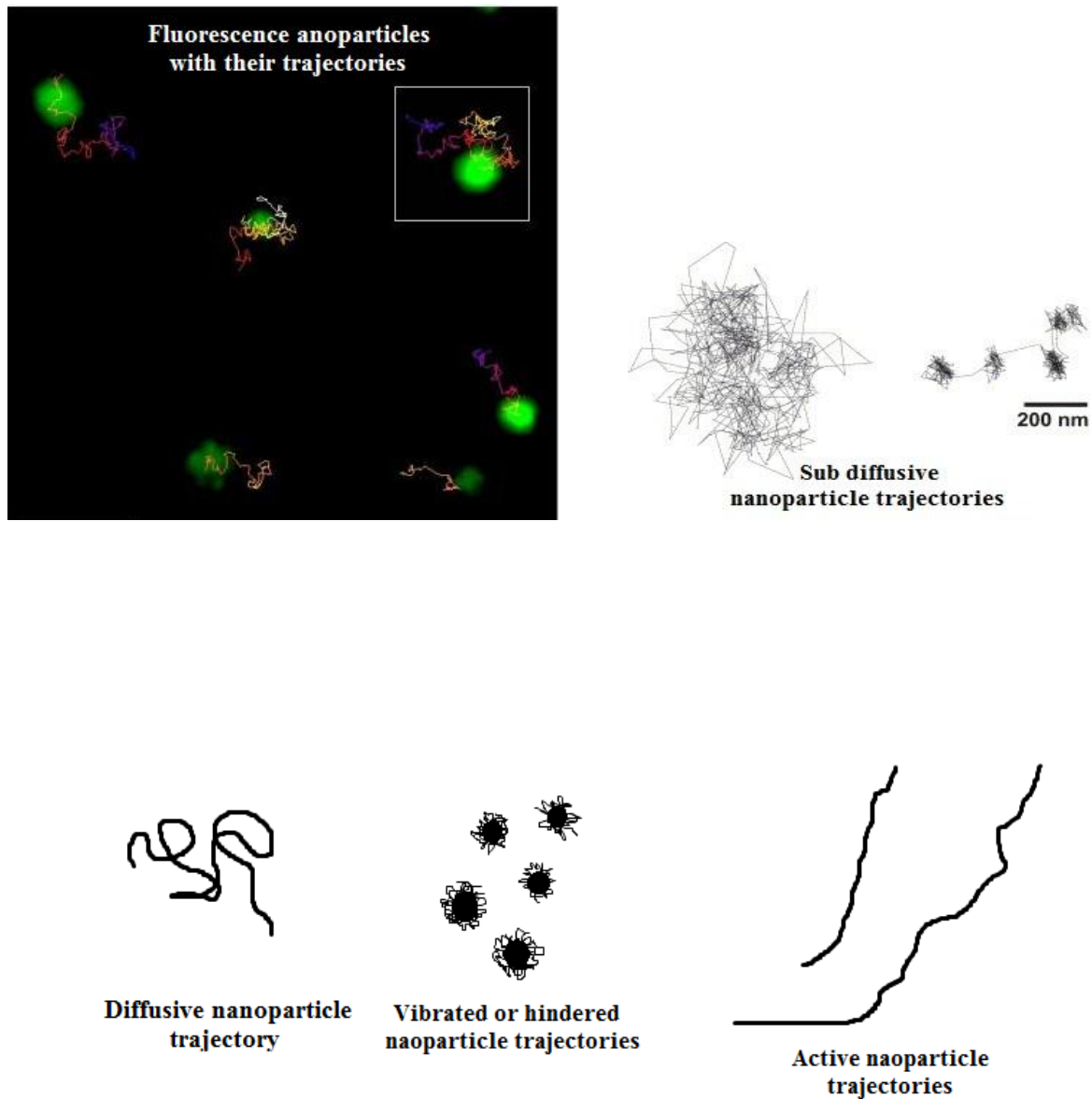


Figure 1.22: Nanoparticle trajectories based on their transport mode in mucus matrix [22, 35].

*SPM= Sigma pig mucus, *PM= Polymeric mucus



1.7.3 Effective diffusivity analysis

The effective diffusivity can be calculated by the given equation [2]:

$$D_{eff} = \frac{\langle \Delta r^2(\tau) \rangle}{4\tau} \quad (2)$$

If D_{eff} plot decreases with time scale nanoparticle display sub-diffusive motion, If D_{eff} plot was constant with time scale nanoparticle display diffusive motion, and if D_{eff} plot increases with time scale nanoparticle display active motion. Immobile particle can be identified by qualitative observations along with mathematical criteria (Figure 1.23) [33, 35].

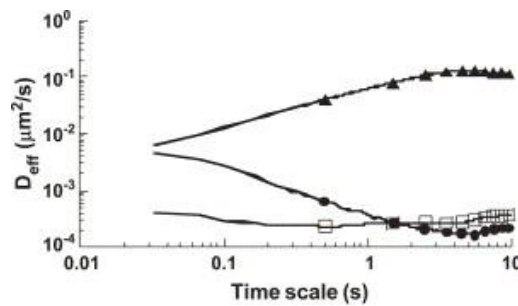


Figure 1.23: Transport mode categorization by MSD plots: Diffusive (□), sub diffusive (●), and active (▲) [35].

Therefore, plotting MSD and D_{eff} values against time scale allows analysis of the mode of particle motion.



1.7.3.1 Diffusivities

1.7.3.1.3 Macroscopic diffusion

The barrier experienced by a particle depends on particle size relative to the mesh size or the matrix (Figure 1.24).

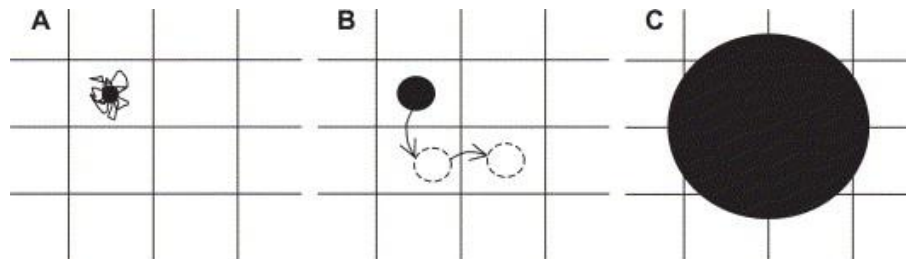


Figure 1.24: Three models of nanoparticle diffusion in biological environment: (A) microscopic, (B) mesoscopic, and (C) macroscopic [35].

Multiple particle tracking may be used to determine the bulk-fluid rheological properties of mucus. In order to estimate the fluid navigation properties, the size of particle should be larger than the fluid pore sizes (Figure 1.24, part C).

1.7.3.1.1 Microscopic diffusion

In complex biological fluids like mucus, the measured fluid viscosity varies with length scale, due to the inhomogeneous nature of the mucus. The cause of the observed heterogeneities within the mucus gel can be attributed to microdomains or pores with lower viscosity fluid (Figure 1.24 A) [35].

Multiple particle tracking can be used to identify the viscosity in these microdomains, where non-adhesive and small particles move freely in the interstitial fluid. By using the Stokes-Einstein equation it is possible to calculate the microviscosity experienced by each particle. This equation is based on particle movement by simple diffusion, meaning that MSD data can be used to calculate the microscopic diffusion at early time scales when particles are under short range Brownian motion [37].

*SPM= Sigma pig mucus, *PM= Polymeric mucus



1.7.3.1.2 Mesoscopic diffusion

The size of particle determines its interactions in a complex biological environment. Particle mobility can be influenced by the dynamic of the fluid microstructure, for instance if the particle has the same size as the fluid pores in the biological environment. In this case, particles may show to be hindered at early time scale. However, alteration in the microstructure of the fluid contributes to particle diffusion which often displays biphasic behavior. This behavior can be seen as a decrease in De_{eff} value with time at short time scales. This behavior can be seen as a decrease in De_{eff} value with time at short time scales and reaches a constant value at long time scales. This constant lower value corresponds to the mesoscopic diffusion coefficient. The viscosity measured from the mesoscopic diffusivity would be lower than values provided by other conventional rheological techniques, due to particle accession to pores with lower viscosity. Therefore, particles have more free motion and using the particle tracking technique gives information about pore sizes in the mucus (Figure 1.24 A) [37].

1.7.4 Beads on string

Analysis of particle mobility does not necessarily explain the molecular origin of the barriers to movement. As shown in figure W, nanoparticle could be trapped in mucus mesh pores and being impeded or nanoparticle could be associated with mucus fibers and such a non-statistic vibration mucus networks and both could result in similar trajectories (beads on a string) one of steric(A) and one of interactive origin (B) (Figure 1.25).

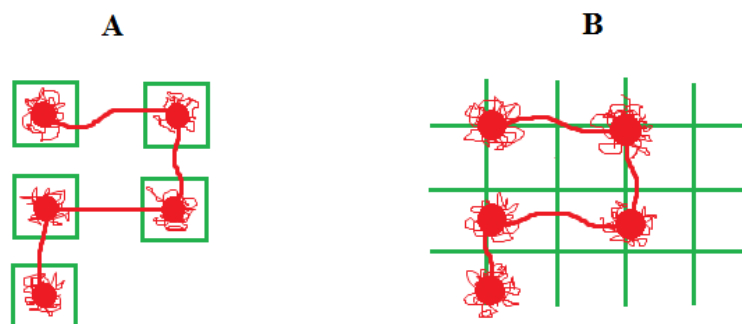


Figure 1.25: Mucus matrix as barrier to nanoparticle transport. Nanoparticle movement limited by both mucus mesh pores (A) and mucus network (B).



Chapter 2

Material and methods

2.1 Nanoparticles

Carboxylate modified microspheres and amine modified microspheres were obtained from Invitrogen. These particles have yellow-green fluorescent color with 200 nm in diameter, and are mixed in distilled water together with 2mM azide (2 % solids).

The carboxylate modified microsphere products (product code: F8811) were made by grafting polymers with functional groups like carboxylic to sulfate chain of microspheres, giving both negative and hydrophilic surface to beads. Amine modified microsphere products (product code: F8764) were prepared by chemical modification hydrophilic with amine groups which gives positive charged beads. The amine and carboxylate nanoparticles are firmly hydrophobic, because they created by polystyrene materials. They greatly excited by setting the argon laser at 488 nm spectral line, results in intense fluorescence color.

2.2 Porcine gastric mucin

Gastric mucin extracted from porcine stomach was purchased from Sigma-Aldrich Norway AS, Tevlingn 23, N-1081 Oslo (Product number: M2378), and was used for experiments in this master thesis.

Porcine gastric mucin is similar to mucus which found in human, and therefore is a good model for studying nanoparticle mobility in mucus.

2.3 Polymeric mucin

Polymeric mucin was obtained from J.P. Pearson University of Newcastle, UK prepared according to the method of F.J.J Fogg et al [38].

Solubilized glycoprotein was purified in a CsCl density gradient (starting density 1.42 g·ml⁻¹) and fractionated by Sepharose CL-2B column chromatography. The void volume fractions were pooled, dialysed, freeze-dried and used as polymeric mucin. Purity of mucin was determined by SDS/PAGE and staining with silver. Purified mucin was digested with papain (0.08 mg of papain/mg of glycoprotein, at 60 °C), for 48 h in 0.067 M sodium phosphate

*SPM= Sigma pig mucus, *PM= Polymeric mucus



Mucus barrier components, challenges for nanoscale drug delivery

buffer, pH 6.25, containing 5 mM cysteine hydrochloride and 5 mM EDTA. Digested mucin was fractionated in a further CsCl gradient, starting density $1.42 \text{ g}\cdot\text{ml}^{-1}$. Polymeric mucin was reduced with 0.2 M mercaptoethanol, for 24 h, at room temperature in 0.2 M Tris/HCl buffer, pH 8.0, containing 0.01 M EDTA, and was subsequently blocked overnight with 0.22 M iodoacetamide. Reduced mucin was fractionated in a further CsCl gradient, starting density $1.42 \text{ g}\cdot\text{ml}^{-1}$ [38].

2.4 G-blocks dried powder

G-blocks dried powder prepared according to the described method by Jørgensen et al [30].

The chemical composition, fraction of diad sequences F_{GG} , F_{MG} , and F_{MM} , determined by high-field ^1H NMR, and intrinsic viscosity, $[\eta]$, in 0.1 M NaCl at $T = 20^\circ\text{C}$ determined in a capillary viscometer are summarized in Table 1. Low molecular weight G block alginates were produced by means of acid hydrolysis as previously described.

2.5 MES sodium salt

MES sodium salt was purchased from Sigma-Aldrich Norway AS, tevlingn 23, N-1081 (product code M3885). MES sodium salt has molecular weight of 195.2 Da and chemical formulae of $\text{C}_6\text{H}_{12}\text{NNaO}_4\text{S}$. In this experiment MES buffer at pH=6 was used as solvent in beads and mucus networks (see the supporting information in appendix). Mucus pH is depends on mucosal surfaces and pH range on mucosal surfaces is from the acidic pH in the gut and close to neutral pH in the lung. Therefore the optimal pH of MES buffer was selected for this experiment.

2.6 Cover glass slide chamber

The chambered cover glass (8 chamber-units, sterile) was purchase form Thermo Fisher Scientific, 75 Panorama creek D.r Rochester, NY 14625 USA. The chambered cover glass is intended to for cell culture applications employing high magnification inverted microscopes. The cover glass allows the microscope objective as close as possible to growing cells. In this master thesis, chambered cover glass was used for investigating nanoparticle motion in mucus samples.



2.7 Phase 1 of experiments

2.7.1 Preparation of mucus matrixes

Sigma pig mucus was prepared by dissolving sigma pig mucin (45 mg/ml) in MES buffer (100mM) at pH 6. Mucus was added to buffer and stirred gently overnight at 4°C.

Chambers were filled with 200 microliter sigma pig mucus (45 mg/ml), and 5 microliter of a mixture of particle-MES buffer stirred gently in 45 mg/ml of sigma pig mucus (a mixture: 10 microliter of nanoparticle suspensions (2% w/w) was mixed with 40 microliter of MES buffer (100mM).

2.7.2 Nanoparticle treatment with G-blocks to apply in mucus

Ten microliter of nanoparticle suspensions (2% w/w) was mixed with 40 microliter of solubilized G-blocks (mg/ml) with MES buffer (100 mM) at pH 6. 5 microliter of this mixture was stirred gently in 200 microliter sigma pig mucus (45 mg/ml).

2.7.3 Preparation of mucus matrixes

A mixture of sigma pig mucus plus polymeric mucus was prepared by dissolving sigma pig mucin + polymeric mucin (30 mg/ml + 15 mg/ml) in MES buffer (100mM) at pH 6. Mucus was added to buffer and stirred gently overnight at 4°C.

Chambers were filled with 200 microliter of the mixture of sigma pig mucus plus polymeric mucin (30 mg/ml + 15 mg/ml), and 5 microliter of a mixture of particle-MES buffer stirred gently in mucus samples (10 microliter of nanoparticle suspensions (2% w/w) was mixed with 40 microliter of MES buffer (100mM).

2.7.4 Nanoparticle treatment with G-blocks to apply in mucus

Ten microliter of nanoparticle suspensions (2% w/w) was mixed with 40 microliter of solubilized G-blocks (mg/ml) with MES buffer (100 mM) at pH 6. 5 microliter of this mixture was stirred gently in 200 microliter of the mixture of sigma pig mucus plus polymeric mucus (30 mg/ml + 15 mg/ml).

*SPM= Sigma pig mucus, *PM= Polymeric mucus



Mucus barrier components, challenges for nanoscale drug delivery

* Mucus samples were sealed with parafilm to prevent of dehydration and left overnight for 24 hours in a cold room (4°C). Chambers were observed and were imaged at room temperature using a Leica microscope (TCS SP5).

* Stirring: the suspensions were mixed in mucus samples.

*Without stirring: the suspensions were added on top of 200 microliter mucus in chambers.

2.8 Phase 2 of experiments

2.8.1 Sample preparation

Sigma pig mucus was prepared by dissolving sigma pig mucin (45 mg/ml) in MES buffer (100mM) plus 0.04 mg/ml G-blocks at pH 6. Mucus was added to buffer and stirred gently overnight at 4°C.

2.8.2 Mucus treatment with G-blocks

Chambers were filled with 150 microliter sigma pig mucus (45 mg/ml) contains G-blocks (0.04 mg/ml) in 100mM MES buffer at pH 6. Then, 55 microliter of nanoparticle-MES buffer stirred gently in 150 microliter mucus (5 microliter of nanoparticle suspension + 50 microliter of MES buffer).

2.8.3 Nanoparticle treatment with G-blocks

Nanoparticles (5 microliter) mixed with 50 microliter of G-blocks solubilized in MES buffer (0.04 mg/ml G-blocks in 100 mM MES buffer) and 55 microliter of the mixture stirred gently in 150 microliter of sigma pig mucus (45 mg/ml) (Ten microliter of nanoparticle suspensions (2% w/w) was mixed with 50 microliter of solubilized G-blocks (0.04 mg/ml) in MES buffer (100 mM) at pH 6).

2.8.4 Sample preparation

Sigma pig mucus was prepared by dissolving sigma pig mucin (45 mg/ml) in MES buffer (100mM) plus 0.5 mg/ml G-blocks at pH 6. Mucus was added to buffer and stirred gently overnight at 4°C.



2.8.5 Mucus treatment with G-blocks

Chambers were filled with 150 microliter sigma pig mucus (45 mg/ml) contains G-blocks (0.5 mg/ml) in 100mM MES buffer at pH 6. Then, 55 microliter of nanoparticle-MES buffer stirred gently in 150 microliter mucus (5 microliter of nanoparticle suspension + 50 microliter of MES buffer).

2.8.6 Nanoparticle treatment with G-blocks

Nanoparticles (5 microliter) mixed with 50 microliter of G-blocks solubilized in MES buffer (0.5 mg/ml G-blocks in 100 mM MES buffer) and 55 microliter of the mixture stirred gently in 150 microliter of sigma pig mucus (45 mg/ml) (Ten microliter of nanoparticle suspensions (2% w/w) was mixed with 50 microliter of solubilized G-blocks (0.5 mg/ml) in MES buffer (100 mM) at pH 6).

*All mucus samples were sealed to prevent of dehydration of mucus, and left overnight for 24 hours in a cold room (°4C).

*The same procedure used to test the motion of both amine and carboxylate modified nanoparticles in sigma pig mucus.

* Mucus samples were sealed with parafilm to prevent of dehydration and left overnight for 24 hours in a cold room (°4C). Chambers were observed and were imaged at room temperature using a Leica microscope (TCS SP5).

2.9 Confocal Laser Scanning Microscopy

Confocal Laser Scanning Microscopy is a powerful technique for observing sample molecules stained with fluorescent dyes. The fluorescent emission, resulting from excitation of electrons caused by an incident light, is focused onto a photo detector. Samples are scanned by laser in order to obtain high resolution optical images with depth selectivity. The confocal microscope was designed with the ability to acquire in-focus images from selected depths, which is known as optical sectioning. Images are acquired point-by-point and displayed at the appropriate spatial position on a TV monitor. This allows three-dimensional reconstructions of topologically complex objects [39].

*SPM= Sigma pig mucus, *PM= Polymeric mucus



2.9.1 Sample visualization

A Leica TCS SP5 laser scanning confocal microscope was used to capture images from mucus samples. Argon laser at 488 nm selected from laser setting to observe fluorescence dye. Laser excitation wavelength was set at 525nm and detection. A 63X 1.2/ water objective lens was used to obtain 512 frame wise images at 73 second time scales (image resolution 512×512 pixels) (See Appendix C, Table C.1).

2.10 Data analysis

Obtained images from amine and carboxylate nanoparticles in mucus samples were process with Image J plugin software. The x and y position of 50 COOH nanoparticle trajectories were extracted with Image J plugin software and further using Matlab predefined script. The mean square displacement (MSD), and the averaged-mean square displacement ($\langle \text{MSD} \rangle$) were calculated by provided values from Matlab software. The calculated MSD values allowed us to calculate the effective diffusivities (D_{eff}) ($\text{MSD}/4 \cdot T$), and the average-mean effective diffusivities ($\langle D_{\text{eff}} \rangle$).



Chapter 3

Results and Discussion

3.1 The motion of carboxylate nanoparticles in sigma pig mucus

To determine the motion of carboxylate-modified nanoparticles (200 nm in diameter) in 45 mg/ml sigma pig mucus, experiments were performed in triplicate repeats for 50 COOH nanoparticles using multiple particle tracking (MPT).

The following sample was studied,

- Carboxylate nanoparticle suspensions were gently stirred in 45 mg/ml sigma pig mucus (stirred → nanoparticle suspensions were mixed in mucus). (Data analysis is provided in Figure 3.1).

The x and y positional coordinates for carboxylate nanoparticle trajectories were imaged frame wise (512 frame obtained at 73-ms time scale), and were tracked by Image J plugin software. The analyzed two dimension (2D) particle motion was used to calculate the mean square displacement (MSD) value for the each carboxylate nanoparticle.

Calculated MSD values allowed us to calculate the effective diffusivity ($Deff$) ($MSD/4*T$), the averaged-mean square displacement ($\langle Deff \rangle$), as well as averaged-mean effective diffusivity ($\langle Deff \rangle$) (note that all values were plotted as function of time scale) (Figure 3.1).

Individual nanoparticle transport mode can be classified based on $Deff$ plot in three modes; sub diffusive, diffusive, and active transport. If $Deff$ plot decreases with time scale nanoparticle display sub-diffusive motion, If $Deff$ plot was constant with time scale nanoparticle display diffusive motion, and if $Deff$ plot increases with time scale nanoparticle display active motion. In addition, $Deff$ plot lower than sub diffusive $Deff$ plot over time scale can be classified as immobile. Immobile particles can be identified by MSD plot which show a constant trend with time scale. Note that there should be no active motion in the mucus matrix, since there is no motor transport in mucus mesh [33, 35, 36].

*SPM= Sigma pig mucus, *PM= Polymeric mucus



Mucus barrier components, challenges for nanoscale drug delivery

The first experiment investigated the motion of carboxylate modified nanoparticle in sigma pig mucus. Three replicate experiments were conducted at the same condition.

There was a large variation in the individual particle trajectories and therefore MSD and Deff values which resulted in variability in the mean MSD and Deff values for 3 replicates.

As can be seen from Figure 3.1, stirred COOH nanoparticles show that sub-diffusive mobility in 45 mg/ml sigma pig mucus, however there is a sub population of nanoparticles show diffusive motion with tendency to time scale.

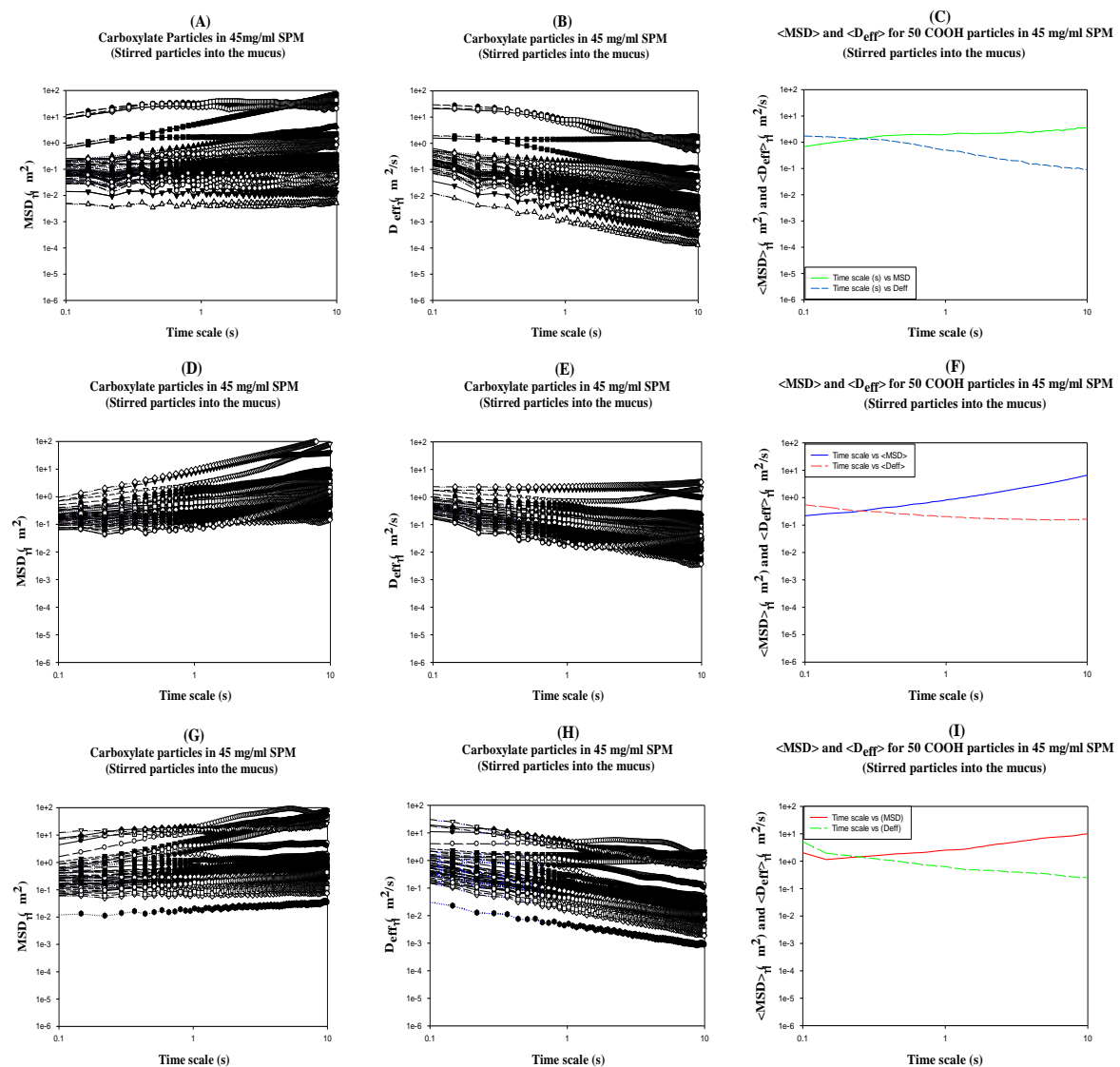


Figure 3.1: The motion of carboxylate nanoparticle in sigma pig mucus. (A, D, G) Triplicates ensemble mean square displacement (MSD), (B, E, H) effective diffusivity, (C, F, I) mean MSD ($\langle MSD \rangle$) (solid line), and mean ($\langle D_{eff} \rangle$) (dashed line) for 50 carboxylate nanoparticles in 45 mg/ml sigma pig mucus (obtained between 0.1 to 10 seconds time scales).



Mucus barrier components, challenges for nanoscale drug delivery

Figure 3.2 provide triplicate mean MSD ($\langle \text{MSD} \rangle$), and mean Deff ($\langle \text{Deff} \rangle$) for 150 COOH-modified polystyrene nanoparticles in 45 mg/ml sigma pig mucus by combining C, F, and I panels from the Figure 3.1.

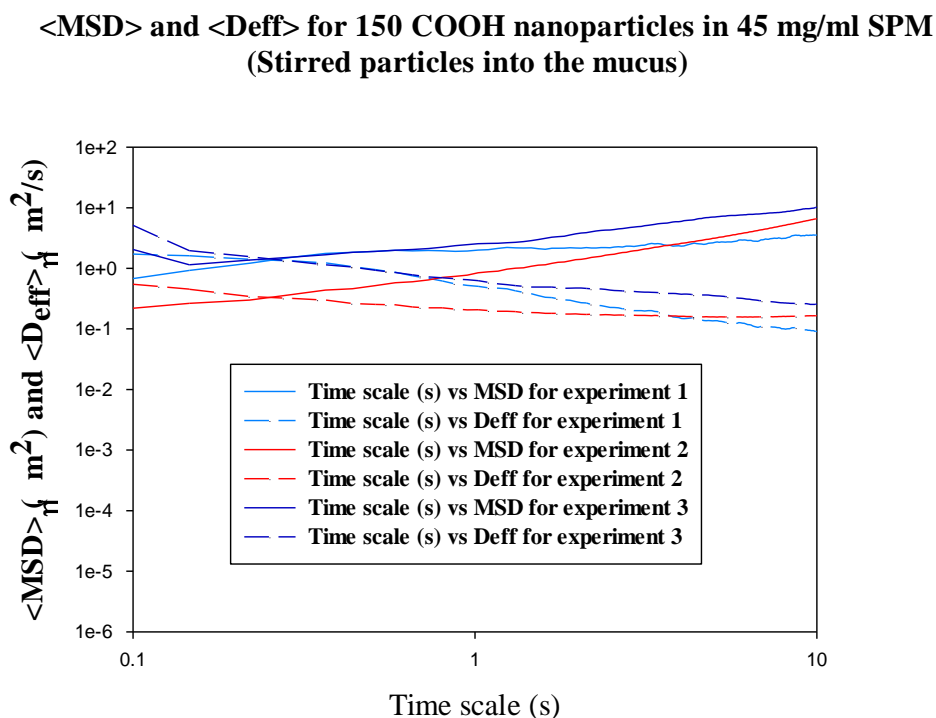


Figure 3.2: Triplicate combined MSD and Deff in sigma pig mucus. Ensemble-averaged mean square displacement $\langle \text{MSD} \rangle$ (solid lines) and mean effective diffusivities $\langle \text{Deff} \rangle$ (dashed lines) of carboxylate-modified nanoparticles (200 nm in diameter) in 45 mg/ml sigma pig mucus provided by three replicate experiments between 0.1 to 10 second of time scales (Figure is combined plot of panels C, F, and I from Figure 3.1).

In order to determine if results were representative, a set of exclusion criteria was applied over all triplicate results to determine if they could be considered as one data set.



3.2 Exclusion criteria

Exclusion criteria are the standards to determine whether a group of data sets can be considered as a single set for data interpretation. The exclusion criteria can be different according to the research standards [40].

The applied exclusion criteria over triplicate results:

Firstly any image series that showed apparent active transport was excluded.

Basically nanoparticles would not show active transport in mucus network, because there is no motor active in there. Reasons for observation of nanoparticle with active movement could be due to sample drift in microscopic field of view or random thermal motion caused by microscope laser beam.

Additionally, the flowing conditions must be satisfied for the replicates to be combined as a single data set.

1. The members of all data set must show same mean MSD and Deff trends (sub diffusion, diffusion).
2. All maximum MSD and Deff at 0.1 s to 10 s time scales must be above the all group mean MSD and mean Deff (represent by colored dots).
4. All minimum MSD and Deff at 0.1 s to 10 s time scales must be below the all group mean MSD and mean Deff (represent by colored dots).

We evaluated results of triplicate experiments and made the assumption if they resembled as same data set we can used them for data interpretation. Also, results of nanoparticles that showed active motion in mucus samples were excluded and did not considered further (nanoparticle with active transport display the effective diffusivity (Deff) increasing with time scale- Excluded results are presented in appendix A, Figures A.1, A.2, A.3, and A.4).



3.3 The comparison between triplicates maximum and minimum MSD and Deff values for carboxylate nanoparticles

To quantify whether these three repeated mean MSD ($\langle \text{MSD} \rangle$) and mean Deff ($\langle \text{Deff} \rangle$) values can be treated as same data set, the maximum and minimum MSD and Deff values of 50 stirred COOH-modified nanoparticles were compared for all group of results (triplicate experiments) and are shown in Figure 3.3 A , B.

Considering point .1 all replicates means showed sub diffusive behavior (Figure 3.2).

Considering point .2 all maximum MSD and Deff values at 0.1 s to 10 s time scales are above the all group mean MSD and mean Deff (represent by colored dots) (Figure 3.3 A and B).

Considering point .3 all minimum MSD and Deff at 0.1 s to 10 s time scales are below the all group mean MSD and mean Deff (represent by colored dots) (Figure 3.3 A and B).

Therefore these 3 replicates satisfy the above criteria and can be treated as a single data set.

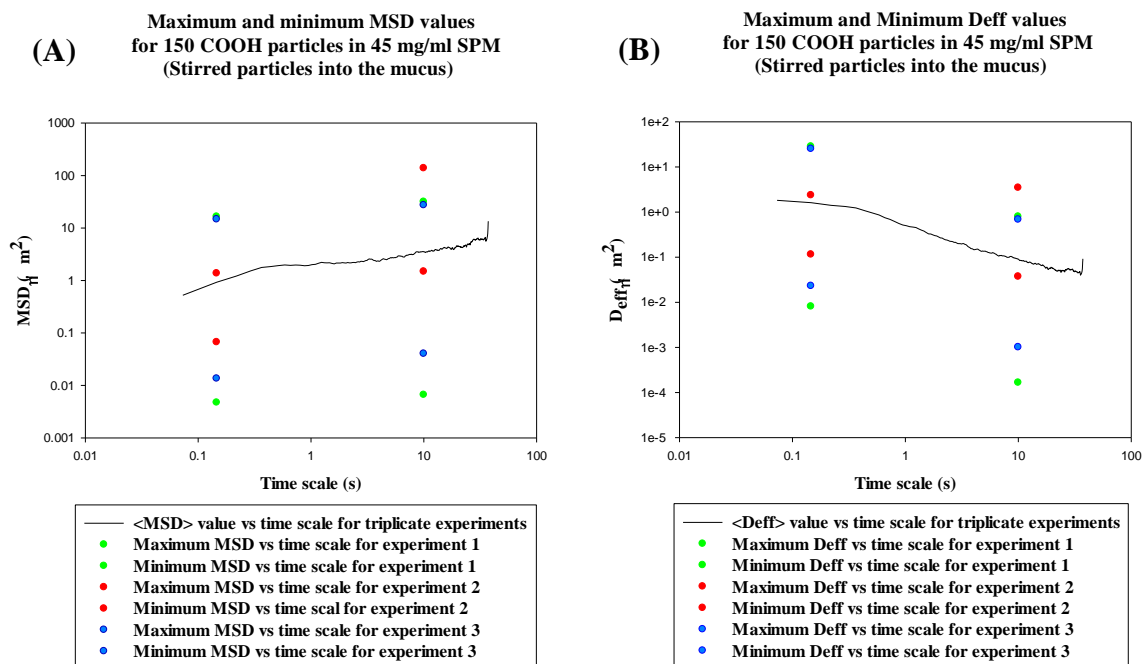


Figure 3.3: Maximum and minimum MSD and Deff values of triplicate experiments for stirred carboxylate nanoparticles in sigma pig mucus. (A) Show maximum and minimum MSD values for 150 stirred carboxylate nanoparticles between 0.1 to 10 second times in 45 mg/ml sigma pig mucus, and (B) Maximum and minimum Deffs values for 150 carboxylate-modified nanoparticles between 0.1 to 10 second time scales in 45 mg/ml sigma pig mucus (Obtained from values in Figure 3.1).

*SPM= Sigma pig mucus, *PM= Polymeric mucus



3.3.1 Discussion

Results from triplicate experiments (MSD and Deff values) were considered as single data set for stirred carboxylate-modified nanoparticles in 45 mg/ml sigma pig mucus and is shown in Figure 3.4. As can be seen, carboxylate particles displayed sub diffusive motion. In general, a typical behavior of nanoparticles is to show sub diffusive motion in mucus matrix, which is in accordance with previous studies [13, 33].

Indeed, nanoparticles can exhibit diffusive, hindered, and immobile motion behavior in mucus matrix based on mucus barrier and the presence of biopolymer for example G-blocks [13, 41, 42].

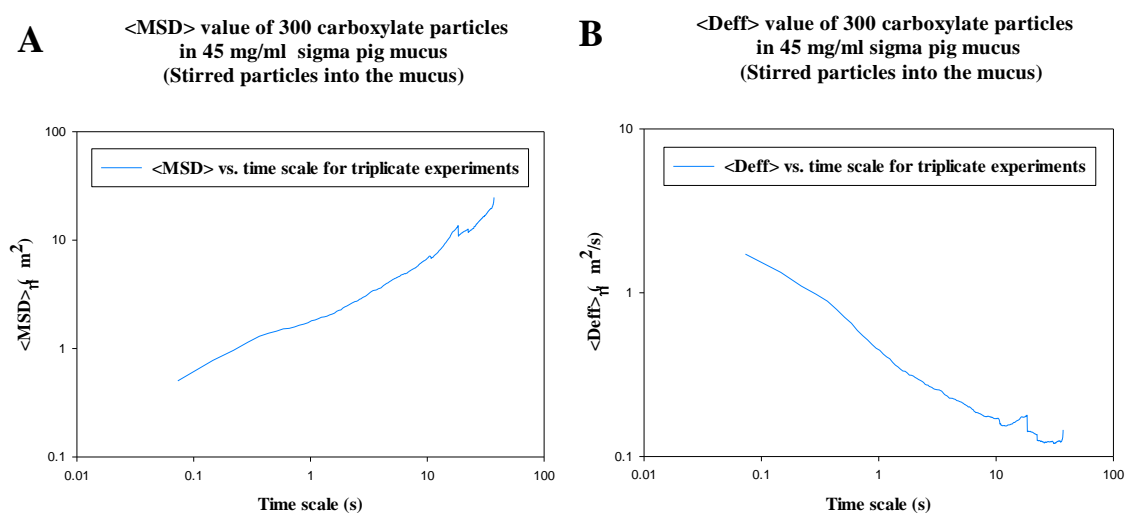


Figure 3.4: Graphical presentation of combined MSD and Deff values from triplicate results as a single data set. MSD plot (A) and Deff plot (B) in 45 mg/ml sigma pig mucus from triplicate experiments which considered as a single data set (Data analysis is shown in Chapter 3, Figure 3.1).



3.4 Study to investigate the effect of G-blocks on nanoparticle mobility in sigma pig mucus

The motion of carboxylate-modified nanoparticles was investigated at 73-ms time interval in 45 mg/ml sigma pig mucus using multiple particle tracking technique (MPT).

The following samples were studied,

1. Carboxylate nanoparticles were gently stirred into 45 mg/ml sigma pig mucus (stirred → nanoparticles suspension mixed into the mucus). (Data analysis is provided in Chapter 3, Figure 3.1).
2. Carboxylate nanoparticle suspensions mixed with 0.04 mg/ml G-blocks and were gently stirred into 45 mg/ml sigma pig mucus (stirred → nanoparticles treated with G-blocks and the suspensions mixed into the mucus). (Data analysis is shown Chapter 5, Figure 5.4,).

From 100-150 nanoparticle trajectories obtained in triplicate experiments, the mean square displacement (MSD) was calculated for each trajectory as well as averaged-mean square displacement ($\langle \text{MSD} \rangle$). The same criteria for treating replicates as a single group was applied as describe in section 3.1.1 (Data analysis are presented in chapter 3, Figure 3.1 and in Chapter 5, Figure 5.4 respectively).

To allow determination diffusive and sub diffusive particles, Deff values ($\text{MSD}/4 \cdot T$) were calculated and plotted as function of time scale. If Deff is constant with time scale, then particle shows diffusive motion. If Deff decreases with time scale, then particle shows sub-diffusive mobility.

We can see in Figure 3.5 B that, particles are sub-diffusive and $\langle \text{deff} \rangle$ values decreased with time scale. The $\langle \text{MSD} \rangle$ and $\langle \text{Deff} \rangle$ plots of carboxylate particles have similar shapes with and without of G-blocks (0.04 mg/ml).

*SPM= Sigma pig mucus, *PM= Polymeric mucus

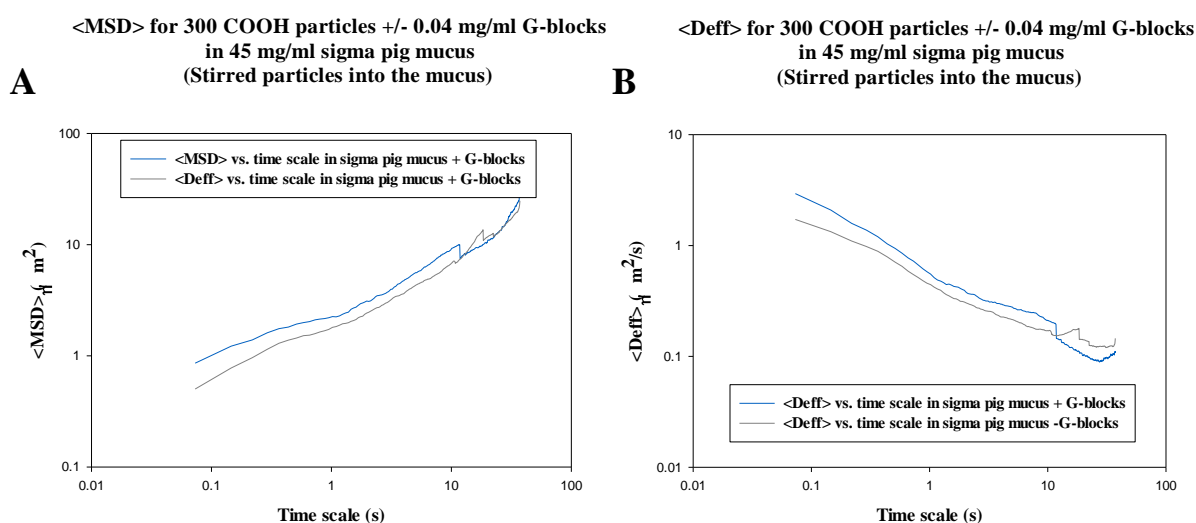


Figure 3.5: The effect of G-blocks on stirred carboxylate nanoparticles motion in sigma pig mucus. Panel A and panel B show mean MSD $\langle \text{MSD} \rangle$ and mean Deff $\langle \text{Deff} \rangle$ values for 300 stirred carboxylate nanoparticles with and without G-blocks (0.04 mg/ml) in 45 mg/ml of sigma pig mucus (obtained at 73-ms time intervals) (Data analysis are presented in chapter 3, Figure 3.1 and in chapter 5, Figure 5.4).

3.4.1 Discussion

Under these conditions G-blocks did not alter particle mobility. This may be because of the relatively degraded nature of sigma pig mucus.



3.5 Study to determine the influence of G-blocks on nanoparticle mobility in sigma pig mucus + polymeric mucus

To determine if an increased content of non-degrade polymeric mucin altered the effect of G-blocks, the motion of carboxylate nanoparticles was investigate in sigma pig mucus + polymeric mucus. Therefore, the following groups were studied,

1. Carboxylate nanoparticles were gently stirred in 45 mg/ml sigma pig mucus + polymeric mucus (30 mg/ml + 15 mg/ml) without G-blocks treatment (stirred → nanoparticle suspensions were mixed into the mucus). (Data analysis is presented in Chapter 5, Figure 5.10).
2. Carboxylate nanoparticles were treated with 0.04 mg/ml G-blocks, and were gently stirred in 45 mg/ml sigma pig mucus + polymeric mucus (30 mg/ml + 15 mg/ml) (nanoparticle suspensions were mixed into the mucus). (Data analysis is shown in Chapter 5, Figure 5.16).

Considering the applied criteria, the analyzed mean $\langle \text{MSD} \rangle$ and mean $\langle \text{Deff} \rangle$ values show no different motion trend for particles treated with G-blocks and without G-blocks treatment, however, there is an indication that G-blocks may have led to more diffusive type motion at longer time scales. At time scales above 10s, treated particles with G-blocks were on average more mobile.

*SPM= Sigma pig mucus, *PM= Polymeric mucus

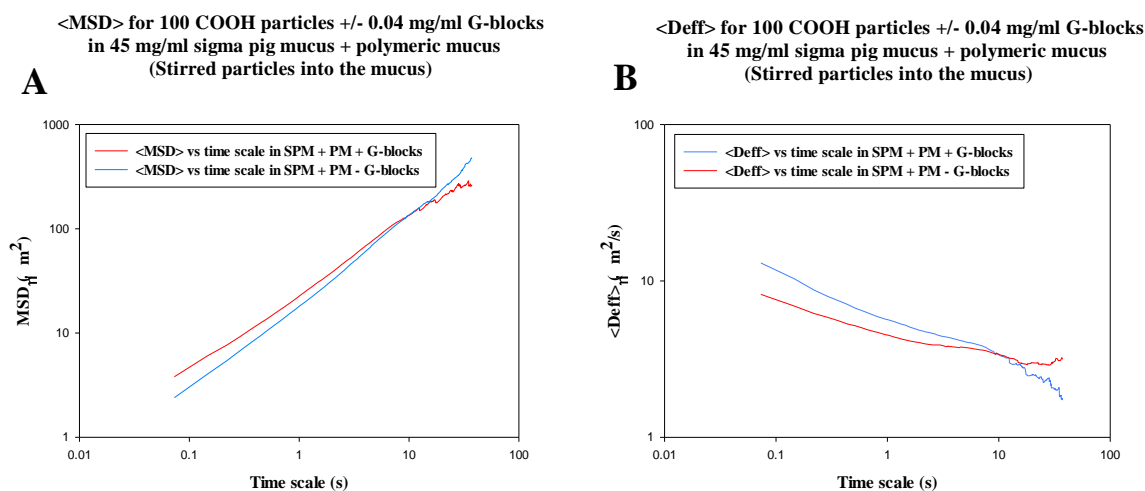


Figure 3.6: The effect of G-blocks on stirred carboxylate nanoparticles motion in sigma pig mucus + polymeric mucus. Panel A and panel B present mean MSD $\langle \text{MSD} \rangle$ and mean Deff $\langle \text{Deff} \rangle$ values for 100 stirred carboxylate nanoparticles with and without 0.04 mg/ml G-blocks in 45 mg/ml of sigma pig mucus + polymeric mucus obtained at 73-ms time interval (Data analysis are presented in chapter 5, Figure 5.10 and Figure 5.16).

3.5.1 Discussion

Comparing Figure 3.5 and Figure 3.6, it can be seen no significant differences in the MSD and Deff values for nanoparticles with and without G-blocks in mucus matrix A or in mucus matrix B, however, a crossover was seen and that may indicate changes with G-blocks treatment that alter barrier at longer timescales. Therefore, further investigation is required.



3.6 Study to compare nanoparticle mobility in mucus types A and B

In this study, multiple particle tracking was employed as previously described to investigate carboxylate nanoparticles motion in mucus matrix A (sigma pig mucus) and mucus matrix B (sigma pig mucus + polymeric mucus). Therefore, the following samples were taken into account,

1. Carboxylate nanoparticles were gently stirred in 45 mg/ml mucus matrix A (sigma pig mucus) (stirred → nanoparticle suspensions were mixed with into the mucus) (Data analysis is shown in Chapter 3, Figure 3.1)
2. Carboxylate nanoparticles were gently stirred in 45 mg/ml mucus matrix B (sigma pig mucus + polymeric mucus) (30 mg/ml + 15 mg/ml) (stirred → nanoparticle suspensions were mixed with into the mucus) (Data analysis is presented in Chapter 5, Figure 5.10).

The averaged-mean square displacement MSD ($\langle \text{MSD} \rangle$) (a) and the averaged-mean effective diffusivity ($\langle \text{Deff} \rangle$) were compared for carboxylate nanoparticles in Mucus A and Mucus B and are shown in Figure 3.7. As can be seen from Figure 3.7 a and b, $\langle \text{MSD} \rangle$ and $\langle \text{Deff} \rangle$ values are approximate 10 fold greater for mucus matrix B than mucus matrix A.

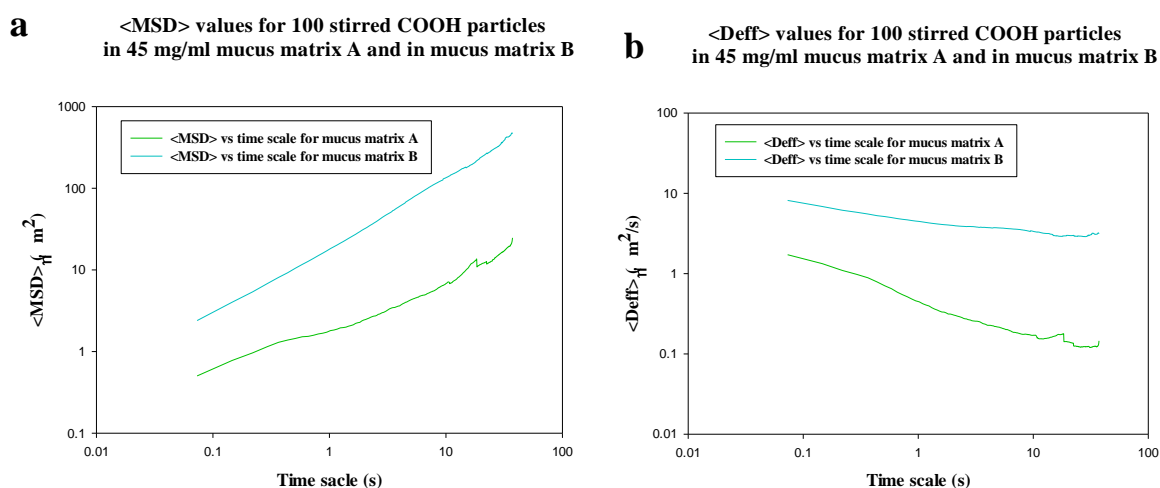


Figure 3.7: Carboxylate nanoparticles motion in mucus matrix A and matrix B. Panel a and b Provide mean MSD $\langle \text{MSD} \rangle$ and mean Deff $\langle \text{Deff} \rangle$ values for 100 stirred carboxylate particles in 45 mg/ml of mucus matrix A (sigma pig mucus) and mucus matrix B (sigma pig mucus + polymeric mucus) (Data analysis are presented in Chapter 3 Figure 3.1, and in chapter 5, Figure 5.10).

*SPM= Sigma pig mucus, *PM= Polymeric mucus



Mucus barrier components, challenges for nanoscale drug delivery

In addition, carboxylate particles appeared to be more diffusive in mucus matrix B (higher Deff plot). It was found that, carboxylate nanoparticles experienced less barrier to movement when polymeric mucus was added into the sigma pig mucus.

3.6.1 Discussion

The results of this study revealed the involvement of mucus components as movement barrier to nanoparticle motion, and existing challenges for nanoscale drug delivery. The degree of nanoparticle motion depends on the spacing between mucus fibers and its elements and the interactions with mucus components. Interestingly, carboxylate-modified nanoparticles diffused rapidly through mucus matrix B than mucus matrix A.

One possible explanation would be that, polymeric mucus makes more pores or provides a scaffold in mucus network and that resulted in increased particle mobility.

It also seems possible that, increased nanoparticle motion in matrix B is most likely due to different matrix architecture between sigma pig mucus and polymeric mucus (Figure 3.8).

Thus, choosing a proper mucus matrix is critical for studying its behavior.

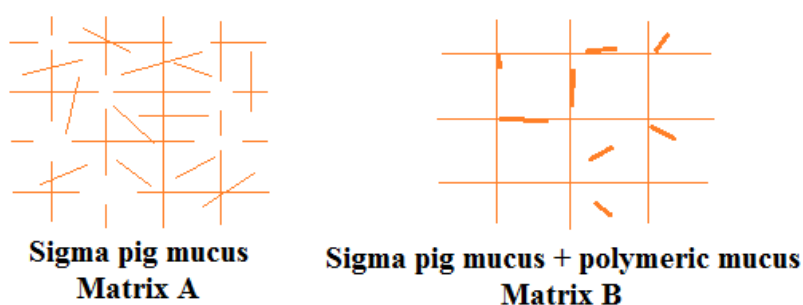


Figure 3.8: Schematic representation of mucus matrix A (sigma pig mucus) and mucus matrix B (sigma pig mucus + polymeric mucus).



3.7 Study to compare nanoparticle motion in mucus matrix A and mucus matrix B in the presence of G-blocks

The same study was performed as section 3.6 to determine changes on carboxylate nanoparticles mobility in the presence of G-blocks in mucus matrix A (sigma pig mucus) and mucus matrix B (sigma pig mucus + polymeric mucus). Therefore, the following samples were taken into account,

Therefore, the following studies were investigated,

1. Carboxylate nanoparticles treated with 0.04 mg/ml G-blocks and were gently stirred in 45 mg/ml mucus matrix A (sigma pig mucus) (stirred → nanoparticle suspensions were mixed with into the mucus) (Data analysis is shown in Chapter 5, Figure 5.4)
2. Carboxylate nanoparticles treated with 0.04 mg/ml G-blocks and were gently stirred in 45 mg/ml mucus matrix B (sigma pig mucus + polymeric mucus) (30 mg/ml + 15 mg/ml) (stirred → nanoparticle suspensions were mixed with into the mucus) (Data analysis is presented in Chapter 5, Figure 5.16).

Analyzed MSD and Deff values confirmed that carboxylate nanoparticles diffused greater in mucus matrix B than in mucus matrix A to an extent similar to study 3.6.

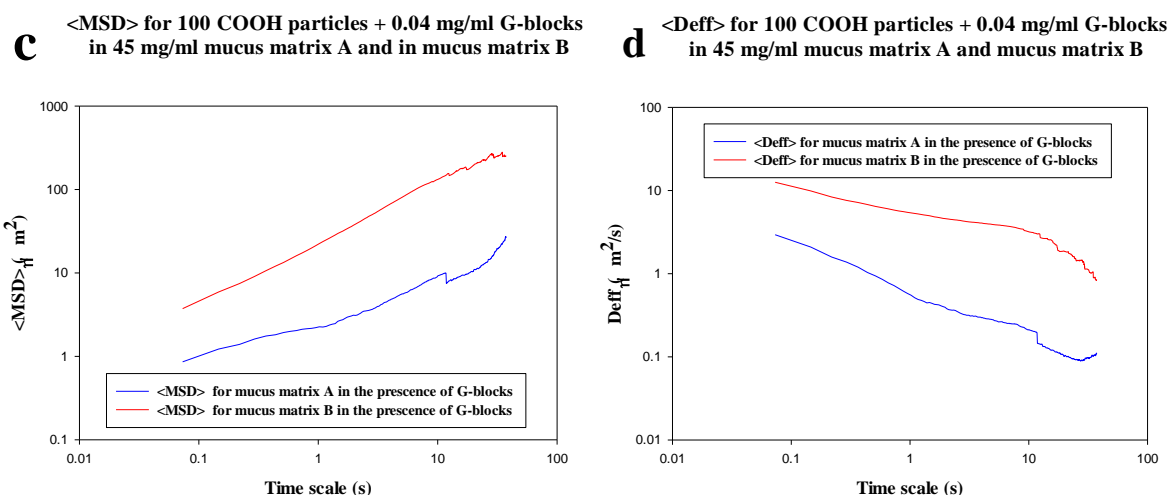


Figure 3.9: Carboxylate nano particles motion in the presence of G-blocks in mucus matrix A and matrix B. Panels c and d provide mean MSD $\langle \text{MSD} \rangle$ and mean Deff $\langle \text{Deff} \rangle$ values for 100 stirred carboxylate particles treated with G-blocks in 45 mg/ml of Mucus matrix A (sigma pig mucus) and Mucus matrix B (sigma pig mucus + polymeric mucus) (200 nm in diameter, obtained at 73-ms time intervals) (Data analysis are provided in chapter 5, Figure 5.4 and in Figure 5.16).

3.7.1 Discussion

As evident from both Figures 3.7 and 3.9 increased carboxylate nanoparticles motion in mucus matrix B is not likely due to G-blocks treatment, but is due to the presence of polymeric mucus in mucus matrix B.

The differences between the two matrices are similar with and without G-block treatment. In this case the matrix is the biggest determinant of particle mobility. Thus it is important to choose appropriate mucus matrix for investigation of nanoparticle motion.

It has been shown that nanoparticle motion can be categorized directly on mucus matrix obtained from animals, reasoning that the unique rheological and barrier properties required at each mucosal surface give rise to different mesh spacings or other structure properties, which has important implications for mucosal drug and gene delivery [43].



3.8 Study to quantify the method of bead addition on nanoparticle mobility in sigma pig mucus

To evaluate whether the method of nanoparticles (beads) addition makes difference to nanoparticle motion, the motion of stirred versus unstirred carboxylate-modified nanoparticles compared in 45 mg/ml sigma pig mucus by MPT.

Therefore, the following examination were taken into account,

1. Carboxylate nanoparticles were gently stirred into 45 mg/ml sigma pig mucus (Stirred → nanoparticle suspensions were mixed in mucus samples). (Data analysis is presented in Chapter 3, Figure 3.1)
2. Carboxylate nanoparticles were added into 45 mg/ml sigma pig mucus (Unstirred → nanoparticle suspensions were added on top in mucus samples in chamber). (Data analysis is shown in Chapter 5, Figure 5.1)
3. Carboxylate nanoparticles treated with 0.04 mg/ml G-blocks and were gently stirred into 45 mg/ml sigma pig mucus (Stirred → nanoparticle suspensions were mixed in mucus samples). (Data analysis is provided in Chapter 5, Figure 5.4)
4. Carboxylate nanoparticles treated with 0.04 mg/ml G-blocks and were added into 45 mg/ml sigma pig mucus (Unstirred → nanoparticle suspensions + G-blocks were added on top in mucus samples in chamber). (Data analysis is shown in Chapter 5, Figure 5.7).



Mucus barrier components, challenges for nanoscale drug delivery

The mean square displacement (MSD) and effective diffusivity (Deff) were calculated for 150 stirred versus unstirred carboxylate-modified nanoparticles treated with and without 0.04 mg/ml G-blocks in 45 mg/ml sigma pig mucus (Figure 3.10).

The mean MSD ($\langle \text{MSD} \rangle$) (A, C) and mean Deff ($\langle \text{Deff} \rangle$) (B, D) plots indicates differences but these are not large enough to be considered significant at these stage (considering the applied exclusion criteria) (Figure 3.10).

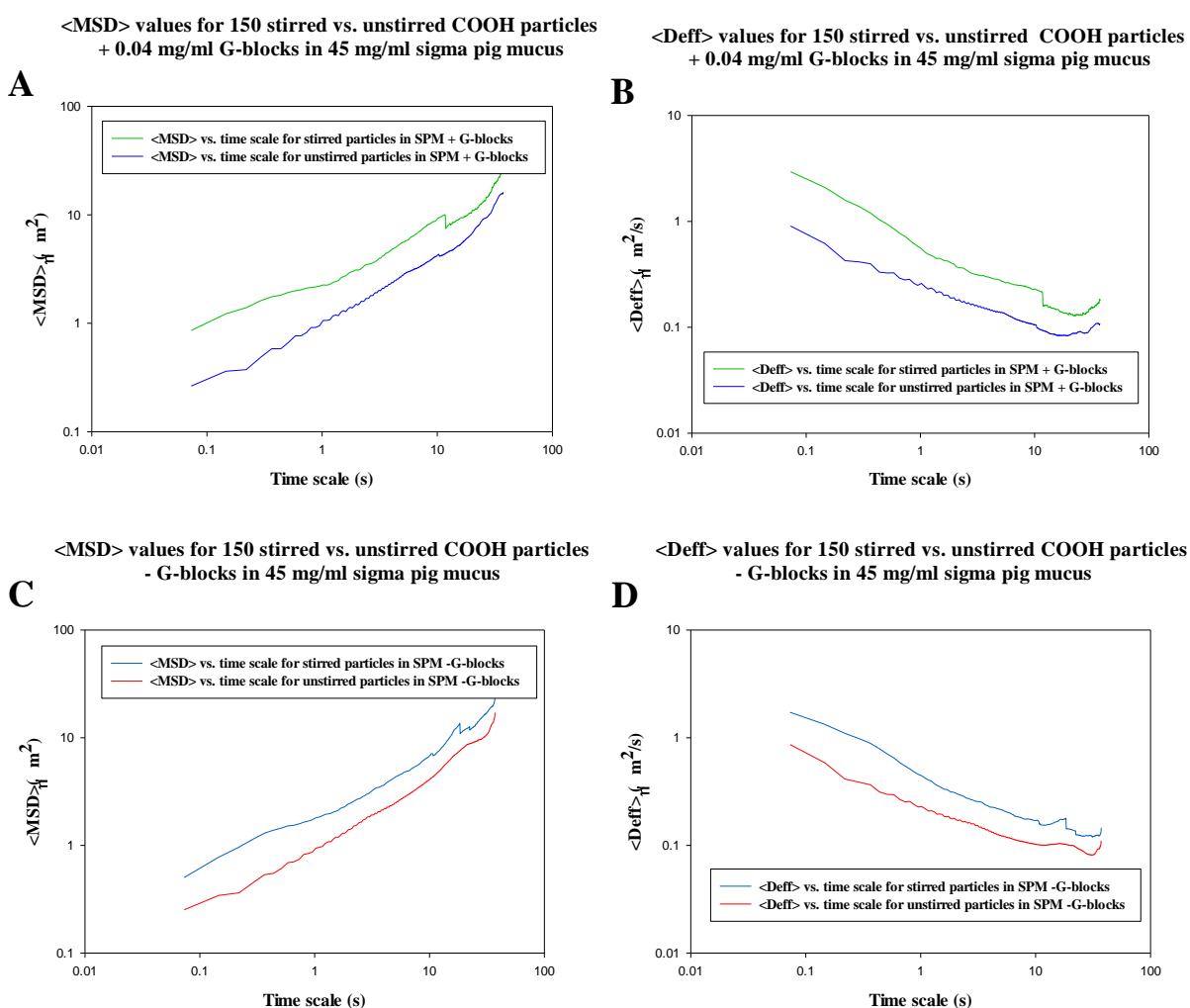


Figure 3.10: Study the method of beads addition on carboxylate particle mobility in sigma pig mucus. Panels A-C and B-D show mean MSD ($\langle \text{MSD} \rangle$) and mean Deff ($\langle \text{Deff} \rangle$) values for stirred versus unstirred particles for 150 carboxylate nanoparticle trajectories (200 nm in diameter, obtained at 73-ms time intervals) in 45 mg/ml sigma pig mucus (Data analysis are provided in Chapter 3, Figure 3.1, and in chapter 5, Figure 5.1, Figure 5.4 and Figure 5.7).



3.8.1 Study to verify the effect of bead addition on nanoparticle mobility in sigma pig mucus + polymeric mucus

The same study as in section 3.8, Figure 3.10 was repeated using mucus matrix B (sigma pig mucus + polymeric mucus). To further understand whether the motion of stirred versus unstirred nanoparticles would differ based on mucus mesh network, the method of beads addition (stirred versus unstirred) was investigated in 45 sigma pig mucus + polymeric mucus (30 mg/ml + 15 mg/ml) using multiple particle tracking.

Therefore, the following samples were taken into account,

1. Carboxylate nanoparticles were gently stirred into 45 mg/ml sigma pig mucus + polymeric mucus (Stirred → nanoparticle suspensions were mixed in mucus samples). (Data analysis is presented in Chapter 3, Figure 3.1)
2. Carboxylate nanoparticles added into 45 mg/ml sigma pig mucus + polymeric mucus (Unstirred → nanoparticle suspensions were added on top in mucus samples in chamber). (Data analysis is shown in Chapter 5, Figure 5.1)
3. Carboxylate nanoparticles treated with 0.04 mg/ml G-blocks and were gently stirred into 45 mg/ml sigma pig mucus + polymeric mucus (Stirred → nanoparticle suspensions were mixed in mucus samples). (Data analysis is provided in Chapter 5, Figure 5.4)
4. Carboxylate nanoparticles treated with 0.04 mg/ml G-blocks and were added into 45 mg/ml sigma pig mucus + polymeric mucus (Unstirred → nanoparticle suspensions + G-blocks were added on top in mucus samples in chamber). (Data analysis is shown in Chapter 5, Figure 5.7).



Mucus barrier components, challenges for nanoscale drug delivery

Figure 3.11 compares the averaged mean square displacement ($\langle \text{MSD} \rangle$) (A, C) and averaged effective diffusivity ($\langle \text{Deff} \rangle$) (B, D) values for 150 stirred versus unstirred COOH nanoparticles in 45 mg/ml sigma pig mucus + polymeric mucus (30 mg/ml + 15 mg/ml).

As can be seen from Figure 3.11, there are no differences between mean MSD ($\langle \text{MSD} \rangle$) (A, C) and mean Deff ($\langle \text{Deff} \rangle$) (B, D) plots for 150 stirred versus unstirred COOH nanoparticles over 73 second of time scales. Stirred nanoparticle versus unstirred nanoparticle showed similar $\langle \text{MSD} \rangle$ and $\langle \text{Deff} \rangle$ plots in the presence and in the absence of 0.04 mg/ml G-blocks.

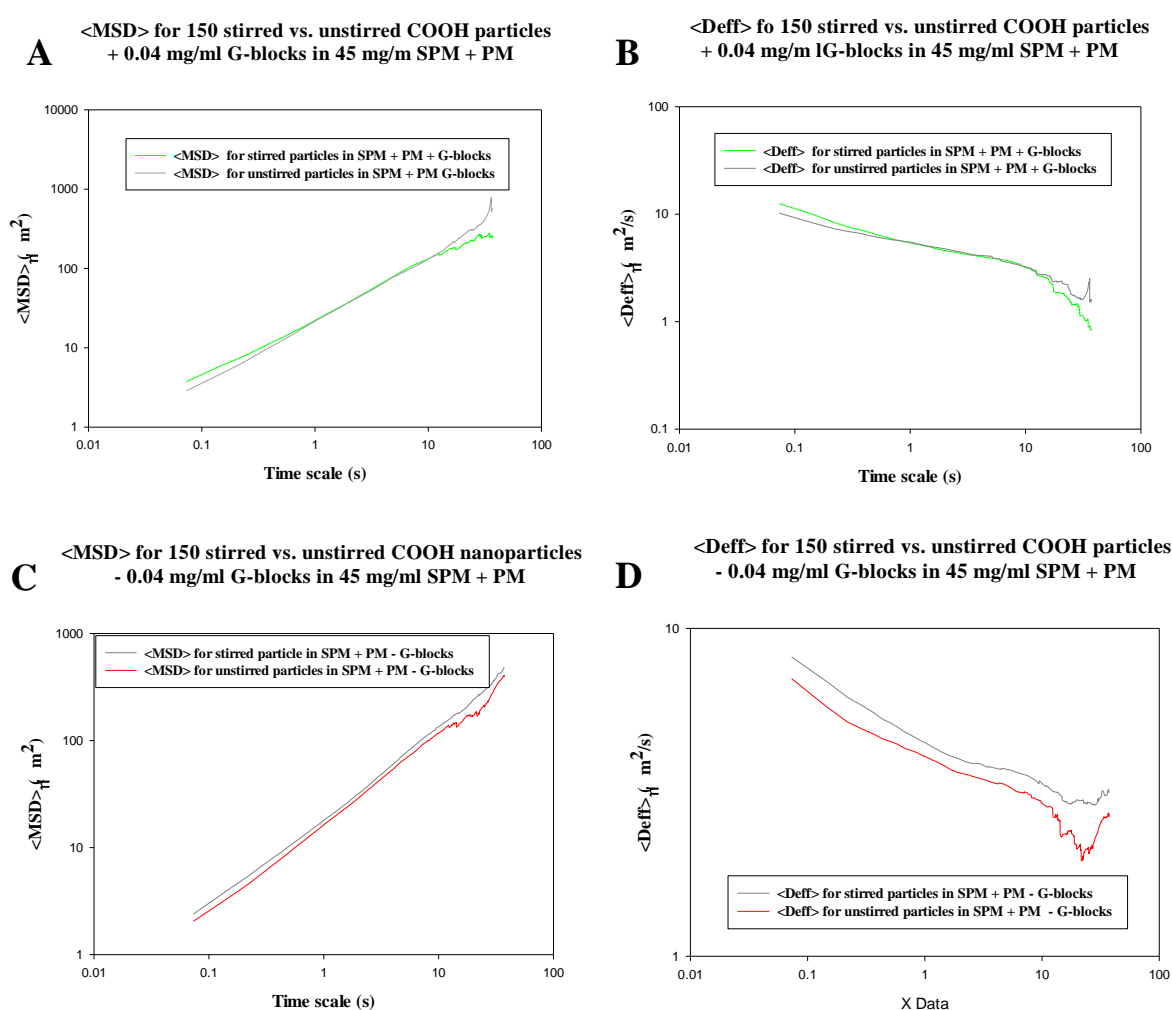


Figure 3.11: Study the method of beads addition on carboxylate nanoparticle mobility in sigma pig mucus + polymeric mucus. Panels A-C and B-D present mean MSD ($\langle \text{MSD} \rangle$) and mean Deff ($\langle \text{Deff} \rangle$) values for stirred versus unstirred particles for 150 carboxylate nanoparticle trajectories with and without 0.04 mg/ml G-blocks treatment in 45 mg/ml polymeric mucus + sigma pig mucus (200 nm in diameter, obtained at 73-ms time intervals) (Data analysis are provided in Chapter 5, Figures 5.10, Figure 5.13, Figure 5.16 and Figure 5.19).



3.8.2 Discussion

Interestingly whilst the results for both matrix A and matrix B for stirred vs. unstirred could not be considered significant based on the exclusion criteria the means MSD plus Deff from matrix B were much more similar than those from matrix A.

It can be reasoned that, similarity between MSD and Deff plot for carboxylate nanoparticles in mucus matrix B is due to ability of mucus matrix B to re-built its network much faster than mucus matrix A, and hence show the functional importance of mucus rheology.



3.9 Alteration mechanisms to mucus barrier function and enhancing uptake of therapeutic in drug delivery system

As earlier pointed out, mucus glycoprotein is highly negatively charged and contains hydrophilic glycosylated protein domains. In the presence of charged nanoparticle (negative or positive surface charge) as well as G-blocks polymer, mucus mesh pores can be modified and promote nanoparticles to cross the mucosal barrier.

G-blocks polymer can alter the mucus matrix through two mechanisms:

- Coating the nanoparticles and mucus matrix with G-blocks alter the interaction between nanoparticle and mucus mesh
- Alter matrix architecture (Figure 3.12).

Referring to Figure 3.12, in the absence of G-blocks polymer nanoparticles were trapped in mucin fibers (A), coating nanoparticles with G-blocks polymer could decrease nanoparticle-mucus interaction and caused nanoparticle to diffuse through mucus mesh (B), and treated mucus network with G-blocks could alter its architecture and nanoparticles could cross the mucus barrier and (C).

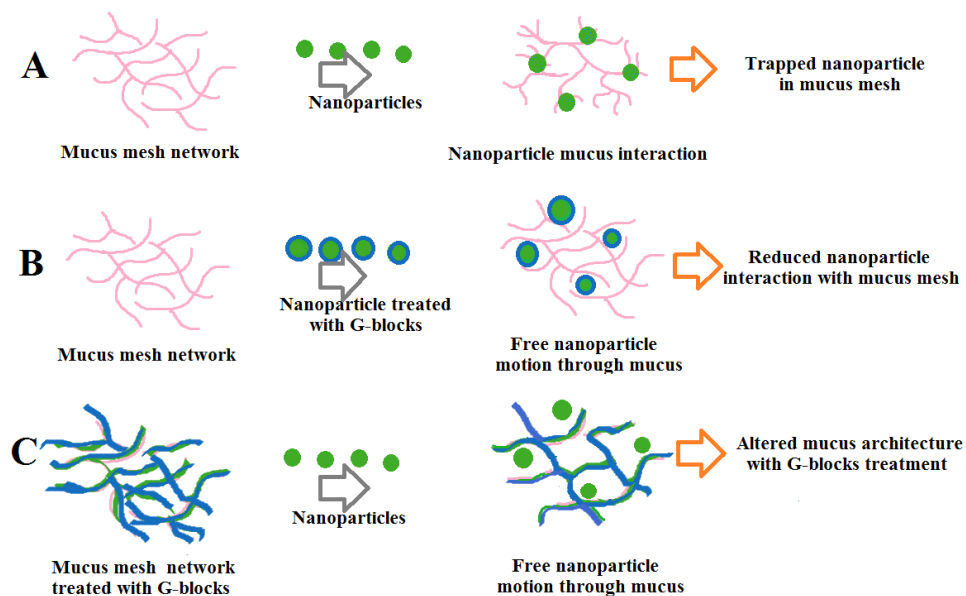


Figure 3.12: Schematic illustration of nanoparticles interaction in mucus network, A) nanoparticles interaction in mucus mesh without G-blocks treatment, B) treated nanoparticles with 0.04 mg/ml G-blocks and were stirred gently in mucus matrix, and C) nanoparticle motion in mucus matrix contained 0.04 mg/ml G-blocks (G-blocks shown in blue).



Mucus barrier components, challenges for nanoscale drug delivery

The previous studies considered situation (A), where particle were mixed with G-blocks before being added to the mucus.

To study the effects of G-blocks on both mucus architecture and nanoparticle in more detail the collective study undertaken to consider;

1. The effect of adding G-blocks to the mucus compared to adding G-blocks to the particles.
2. Testing amine nanoparticle together with carboxylate nanoparticles which have positive and negative surface charges respectively is critical to see the effect of surface chemistry in mucus matrix.

In this study 1 matrix was chosen (45 mg/ml of sigma pig mucus), because this removes a potential variation of the two mucin types.

Additionally, nanoparticle suspensions were stirred into the mucus, because the matrices were subjected to mixture with the addition of G-blocks (stirred → nanoparticle suspensions were mixed in mucus).



3.10 Transport of carboxylate-modified nanoparticles in sigma pig mucus mixed with G-blocks

The transport of carboxylate-modified nanoparticles was investigated in mucus samples using multiple particle tracking technique (MPT).

The following samples were studied,

- Carboxylate nanoparticles motion in 45 mg/ml sigma pig mucus without G-blocks treatment. (Data analysis is provided in Chapter 5, Figure 5.23, panels M, N, and O)
- Carboxylate nanoparticles motion in 45 mg/ml sigma pig mucus mixed with 0.04 mg/ml G-blocks. (Data analysis is provided in Chapter 5, Figure 5.22, panels A, B, and C)
- Carboxylate nanoparticles motion in 45 mg/ml sigma pig mucus mixed with 0.5 mg/ml G-blocks. (Data analysis is provided in Chapter 5, Figure 5.22, panels D, E, and F).

For all three screens above (1, 2, and 3), nanoparticle suspensions were gently stirred in mucus samples (Stirred → nanoparticle suspensions were mixed in mucus samples).

The mean MSD ($\langle \text{MSD} \rangle$) values (**A**) and mean Deff ($\langle \text{Deff} \rangle$) values (**B**) of 300 individual carboxylate-modified nanoparticles are presented in Figure 3.13. As can be seen from Figure 3.13 there are differences between mean MSD and mean Deff plots for carboxylate nanoparticles in the presence of G-blocks in mucus compared with $\langle \text{MSD} \rangle$ and $\langle \text{Deff} \rangle$ plots control of carboxylate nanoparticles in mucus with no G-blocks (MSD and Deff plots).

The $\langle \text{MSD} \rangle$ and $\langle \text{Deff} \rangle$ plots were greater for COOH nanoparticles in the presence of 0.04 mg/ml G-blocks in mucus. In contrast, $\langle \text{MSD} \rangle$ and $\langle \text{Deff} \rangle$ plots displayed a trend toward less movement for COOH nanoparticles in 45 mg/ml sigma pig mucus treated with 0.5 mg/ml G-blocks (green plot versus red plot) (Figure 3.13).

Interestingly, the differences between MSD and Deff plots were reduced at longer time scales for carboxylate nanoparticles in mucus sample treated with 0.5 mg/ml G-blocks and in mucus sample without G-blocks inside it (red and blue plots) (Figure 3.13).

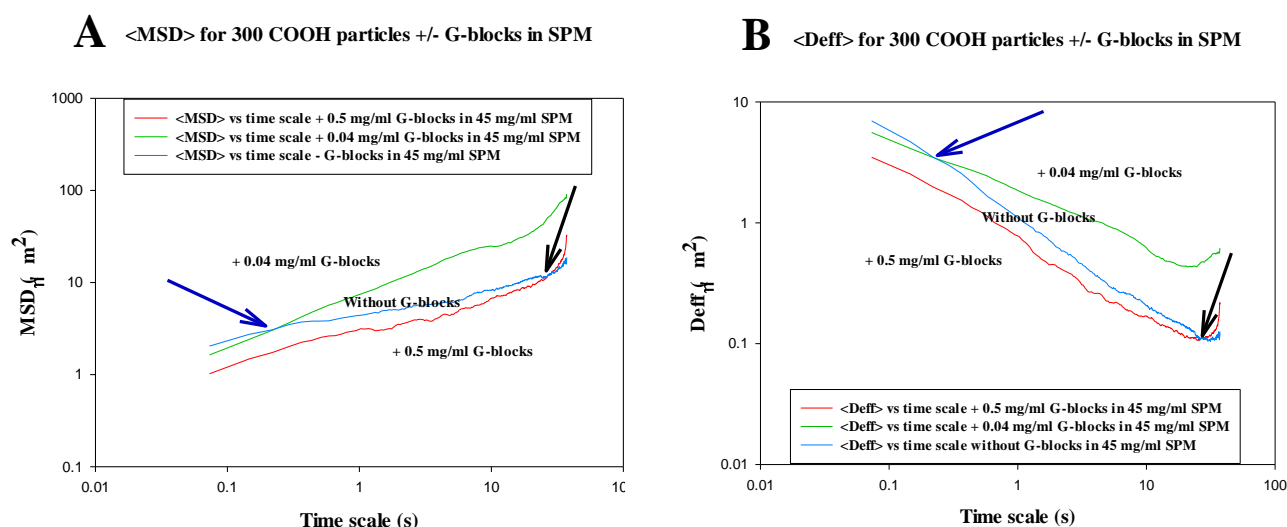


Figure 3.13: Transport of carboxylate nanoparticle in sigma pig mucus contains G-blocks. Ensemble $\langle \text{MSD} \rangle$ (A) and $\langle \text{Deff} \rangle$ (B) values of 300 COOH-modified nanoparticles in 45 mg/ml sigma pig mucus with no G-blocks treatment, in 45 mg/ml sigma pig mucus treated with 0.04 mg/ml G-blocks, and in 45 mg/ml sigma pig mucus treated with 0.5 mg/ml G-blocks obtained at 73-ms time interval (Figure 5.23, panels M, N, and O, Figure 5.22, panels A, B, and C, and Figure 5.22, panels D, E, and F).

*SPM= Sigma pig mucus, *PM= Polymeric mucus



3.10.1 Transport of carboxylate-modified nanoparticles treated with G-blocks in sigma pig mucus

The transport of carboxylate-modified nanoparticles was investigated in 45 mg/ml sigma pig mucus using multiple particle tracking (MPT).

The following samples were studied,

- Carboxylate nanoparticle suspensions were gently stirred in 45 mg/ml sigma pig mucus (stirred → nanoparticle suspensions were mixed in mucus). (Data analysis is provided in Chapter 5, Figure 5.23, panels M, N, and O).
- Carboxylate nanoparticle suspensions mixed with 0.04 mg/ml G-blocks and were stirred gently in 45 mg/ml sigma pig mucus (stirred → nanoparticle suspensions were mixed in mucus). (Data analysis is shown in Chapter 5, Figure 5.23, panels G, H, and I)
- Carboxylate nanoparticle suspensions mixed with 0.5 mg/ml G-blocks and were stirred gently in 45 mg/ml sigma pig mucus (stirred → nanoparticle suspensions mixed in mucus). (Data analysis is presented in Chapter 5, Figure 5.23, panels J, K, and L).

The averaged-mean square displacement ($\langle \text{MSD} \rangle$) values (a) and averaged-mean effective diffusivity ($\langle \text{Deff} \rangle$) values (b) of 300 individual carboxylate-modified nanoparticles are shown in Figure 3.14. As can be seen from Figure 3.14, there are slight differences between mean MSD and mean Deff plots for carboxylate nanoparticles treated with two G-blocks concentrations (0.04 and 0.5 mg/ml respectively) compared to carboxylate nanoparticles without G-blocks treatment in 45 mg/ml sigma pig mucus (red, blue, and green plots).

It is apparent from Figure 3.14 $\langle \text{MSD} \rangle$ and $\langle \text{Deff} \rangle$ plots displayed greater motion for COOH nanoparticles treated with 0.5 mg/ml G-blocks than those for COOH nanoparticles with 0.04 mg/ml G-blocks as well without G-blocks treatment (read plot versus green and blue plots) (Figure 3.14).

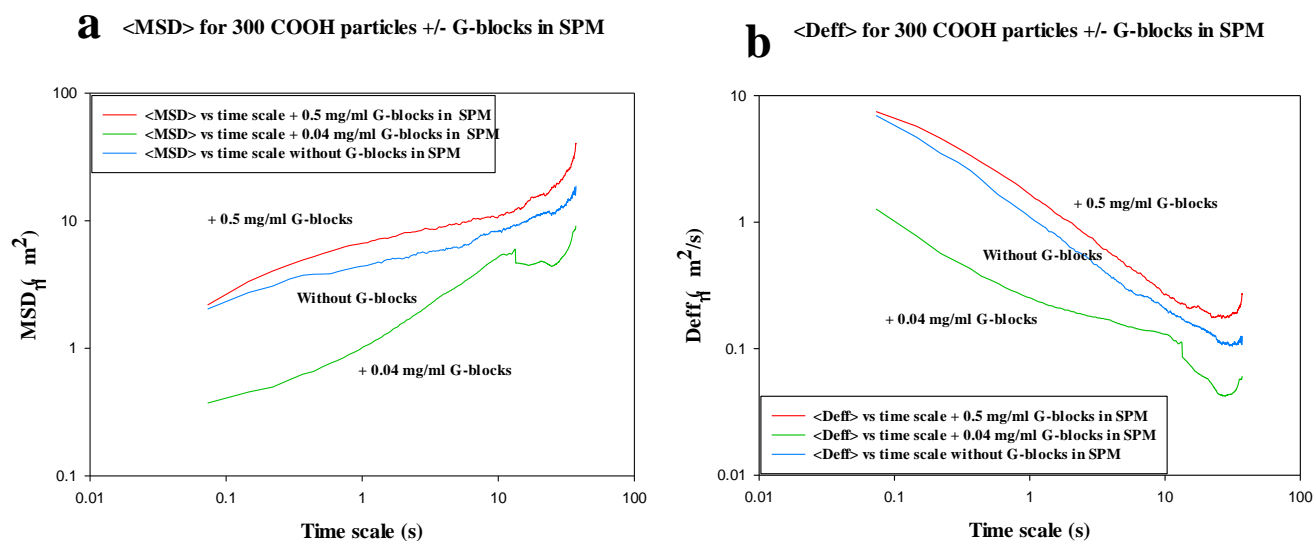


Figure 3.14: Transport of carboxylate nanoparticles treated with G-blocks in sigma pig mucus. Ensemble $\langle \text{MSD} \rangle$ (a) and $\langle \text{Deff} \rangle$ (b) values of 300 carboxylate-modified nanoparticles with no G-blocks treatment, treated with 0.04 mg/ml G-blocks, and treated with 0.5 mg/ml G-blocks in 45 mg/ml sigma pig mucus obtained at 73-ms time interval (Data analysis are shown in Chapter 5, Figure 5.23, panels M, N, and O, Figure 5.23, panels G, H, and I, and Figure 5.23, panels J, K, and L).

3.10.1.2 Discussion

Comparing with section 3.10, Figure 3.13, it is somewhat surprising that the method of G-blocks addition makes such a difference to the results because both G-blocks and nanoparticles are negatively charged so it is not expected that G-blocks would interact strongly with the nanoparticle, and therefore it might be assumed that order of mixing would not have a significant effect at this stage it is unclear why there differences are seen.

Lai et al [41] reported that, polystyrene beads without PEGylated coating form polyvalent bonds with hydrophobic domain distributed along mucus fibers. In addition they found that, the rapid diffusion of PEGlyted nanoparticles is because of nanoparticles movement in low viscosity channels or pores within the mucus.

*SPM= Sigma pig mucus, *PM= Polymeric mucus



Mucus barrier components, challenges for nanoscale drug delivery

Benjamin S. Schuster [42] found that nanoparticles coated with PEG as large as 200 nm in diameter can diffuse faster in human respiratory mucus without lung diseases. They suggested that, PEG coating nanoparticle reduces particle adhesion to mucus matrix, and that lead to freely particle diffusion through mucus. The carboxylate particles showed sub diffusive motion which is similar with published studies [3,13, 41].

G-blocks altered particle mobility but it is not clear how.

There are several possible explanations for these results. A possible explanation would be that G-blocks alter porous structure of mucus network to more favorable for nanoparticles to traverse in. The alteration might be due to formation of covalent bound between G-blocks polymer and mucus fibers, making a new mucus matrix rearrangement which is easier to pass through.

Another possible explanation for this is that, the present of sodium salt (MES buffer) together with G-blocks, making mucus as electrolyte solution resulting in dissolution of mucus matrix and therefore, nanoparticle could penetrate in mucus network.

It is not clear why a low concentration of G-blocks would negatively influence particle mobility based on these ideas.

To investigate the effect of mixing order further amine nanoparticles were used. These particles have a positive surface charge and can be coated by G-blocks (negative charge). So the mixing order may be expected to alter the results.



3.11 Transport of amine-modified nanoparticles in sigma pig mucus mixed with G-blocks

To explore changes in the interaction between nanoparticles and mucus network in the presence of G-blocks, amine nanoparticles were used.

The following samples were studied,

- Amine nanoparticles were gently stirred in 45 mg/ml sigma pig mucus (Stirred → nanoparticle suspensions mixed in mucus sample) (Data analysis is provided in Chapter 5, Figure 5.25, panels B, C, and D)
- Amine nanoparticles were gently stirred in 45 mg/ml sigma pig mucus mixed with 0.04 mg/ml G-blocks (Stirred → nanoparticle suspensions mixed in mucus sample) (Data analysis is provided in Chapter 5, Figure 5.24, panels V, W, and X)
- Amine nanoparticles were gently stirred in 45 mg/ml sigma pig mucus mixed with 0.5 mg/ml G-blocks (Stirred → nanoparticle suspensions mixed in mucus sample) (Data analysis is provided in Chapter 5, Figure 5.24, panels Y, Z, and A).

Figure 3.15 presents the results of the ensemble averaged-mean square displacement ($\langle \text{MSD} \rangle$) (C) and averaged effective diffusivity ($\langle \text{Deff} \rangle$) (D) values over 300 amine-modified nanoparticles in 45 mg/ml sigma pig mucus.

There was a significant difference between mean MSD ($\langle \text{MSD} \rangle$) and mean Deff ($\langle \text{Deff} \rangle$) of amine nanoparticles in 45 mg/ml sigma pig mucus mixed with 0.5 mg/ml and 0.04 mg/ml of G-blocks respectively.

Amine nanoparticles showed sub diffusive $\langle \text{MSD} \rangle$ and $\langle \text{Deff} \rangle$ plots in sigma pig mucus mixed with 0.04 mg/ml G-blocks and 0.5 mg/ml G-blocks respectively (Green and black plots) (Figure 3.15 D).

Amine nanoparticles displayed greater Deff plot in sigma pig mucus without G-blocks treatment at short time scale, however, at longer time scale deff plot showed downward trend, and hence less motion of amine nanoparticles (blue plot) (Figure 3.15 D).

A shift toward more diffusive motion acquired in mild time scales for amine nanoparticles in sigma pig mucus mixed with 0.04 mg/ml G-blocks (green plot) (Figure 3.15 D).

*SPM= Sigma pig mucus, *PM= Polymeric mucus

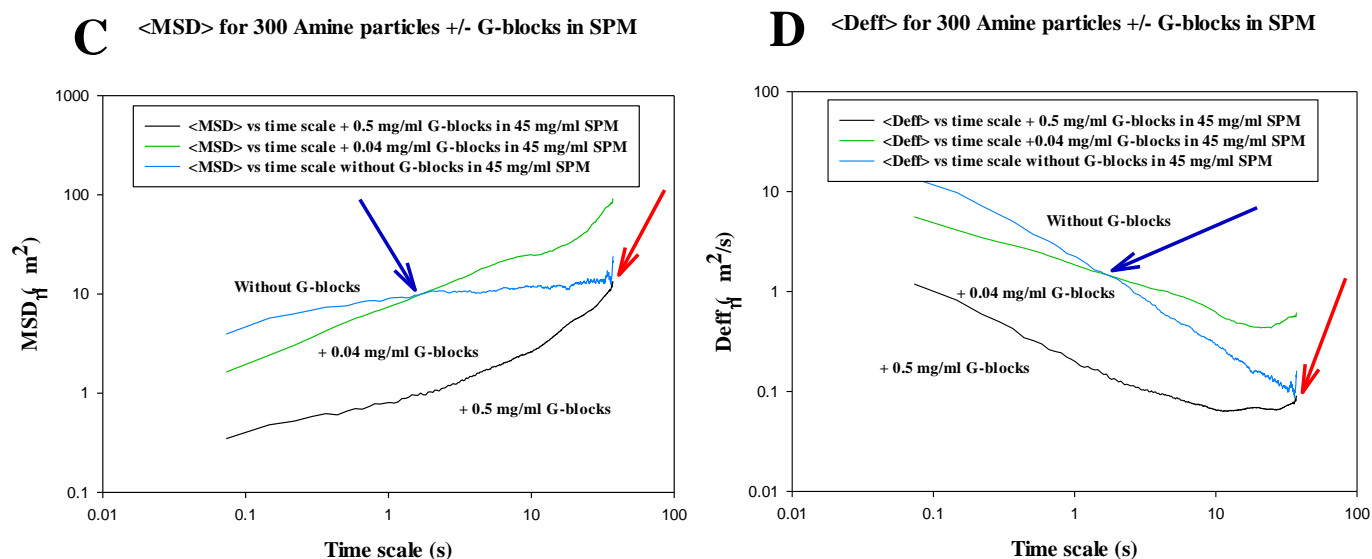


Figure 3.15: Transport of amine nanoparticle in sigma pig mucus contains G-blocks. Ensemble $\langle \text{MSD} \rangle$ (C) and $\langle \text{Deff} \rangle$ (D) values of 300 Amine-modified nanoparticles in 45 mg/ml sigma pig mucus with no G-blocks treatment, in 45 mg/ml sigma pig mucus treated with 0.04 mg/ml G-blocks, and in 45 mg/ml sigma pig mucus treated with 0.5 mg/ml G-blocks obtained at 73-ms time interval (Data analysis are provided in Chapter 5, Figure 5.25, panels B, C, D, Figure 5.24, panels P, Q, and R, and Figure 5.24, panels S, T, and T).



3.11.1 Discussion

Amine particles without G-blocks treatment showed MSD curve flattens out with increased time scale indicates that over a certain time scale nanoparticle are not moving further. Treated amine particles with lower concentration of G-blocks (0.04 mg/ml) exhibit a significant motion improvement at longer time scale.

Treated amine particles with higher concentration of G-blocks (0.5 mg/ml) exhibit a slower trend toward motion improvement. Amine particles displayed sub diffusive mobility by treating with both G-blocks concentrations (0.04 and 0.5 mg/ml G-blocks).

This finding lead to our hypothesis that, the amine nanoparticles were trapped in electrostatic interaction at short time scale, but the effect reduced at longer time scales due to the presence of G-blocks in mucus network, resulting in less hindered nanoparticles at longer time scales.



3.11.2 Transport of amine-modified nanoparticles treated with G-blocks in sigma pig mucus

The motion of amine-modified nanoparticles treated with 0.04 and 0.5 mg/ml G-blocks were studied individually and compared to amine nanoparticles without G-blocks treatment in 45 mg/ml sigma pig mucus

Therefore, the following samples were studied,

- Amine nanoparticle suspensions were gently stirred in 45 mg/ml sigma pig mucus (stirred → nanoparticle suspensions mixed in mucus) (Data analysis is provided in Chapter 5, Figure 5.25, panels B, C, and D).
- Amine nanoparticle suspensions mixed with 0.04 mg/ml G-blocks and were stirred gently in 45 mg/ml sigma pig mucus (stirred → nanoparticle suspensions mixed in mucus) (Data analysis is shown in Chapter 5, Figure 5.25, panels V, W, and X)
- Amine nanoparticle suspensions mixed with 0.5 mg/ml G-blocks and were stirred gently in 45 mg/ml sigma pig mucus (stirred → nanoparticle suspensions mixed in mucus) (Data analysis is presented in Chapter 5, Figure 5.25, panels Y, Z, and A).

The analyzed averaged-mean square displacement $\langle \text{MSD} \rangle$ (c) and averaged-mean effective diffusivity $\langle \text{Deff} \rangle$ values (d) for 300 individual amine-modified nanoparticles are shown in Figure 3.16.

Amine nanoparticles showed greater sub diffusive movement at short time scales and hence higher MSD and Deff plots, however, this trend motion decreased at longer time scales (blue plot) (Figure 3.16).

Remarkably, treated amine nanoparticles with 0.04 mg/ml G-blocks results in a shift to better mobility at longer time scales as shown by MSD and Deff plots (green plot) (Figure 3.16 c and d). In contrast, treated amine nanoparticles with 0.5 mg/ml G-blocks exhibited the lowest MSD and Deff plots, and therefore less mobility (black plot) (Figure 3.16 c and d).

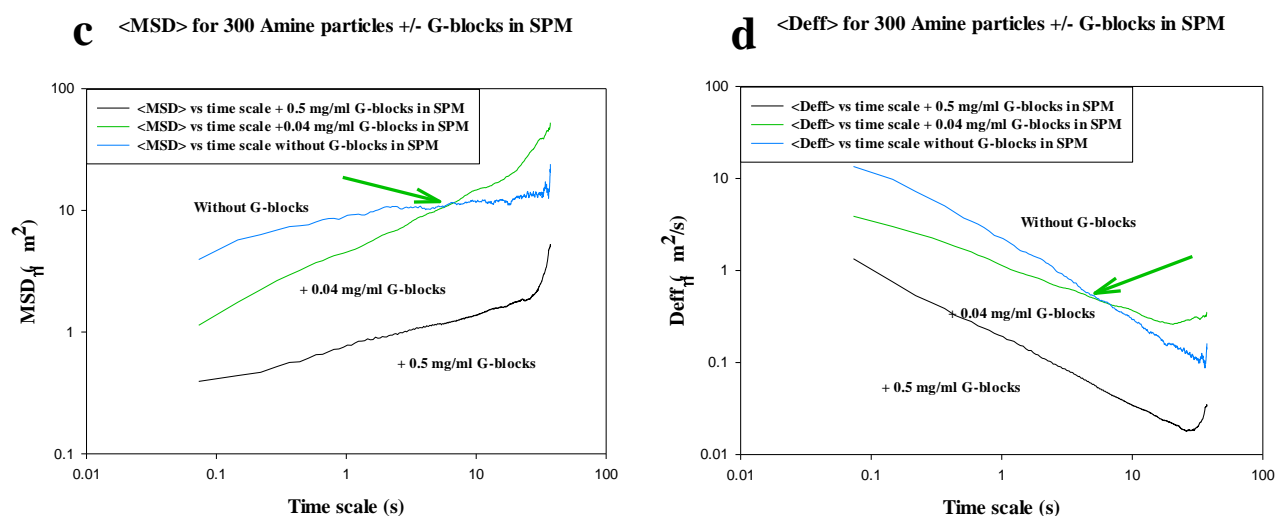


Figure 3.16: Transport of amine nanoparticles treated with G-blocks in sigma pig mucus. Ensemble $\langle \text{MSD} \rangle$ (c) and $\langle \text{Deff} \rangle$ (d) values of 300 amine-modified nanoparticles with no G-blocks treatment, treated with 0.04 mg/ml G-blocks, and treated with 0.5 mg/ml G-blocks in 45 mg/ml sigma pig mucus obtained at 73-ms time interval (This data analysis is presented in chapter 4 Figure 4.25, panels B, C, D, Figure 4.25, panels V, W, X, and Figure 4.25, panels B, C, D).

3.11.3 Discussion

Interestingly the mixing order did not alter the mobility of the particles to a large degree. However, the shift toward greater motion was observed at longer time scales (approximation 10 second) for amine nanoparticles treated with 0.04 mg/ml G-blocks.

Mucus treatment with G-blocks was more effective than nanoparticle treatment with G-blocks in both studies on amine and carboxylate nanoparticles.

This might indicate that G-blocks induced changes occur at a matrix level not a particle level. In both cases higher levels of G-blocks cause a significant decrease in particle motion. If G-blocks alter the matrix it is possible that high levels of G-blocks collapse all the structure and increase the mucus barrier.

*SPM= Sigma pig mucus, *PM= Polymeric mucus



Mucus barrier components, challenges for nanoscale drug delivery

If the G-blocks are mixed directly into the mucus matrix they can alter mucus architecture. If the G-blocks are mixed first with the nanoparticle then they must compete more with nanoparticle to the mucus matrix before they can alter mucus architecture.

Mucus barriers can be up to 450 μm for example in gastrointestinal tract or in respiratory tract with averaged size of 15 μm . Improvement in nanoparticle mobility at longer time scales (longer distances) could be relevant for drug delivery to engineer medical nanoparticles that can experience mucus barrier for a longer times, and hence release their pharmaceuticals through mucus matrix.

It can thus be suggested that, improvements in increasing nanoparticle motion can be achieved by G-blocks treatment. However, more research on this topic needs to be undertaken before identifying the mechanism implications of G-blocks in the mucus network.



3.12 The transport of amine nanoparticle vs. carboxylate nanoparticles in sigma pig mucus

To compare the transport of amine particle vs. carboxylate particles in 45 mg/ml sigma pig mucus, the averaged-mean square displacement ($\langle \text{MSD} \rangle$) and the averaged-mean square displacement ($\langle \text{Deff} \rangle$) of amine versus carboxylate nanoparticles were plotted as function of time scale and are present in Figure 3.17 A and B respectively.

Therefore, the following studies were taken into account,

- Amine nanoparticle suspensions were gently stirred in 45 mg/ml sigma pig mucus without G-blocks treatment (Stirred \rightarrow Nanoparticle suspensions were mixed into mucus samples). (Data analysis is presented in Chapter 5, Figure 5.25, panels B, C, and D).
- Carboxylate sigma pig mucus nanoparticle suspensions were gently stirred in 45 mg/ml sigma pig mucus without G-blocks treatment (Stirred \rightarrow Nanoparticle suspensions were mixed into mucus samples). (Data analysis is provided in Chapter 5, Figure 5.23, panels M, N, and O).

As can be seen from Figure 3.17 A and B, there are differences between amine particle's $\langle \text{MSD} \rangle$ and $\langle \text{Deff} \rangle$ plots vs. carboxylate particle's $\langle \text{MSD} \rangle$ and $\langle \text{Deff} \rangle$ plots over time scales. The amine particle displayed higher transport rate than carboxylate particle did.

The differences were reduced at longer time scales, and that were appeared by overlapped mean MSD ($\langle \text{MSD} \rangle$) and mean Deff ($\langle \text{Deff} \rangle$) plots for both amine and carboxylate particles (Figure 3.17 A and B).

Importantly, amine particle showed greater mobility at shorter timescales but more hindered at longer timescales, while, carboxylate particle motion were more linear over time scale and got closer to amine plot at the end of time scale (Figure 3.17 A and B).

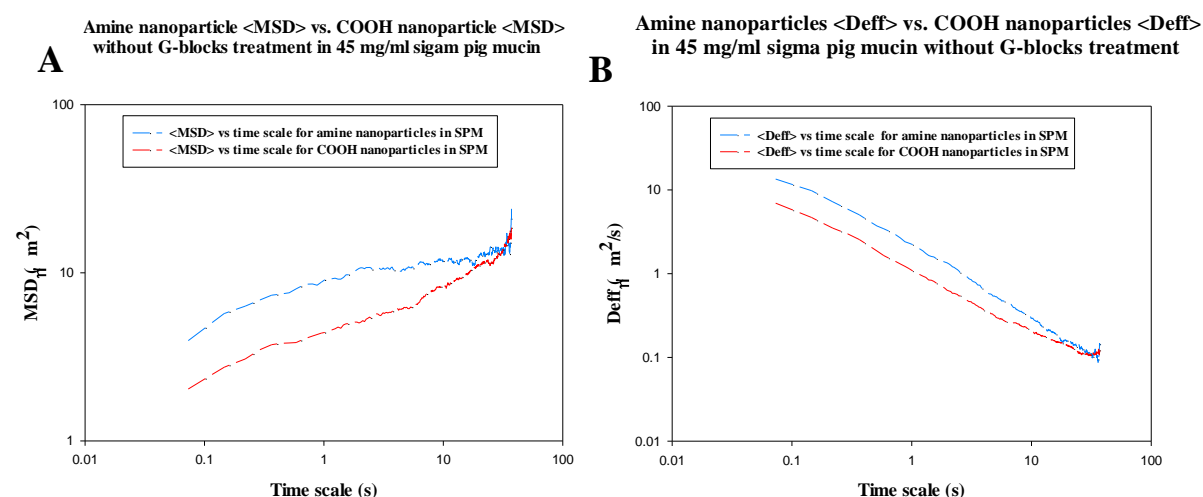


Figure 3.17: Transport of amine particle versus carboxylate particle in sigma pig mucus. (A) Ensemble-averaged mean square displacement ($\langle \text{MSD} \rangle$) and (B) effective diffusivity ($\langle \text{Deff} \rangle$) versus time scale for amine and carboxylate nanoparticles in 45 mg/ml sigma pig mucus contains. Data represents average MSD and Deff values for 100 nanoparticles were obtained at 73-ms time interval (Data analysis are shown in Chapter 5, Figure 5.25, panels B, C, and D and in Figure 5.23, panels M, N, and O).

3.12.1 Discussion

We observed that, nanoparticle motion in mucus matrix is dependent of their surface chemistry. This assumption is verified by gentle stirring amine and carboxylate nanoparticles in 45 mg/ml sigma pig mucus.

Wang and co-worker, 2011 characterized the influence of synthetic particles on the mucus mesh networks. They reported that, both particle concentration and surface chemistry are critical contributors in compromising the mucus barrier. They observed that, high concentration of mucoadhesive nanoparticles (MAP) can increase pore size in mucus through the crosslinking of bundling of mucus fibers, allowing greater penetration of foreign particles across mucus [3].

This study produced results which corroborate the findings of Wang and co-workers, that suggested the effect of surface chemistry as key factor for particle motion through mucus network [3].

Siguerdsson and et al showed that, size filtering and interaction filtering are two major mechanisms that may prevent nanoparticle to diffuse freely through mucus. Size filtering



Mucus barrier components, challenges for nanoscale drug delivery

mechanism could not be considered here, as all nanoparticles used in this study had the same size (200 nm in diameter). Interaction filtering stops nanoparticle transport based on nanoparticle surface chemistry and its interaction with mucus components. Therefore, nanoparticles with strong interaction within mucus components could not cross the mucus barrier and being trapped in mucus network, whereas, nanoparticle with weak degree of interaction within mucus components could pass the mucus elements without being trapped [7]. This finding by Siguerdsson et al corroborates with my ideas that is presented in Figure 3.12.

As shown in Figure 3.18 upon adding nanoparticle (here amine nanoparticles with positive surface charge) to mucus matrix, the architecture of mucus altered and forms bundles around particle, so particle would not move up stream the mucus and being trapped in mucus fibers. That would be due to ionic interaction between positively charged amine particle and negatively charged mucus network which lead particle to attach to mucus elements. Therefore, at longer time scales mucus become thicker and particles trap in mucus bundles, eventually particles will not able to move further in mucus mesh.

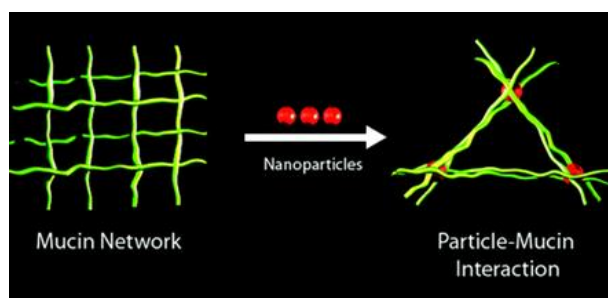


Figure 3.18: Schematic illustration of nanoparticle induced disruption of mucus [44].

Munkhopadhyay and colleagues reported that, polystyrene nanoparticles labeled with amine or COOH functional groups can assemble ordered structures on hydrophobic surfaces in liquid media [45].

Taken together, our results suggest that, nanoparticle motion can be influenced by labeling nanoparticle with functional groups like amine and carboxylate in mucus networks must likely due to formation of hydrophobic bond with negatively charge glycosylated segments along mucus fibers. Results suggest that G-blocks may reduce particle mobility at short time scale by interacting with this process.

*SPM= Sigma pig mucus, *PM= Polymeric mucus



3.13 Trajectory patterns of nanoparticle over time scales

Observations at short time scales show movement over short distances. Trajectory patterns at short time scales could reflect particle interaction with the matrix architecture or moving within network pores but are unlikely to show particles crossing matrix pores elements (Figure 3.19 A).

As long as time scales rise, nanoparticles face with greater barrier movement, being trapped in mucus fibers or wrapped around mucus bundles, result in impeding or vibrating nanoparticle motion in mucus network (Figure 3.19 B, blue and black arrows respectively).

In addition, nanoparticle could exhibit diffusive movement through mucus matrix over time scales if nanoparticle avoided mucoadhesive interaction in this biological system (Figure 3.19 B, orange arrow).

If the matrix architecture was more open such long time scale, particle diffusion would be more higher. Although, amine particle may alter the matrix architecture this did not result in diffusive motion at longer time scales. This may be because the particle plus mucin interact creates a matrix that is less penetrable over longer time scales.

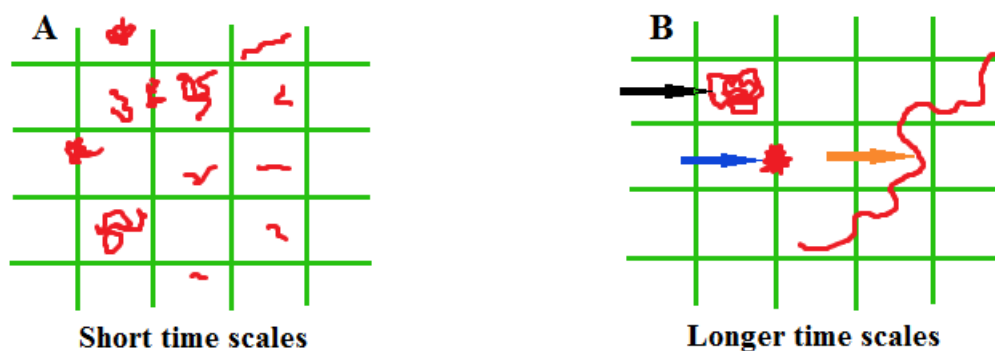


Figure 3.19: Representative trajectories of nanoparticles in mucus over time scale.



Chapter 4

Conclusion

Mucus barrier is complex and poses a crucial limit to nanoparticle diffusion. To overcome barrier properties of mucosal layer, nanoparticle needs to cross the mucus elements.

A key success in nanoparticle transport is to avoid adhesive interaction within mucus components. Results of this study indicate that, G-blocks have enough potential to engineer nanoparticle in order to traverse mucus matrix and reach targeted sites in the body.

Reduction of barrier properties of the mucus layer would be associated to G-blocks ability to alter mucus rheology in a favorable manner to uptake nanoparticle.

Whether the barrier decreases or increases by G-blocks depends on amount of G-blocks, Nanoparticle surface, addition of G-blocks in mucus matrix, as well as time scale.

Such an improvement in nanoparticle transport through mucus blanket can lead to innovative drug delivery system for site specific target drug release, in order to combat against respiratory disease particularly cystic fibrosis disorder.

The data presented here may be consistent with a model where G-blocks alter the mucus barrier architecture. This study must be repeated in ex vivo native matrices because it has been clearly shown here that the matrix components is critical to the barrier properties.

*SPM= Sigma pig mucus, *PM= Polymeric mucus



Chapter 5

Data analysis

5.1 The motion of carboxylate-modified nanoparticles in sigma pig mucus

To determine nanoparticles motion in sigma pig mucus, multiple particle tracking technique was used. The following sample was studied,

- Carboxylate nanoparticles were added on top left side of chamber contains 45 mg/ml sigma pig mucus (Unstirred) (Data analysis is shown in Figure 5.1).

Changes on x and y positions of nanoparticle trajectories were imaged by confocal microscope and were processed with Image J plugin software. The mean square displacement (MSD) was calculated and used to calculate effective diffusivity (D_{eff}).

The averaged-mean square displacement ($\langle D_{eff} \rangle$) and average effective diffusivity ($\langle D_{eff} \rangle$) are presented in Figure 5.1. As can be seen from Figure 5.1, unstirred COOH nanoparticles show sub-diffusive mobility in 45 mg/ml sigma pig mucus.



Mucus barrier components, challenges for nanoscale drug delivery

Three replicate experiments were conducted at the same condition. There was a large variation in the individual particle trajectories and therefore MSD and Deff values which resulted in variability in the mean MSD and Deff values for 3 replicates.

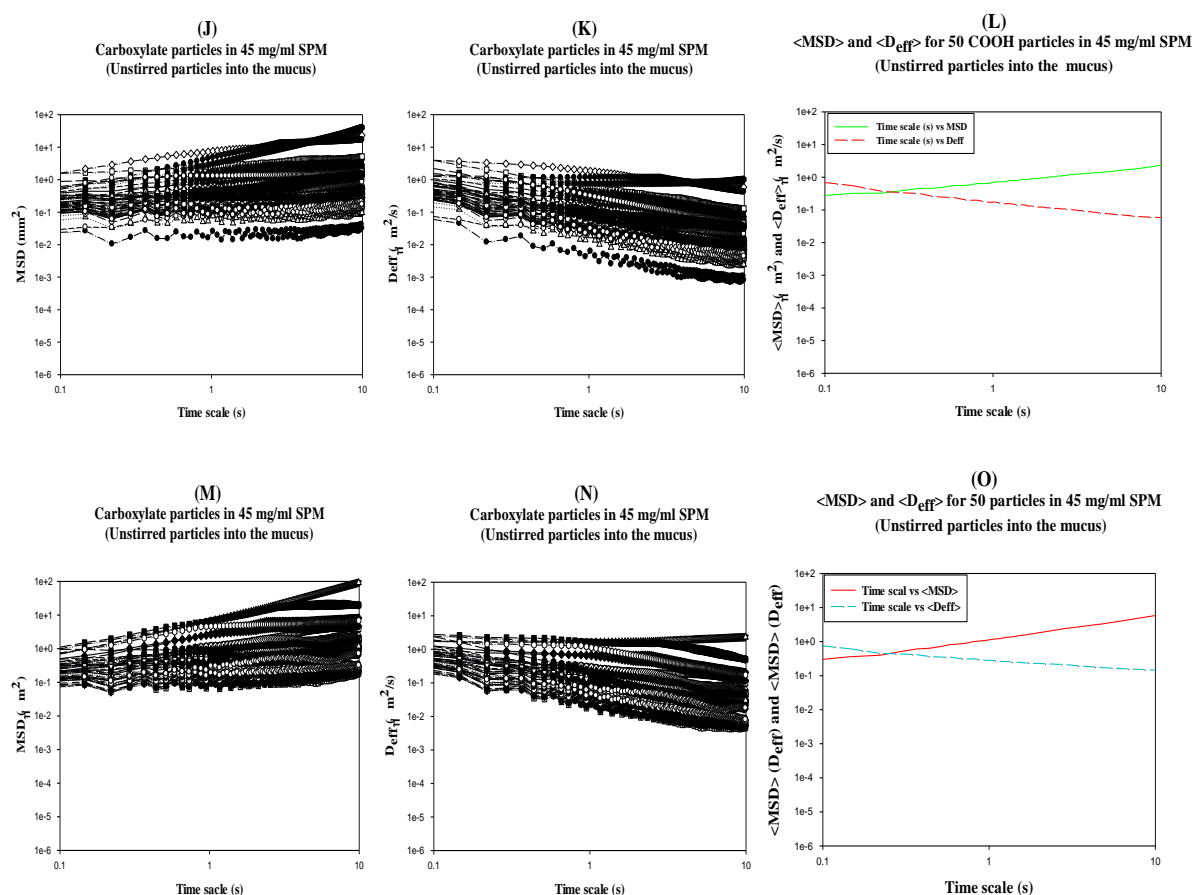


Figure 5.1: The motion of unstirred carboxylate nanoparticle in sigma pig mucus. Duplicate ensemble mean square displacement (MSD) (J, M), effective diffusivity (K, N), and mean MSD (MSD) (solid line) plus mean (Deff) (dashed line) (L, O) for 50 unstirred COOH-modified nanoparticles in 45 mg/ml sigma pig mucus.

*SPM= Sigma pig mucus, *PM= Polymeric mucus



Mucus barrier components, challenges for nanoscale drug delivery

Figure 5.2 Provides duplicate mean MSD ($\langle \text{MSD} \rangle$) and mean Deff ($\langle \text{Deff} \rangle$) for 100 unstirred COOH-modified nanoparticles in 45 mg/ml sigma pig mucus by combing L and O panels from 5.1.

In order to quantify if results were representative, a set of exclusion criteria was applied over all triplicate results to determine if they could be considered as one data set (refer to Chapter 3, section 3.2, Exclusion criteria, page 47).

$\langle \text{MSD} \rangle$ and $\langle \text{D}_{\text{eff}} \rangle$ for 100 COOH particles in 45 mg/ml SPM (Unstirred particles into the mucus)

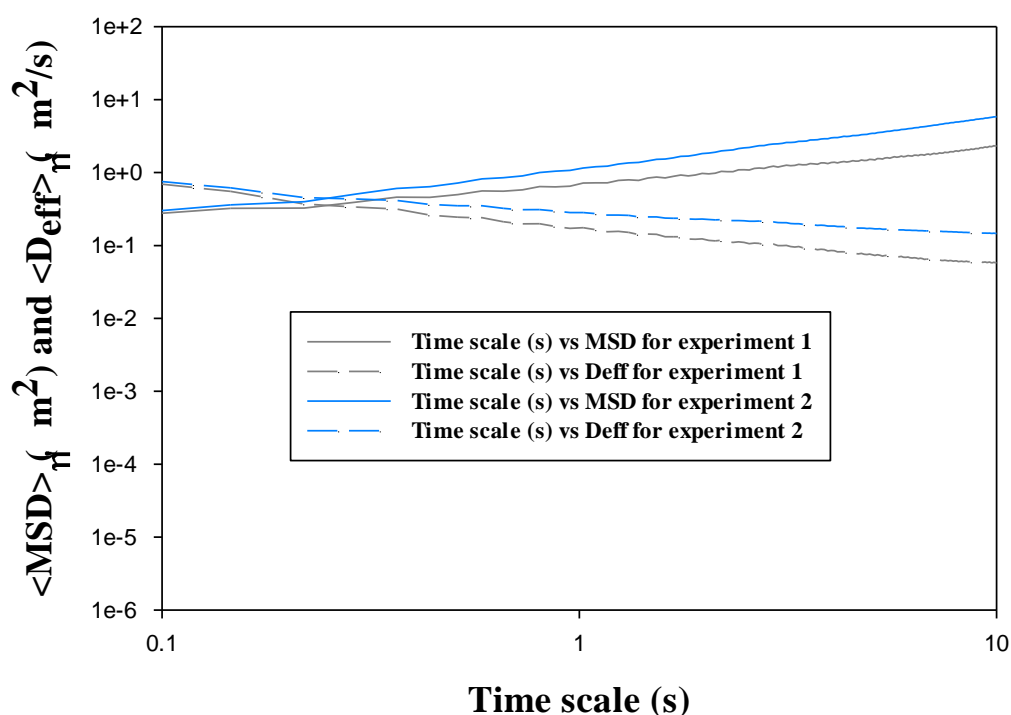


Figure 5.2: Duplicate combined MSD and Deff plots for unstirred carboxylate nanoparticle in sigma pig mucus. Ensemble-averaged mean square displacement $\langle \text{MSD} \rangle$ (solid lines) and mean effective diffusivities $\langle \text{Deff} \rangle$ (dashed lines) of 100 stirred carboxylate nanoparticles (200 nm in diameter) in 45 mg/ml sigma pig mucus provided by two replicated experiments (this figure is combined plot of L, and O from Figure 5.1 as function of time scale).



Mucus barrier components, challenges for nanoscale drug delivery

To quantify whether these two repeated mean MSD ($\langle \text{MSD} \rangle$) and mean Deff ($\langle \text{Deff} \rangle$) values can be treated as same data set, the maximum and minimum MSD and Deff values of 50 stirred COOH-modified nanoparticles were compared for all group of results (duplicate experiments) and are shown in Figure 5.3 A ,B.

Considering points 1, 2, and 3 of defined exclusion criteria, results are representative, and therefore these two replicates satisfy the applied criteria and can be treated as a single data set (See applied exclusion criteria in Chapter 3, section 3.2, Exclusion criteria, page 47).

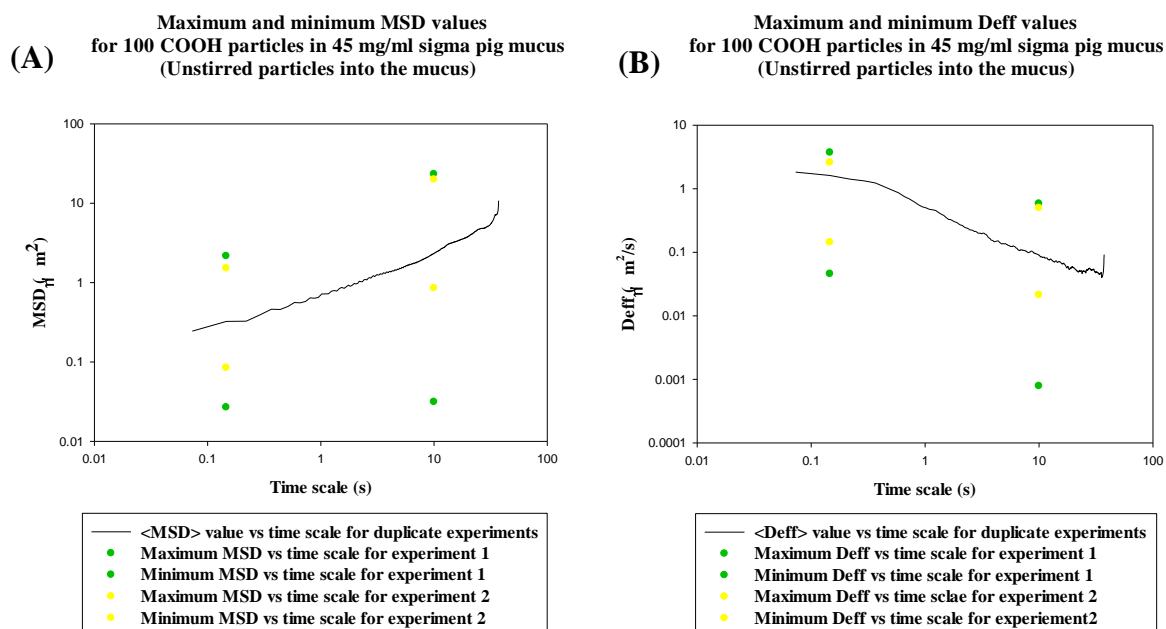


Figure 5.3: Maximum and minimum MSD and Deff values from duplicate experiments for unstirred carboxylate nanoparticle in sigma pig mucus. Panel A present max and min MSD values for 100 carboxylate particles in 45 mg/ml sigma pig mucus between 0.1 to 10 second time scales, and panel B show max and min Deffs values for 100 carboxylate particles in 45 mg/ml sigma pig mucus between 0.1 to 10 second time scales.

*SPM= Sigma pig mucus, *PM= Polymeric mucus



Mucus barrier components, challenges for nanoscale drug delivery

5.2 The effect of G-blocks treatment on carboxylate nanoparticles motion in sigma pig mucus by MPT

The motion of nanoparticles was investigated in sigma pig mucus using multiple particle tracking. Therefore, the following sample taken in account,

- Carboxylate nanoparticles treated with 0.04 mg/ml G-blocks and nanoparticle suspensions were gently stirred in 45 mg/ml sigma pig mucus (stirred → nanoparticle suspensions were mixed into mucus sample) (Data analysis is provided in Figure 5.4).

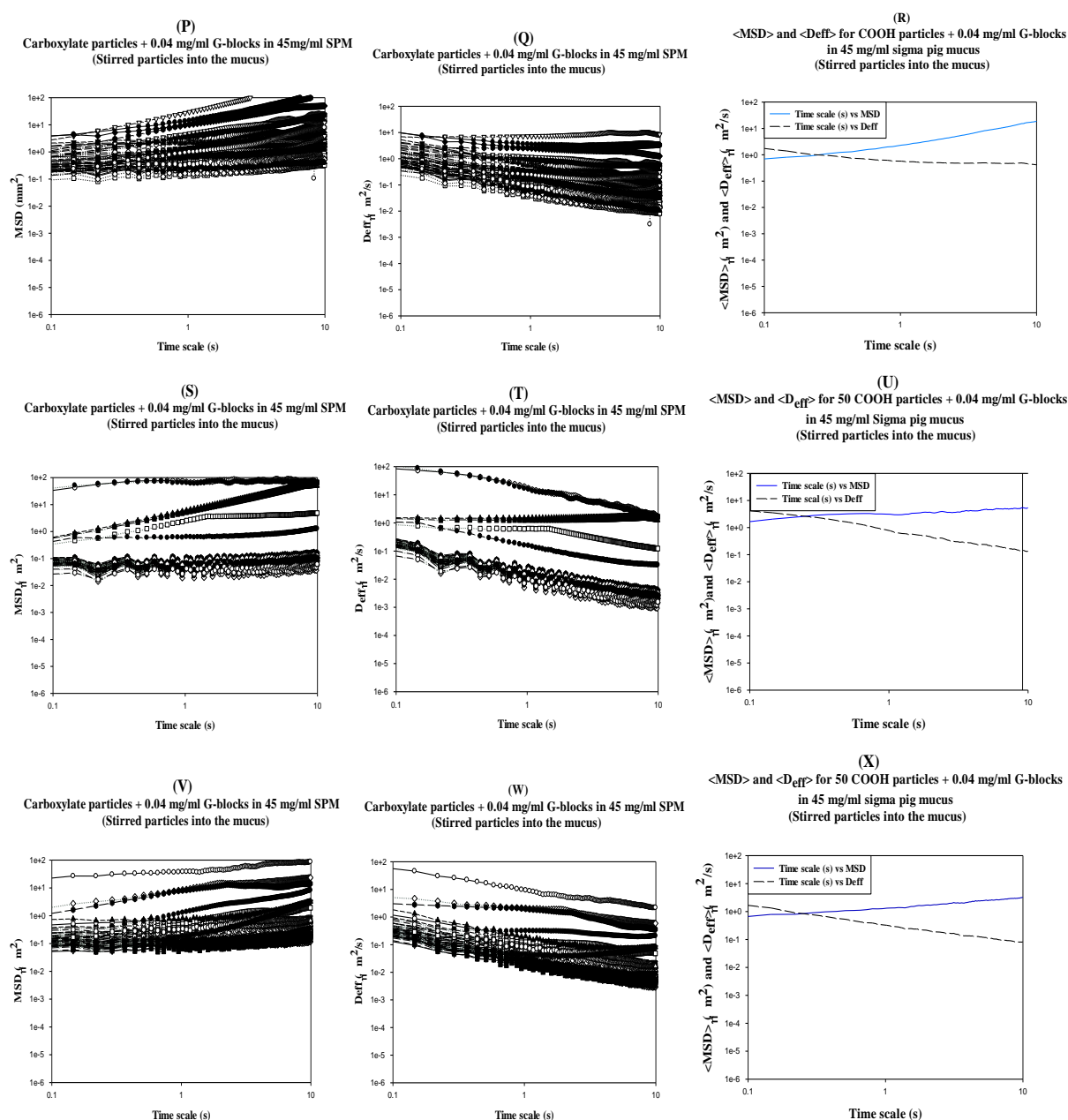


Figure 5.4: The motion of stirred carboxylate nanoparticle treated with G-blocks in sigma pig mucus. Triplicate ensemble mean square displacement (MSD) (P, S, V), effective diffusivity (Q, T, W), and mean MSD (MSD) (solid line) plus mean (Deff) (dashed line) (R, U, X) for 50 stirred carboxylate nanoparticles treated with 0.04 mg/ml G-blocks in 45 mg/ml sigma pig mucus.

*SPM= Sigma pig mucus, *PM= Polymeric mucus



Mucus barrier components, challenges for nanoscale drug delivery

Figure 5.5 Provides triplicate mean MSD ($\langle \text{MSD} \rangle$) and mean Deff ($\langle \text{Deff} \rangle$) for 150 stirred carboxylate-modified nanoparticles in 45 mg/ml sigma pig mucus by combining R, U, and X panels from the Figure 5.4.

In order to validate if results were representative, a set of exclusion criteria was applied over all triplicate results to determine if they could be considered as one data set (refer to Chapter 3, section 3.2, Exclusion criteria, page 47).

$\langle \text{MSD} \rangle$ and $\langle \text{Deff} \rangle$ for 150 COOH particles + 0.04 mg/ml G-blocks in 45 mg/ml Sigma pig mucus (Stirred particles into the mucus)

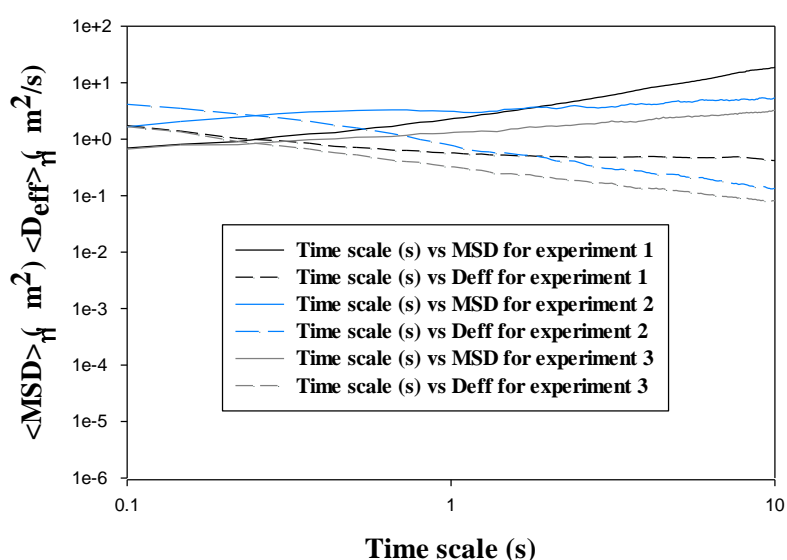


Figure 5.5: Triplicate combined MSD and Deff plots for stirred carboxylate nanoparticle treated with G-blocks in sigma pig mucus. Ensemble-averaged mean square displacement $\langle \text{MSD} \rangle$ (solid lines) and mean effective diffusivities $\langle \text{Deff} \rangle$ (dashed lines) of 150 carboxylate nanoparticles (200 nm in diameter) treated with 0.04 mg/ml G-blocks in 45 mg/ml sigma pig mucus provided by three replicated experiments (This Figure is Combined plot of R, U, and X from Figure 5.4 as function of time scale).



5.3 The comparison between triplicate maximum and minimum MSD and Deff values for 150 COOH-modified nanoparticles treated with G-blocks

To quantify whether these three repeated mean MSD ($\langle \text{MSD} \rangle$) and mean Deff ($\langle \text{Deff} \rangle$) values can be treated as same data set, the maximum and minimum MSD and Deff values of 50 stirred COOH-modified nanoparticles were compared for all group of results (triplicate experiments) and are shown in Figure 5.6 A ,B.

Considering points 1, 2, and 3 of defined exclusion criteria, results are representative, and therefore these three replicates satisfy the applied criteria and can be treated as a single data set (See applied exclusion criteria in Chapter 3, section 3.2, Exclusion criteria, page 47).

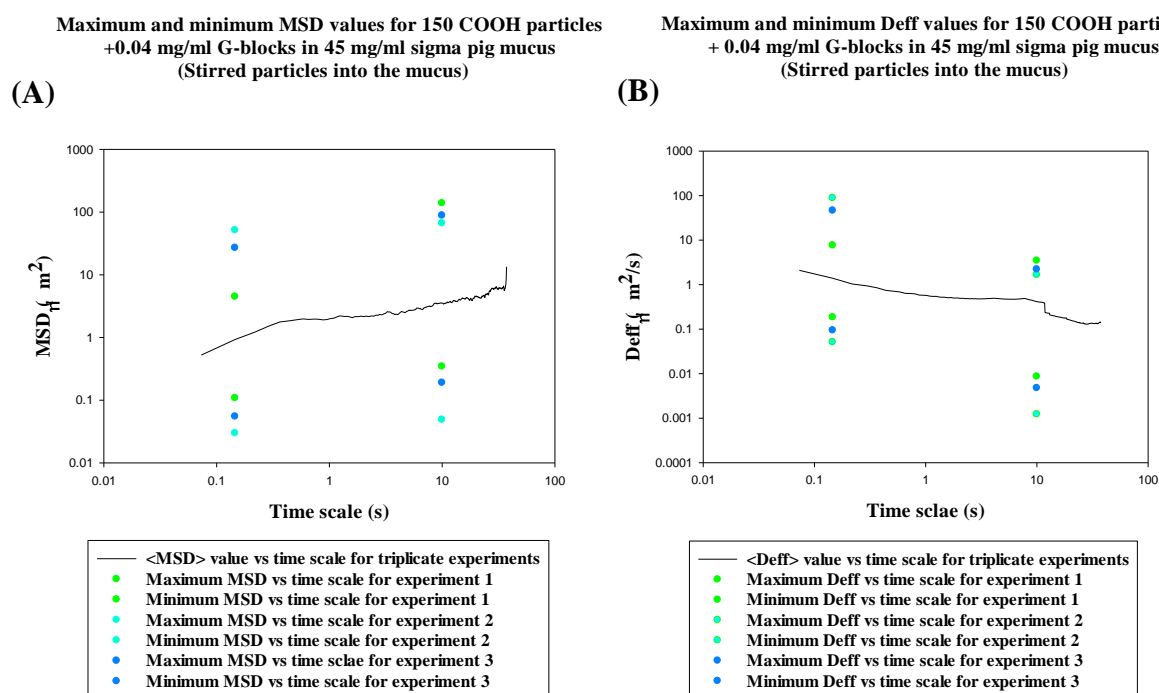


Figure 5.6: Maximum and minimum MSD and Deff values from triplicate experiments for stirred carboxylate nanoparticle treated with G-blocks in sigma pig mucus. Panel A presents maximum and minimum MSD values for 150 stirred carboxylate-modified nanoparticles treated with 0.04 mg/ml G-blocks in 45 mg/ml sigma pig mucus between 0.1 to 10 second time scales, and panel B shows mean maximum and minimum Deffs values for 150 carboxylate-modified nanoparticles in 45 mg/ml sigma pig mucus between 0.1 to 10 second time scales.

*SPM= Sigma pig mucus, *PM= Polymeric mucus



5.4 The transport of carboxylate nanoparticles in the presence of G-blocks in sigma pig mucus

The transport of carboxylate nanoparticles treated in sigma pig mucus was studied in the presence of G-blocks using multiple particle tracking technique. Therefore, the following sample was investigated,

- Carboxylate nanoparticles treated with 0.04 mg/ml G-blocks and were added gently on top left side of chamber contains 45 mg/ml sigma pig mucus (unstirred) (Data analysis is provided in Figure 5.7).

The mean square displacement (MSD) was calculated and used to calculate effective diffusivity (D_{eff}). The averaged-mean square displacement ($\langle D_{eff} \rangle$) and mean D_{eff} ($\langle D_{eff} \rangle$) values are shown in Figure 5.7. As can be seen from Figure 5.7, unstirred COOH nanoparticles which treated with 0.04 mg/ml G-blocks show sub-diffusive motion in 45 mg/ml sigma pig mucus.

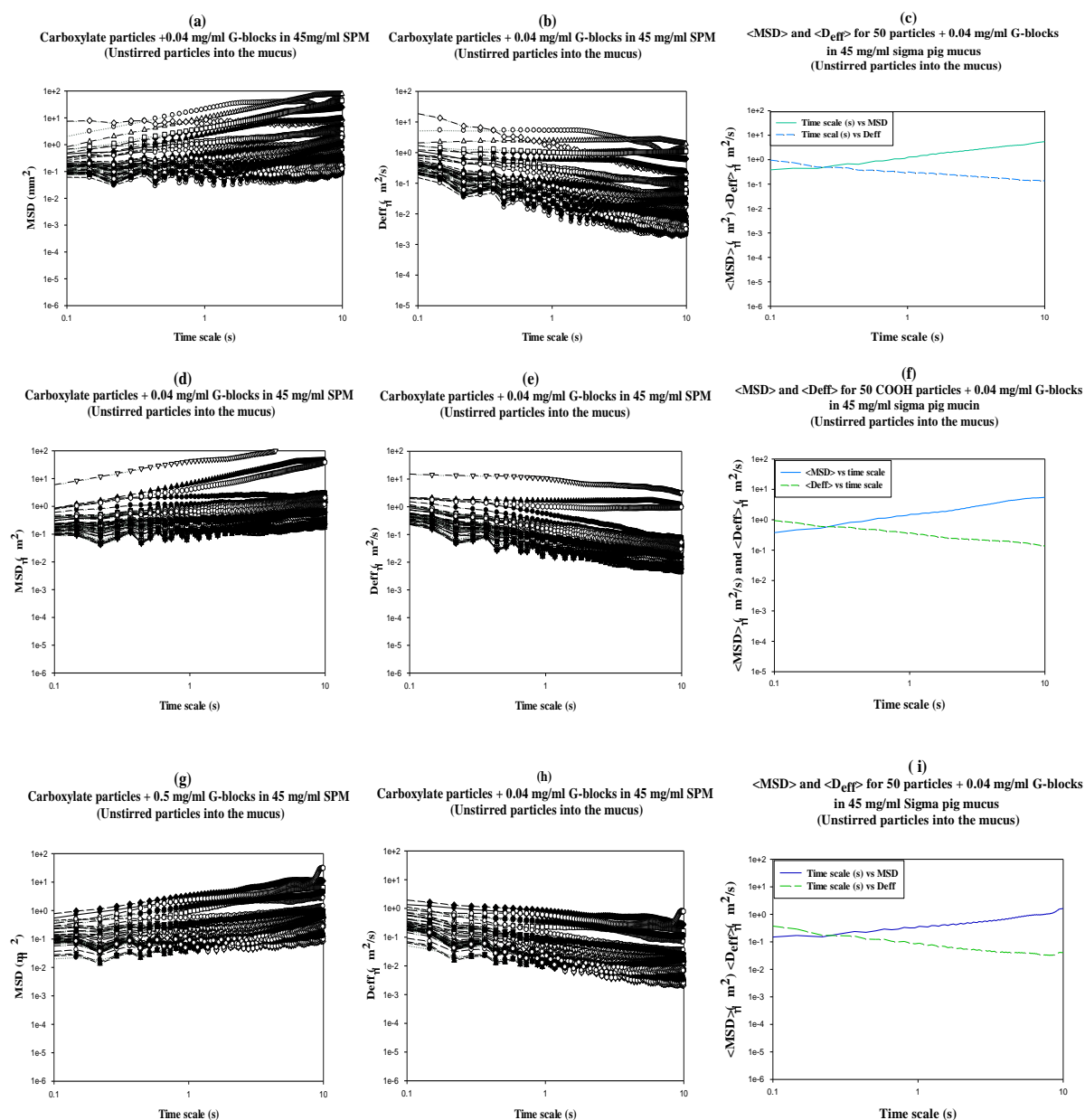


Figure 5.7: The motion of unstirred carboxylate nanoparticle treated with G-blocks in sigma pig mucus. Triplicate ensemble mean square displacement (MSD) (a, d, g), effective diffusivity (b, e, h), mean MSD (MSD) (solid line), and mean (Deff) (dashed line) (c, f, i) for 50 unstirred COOH-modified nanoparticles treated with 0.04 mg/ml G-blocks in 45 mg/ml sigma pig mucus.

*SPM= Sigma pig mucus, *PM= Polymeric mucus



Mucus barrier components, challenges for nanoscale drug delivery

Figure 5.8 provides triplicate mean MSD ($\langle \text{MSD} \rangle$) and mean Deff ($\langle \text{Deff} \rangle$) for 150 unstirred COOH-modified nanoparticles in 45 mg/ml sigma pig mucus by combining c, f, and i panels from Figure 5.7.

In order to quantify if results were representative, a set of exclusion criteria was applied over all triplicate results to determine if they could be considered as one data set (refer to Chapter 3, section 3.2, Exclusion criteria).

$\langle \text{MSD} \rangle$ and $\langle \text{Deff} \rangle$ for 150 COOH particles + 0.04 mg/ml G-blocks in 45 mg/ml sigma pig mucus
(Unstirred particles into the mucus)

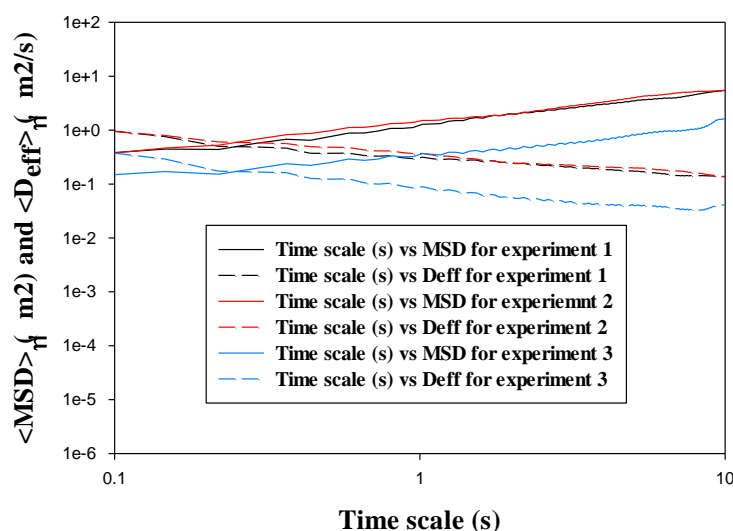


Figure 5.8: Triplicate combined MSD and Deff plots for unstirred carboxylate nanoparticle treated with G-blocks in sigma pig mucus. Ensemble-averaged mean square displacement $\langle \text{MSD} \rangle$ (solid lines) and mean effective diffusivities $\langle \text{Deff} \rangle$ (dashed lines) of 150 unstirred carboxylate particles (200 nm in diameter) in 45 mg/ml Sigma pig mucus provided by three replicated experiments (this figure is combined plot of c, f and i from Figure 5.7 as function of time scale).



Mucus barrier components, challenges for nanoscale drug delivery

To quantify whether these three repeats mean MSD ($\langle \text{MSD} \rangle$) and mean Deff ($\langle \text{Deff} \rangle$) values can be treated as same data set, we compared maximum and minimum MSD and Deff values of COOH-modified nanoparticles from the each triplicate experiment and are shown in Figure 5.9, A ,B.

Considering points 1, 2, and 3 of defined exclusion criteria, results are representative, and therefore these three replicates satisfy the applied criteria and can be treated as a single data set (See applied exclusion criteria in Chapter 3, section 3.2, Exclusion criteria, page 47).

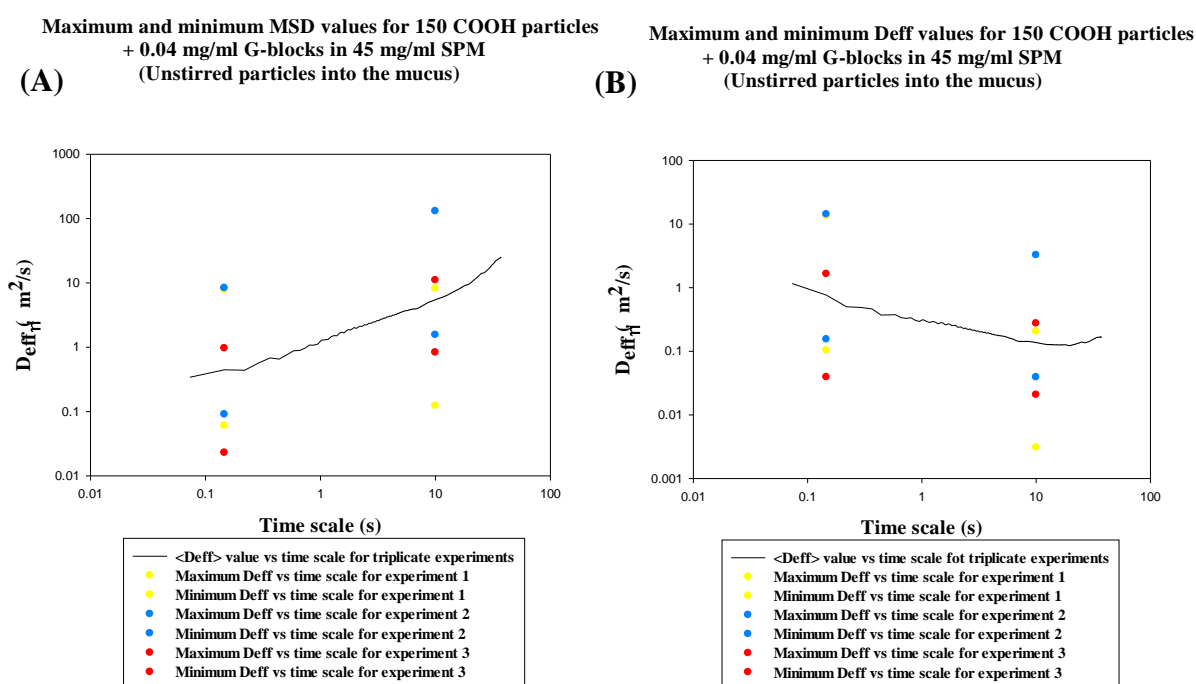


Figure 5.9: Maximum and minimum MSD and Deff values from triplicate experiments for unstirred carboxylate nanoparticle treated with G-blocks in sigma pig mucus. Panel A Presents maximum and minimum MSD values for 150 unstirred carboxylate nanoparticle in 45 mg/ml sigma pig mucus between 0.1 to 10 second time scales, Panel B shows maximum and minimum Deffs values for 150 unstirred carboxylate particles in 45 mg/ml sigma pig mucus between 0.1 to 10 second time scales.

*SPM= Sigma pig mucus, *PM= Polymeric mucus



5.5 The motion of carboxylate nanoparticles in sigma pig mucus + polymeric mucus by MPT

The motion of nanoparticles was investigated in sigma pig mucus + polymeric mucus using multiple particle tracking. Therefore, the following sample taken in account,

- Carboxylate nanoparticles were gently stirred in 45 mg/ml sigma pig mucus + polymeric mucus (30 and 15 mg/ml respectively) (stirred → nanoparticle suspensions were mixed into mucus sample) (Data analysis is provided in Figure 5.10).

The mean square displacement (MSD) was calculated and used to calculate effective diffusivity (D_{eff}). The averaged-mean square displacement ($\langle D_{eff} \rangle$) and mean D_{eff} ($\langle D_{eff} \rangle$) values are shown in Figure 5.10. As can be seen from Figure 5.10, unstirred COOH nanoparticles that show sub-diffusive motion in 45 mg/ml sigma pig mucus + polymeric mucus.



Mucus barrier components, challenges for nanoscale drug delivery

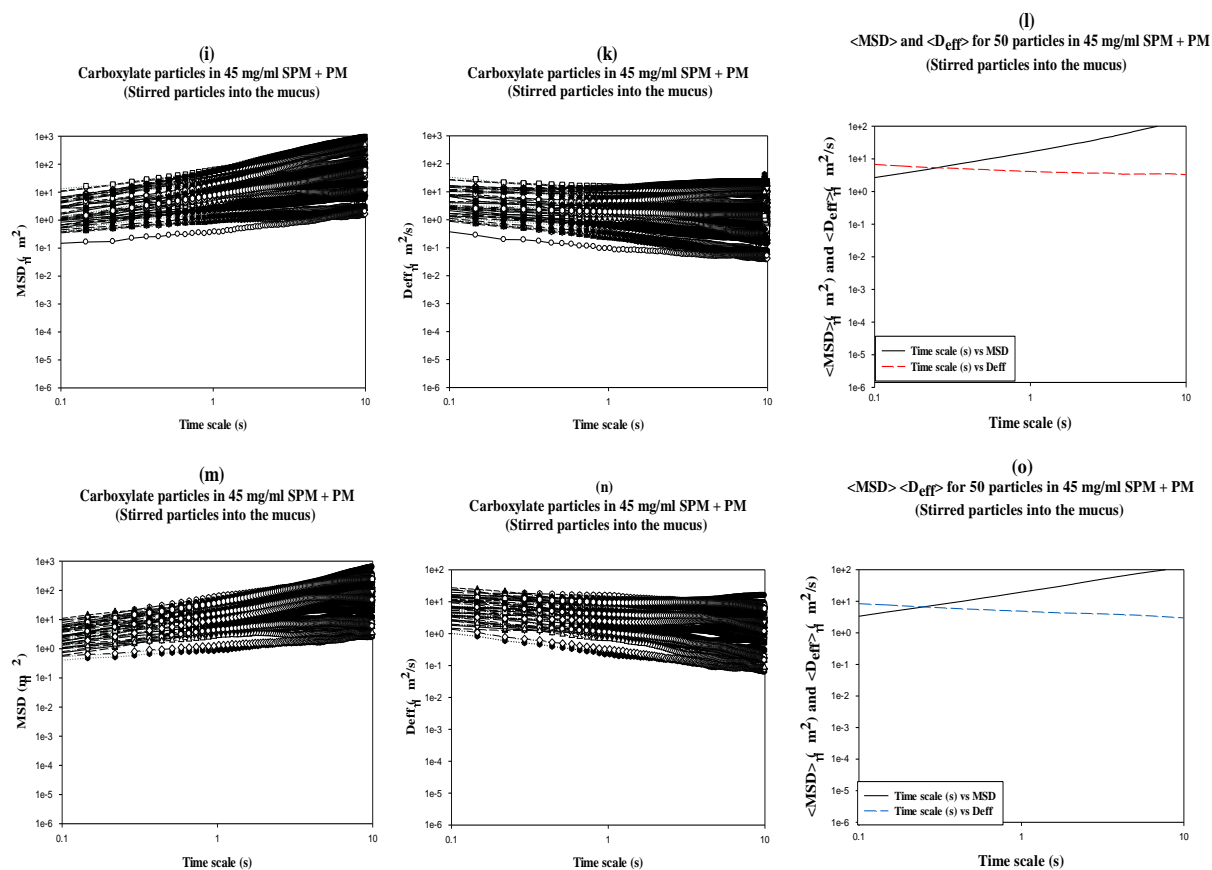


Figure 5.10: The motion of stirred carboxylate nanoparticle in sigma pig mucus + polymeric mucus. Duplicate ensemble mean square displacement (MSD) (j, m), effective diffusivity (k, n), mean MSD (MSD) (solid line) and mean (D_{eff}) (dashed line) (l, o) for 50 stirred COOH-modified nanoparticles in 45 mg/ml sigma pig mucus + polymeric mucus.

*SPM= Sigma pig mucus, *PM= Polymeric mucus



Mucus barrier components, challenges for nanoscale drug delivery

Figure 5.11 provides duplicate mean MSD ($\langle \text{MSD} \rangle$) and mean Deff ($\langle \text{Deff} \rangle$) for 100 stirred COOH-modified nanoparticles in 45 mg/ml sigma pig mucus + polymeric mucus by combining l and o and panels from the Figure 5.10.

In order to quantify if results were representative, a set of exclusion criteria was applied over all triplicate results to determine if they could be considered as one data set (refer to Chapter 3, section 3.2, Exclusion criteria).

$\langle \text{MSD} \rangle$ and $\langle \text{Deff} \rangle$ for 100 COOH particles in 45 mg/ml sigma pig mucus + polymeric mucus (Stirred particles into the mucus)

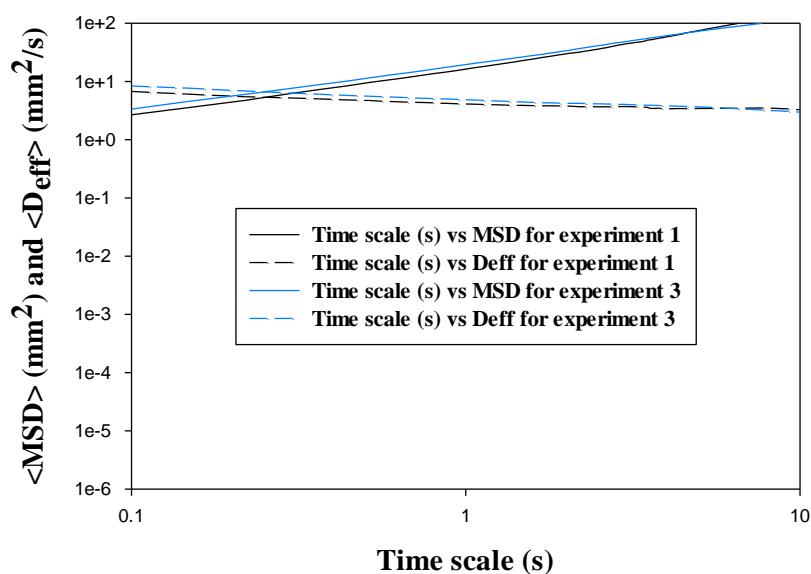


Figure 5.11: Duplicate combined MSD and Deff plots for stirred carboxylate nanoparticle in sigma pig mucus + polymeric mucus. Ensemble-averaged mean square displacement $\langle \text{MSD} \rangle$ (solid lines) and mean effective diffusivities $\langle \text{Deff} \rangle$ (dashed lines) of carboxylate-modified nanoparticles (200 nm in diameter) in 45 mg/ml sigma pig mucus + polymeric mucus provided by two replicated experiments (this Figure is combined plot of l, and o from Figure 5.10 as function of time scale).



Mucus barrier components, challenges for nanoscale drug delivery

To quantify whether these two repeats mean MSD ($\langle \text{MSD} \rangle$) and mean Deff ($\langle \text{Deff} \rangle$) values can be treated as same data set, we compared maximum and minimum MSD and Deff values of 50 stirred COOH-modified nanoparticles from triplicate experiments and are shown in Figure 5.12 A and B.

Considering points 1, 2, and 3 of defined exclusion criteria, results are representative, and therefore these two replicates satisfy the applied criteria and can be treated as a single data set (See applied exclusion criteria in Chapter 3, section 3.2, Exclusion criteria, page 47).

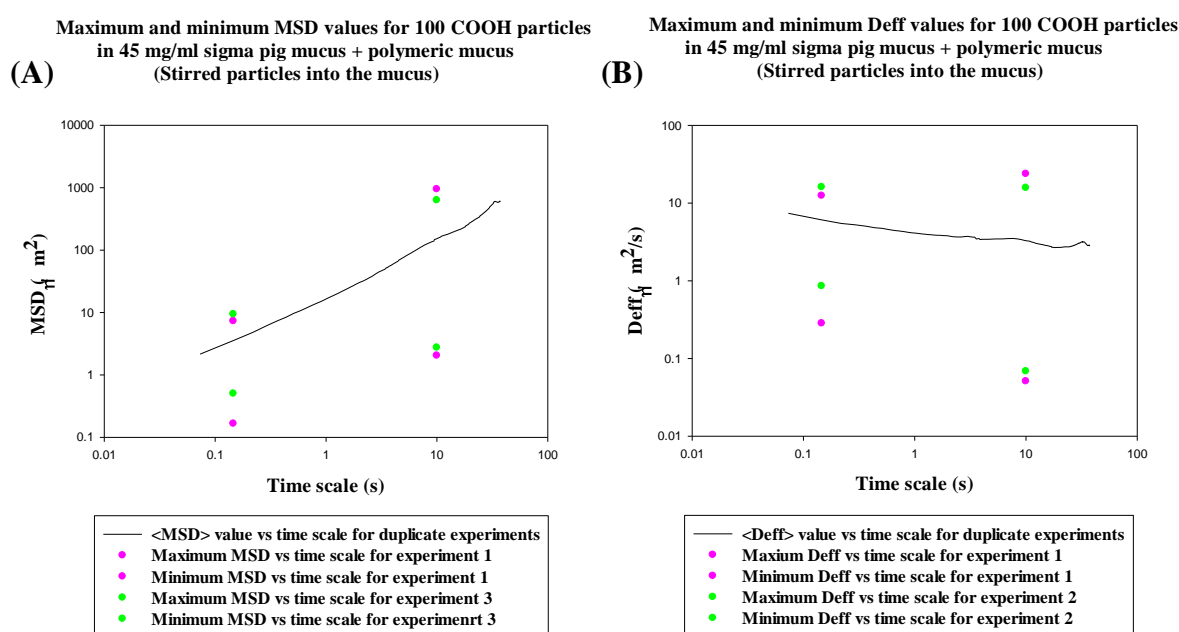


Figure 5.12: Maximum and minimum MSD and Deff values from duplicate experiments for stirred carboxylate in sigma pig mucus + polymeric mucus. Panel A presents maximum and minimum MSD values for 100 stirred carboxylate particles in 45 mg/ml sigma pig mucus + polymeric mucus between 0.1 to 10 second time scales, Panel B presents maximum and minimum Deffs values for 100 stirred carboxylate particles in 45 mg/ml sigma pig mucus + polymeric mucus between 0.1 to 10 second time scales.

*SPM= Sigma pig mucus, *PM= Polymeric mucus



5.6 The transport of carboxylate nanoparticles in sigma pig mucus + polymeric mucus

The motion of nanoparticles was investigated in sigma pig mucus + polymeric mucus using multiple particle tracking. Therefore, the following sample taken in account,

- Carboxylate nanoparticles were added on top left side of chamber contains 45 mg/ml sigma pig mucus + polymeric mucus (30 and 15 mg/ml respectively) (unstirred) (Data analysis is provided in Figure 5.10).

The mean square displacement (MSD) was calculated and used to calculate effective diffusivity (D_{eff}). The averaged-mean square displacement ($\langle D_{eff} \rangle$) and mean D_{eff} ($\langle D_{eff} \rangle$) values are shown in Figure 5.13. As can be seen from Figure 5.13, unstirred COOH nanoparticles that show sub-diffusive motion in 45 mg/ml sigma pig mucus + polymeric mucus.



Mucus barrier components, challenges for nanoscale drug delivery

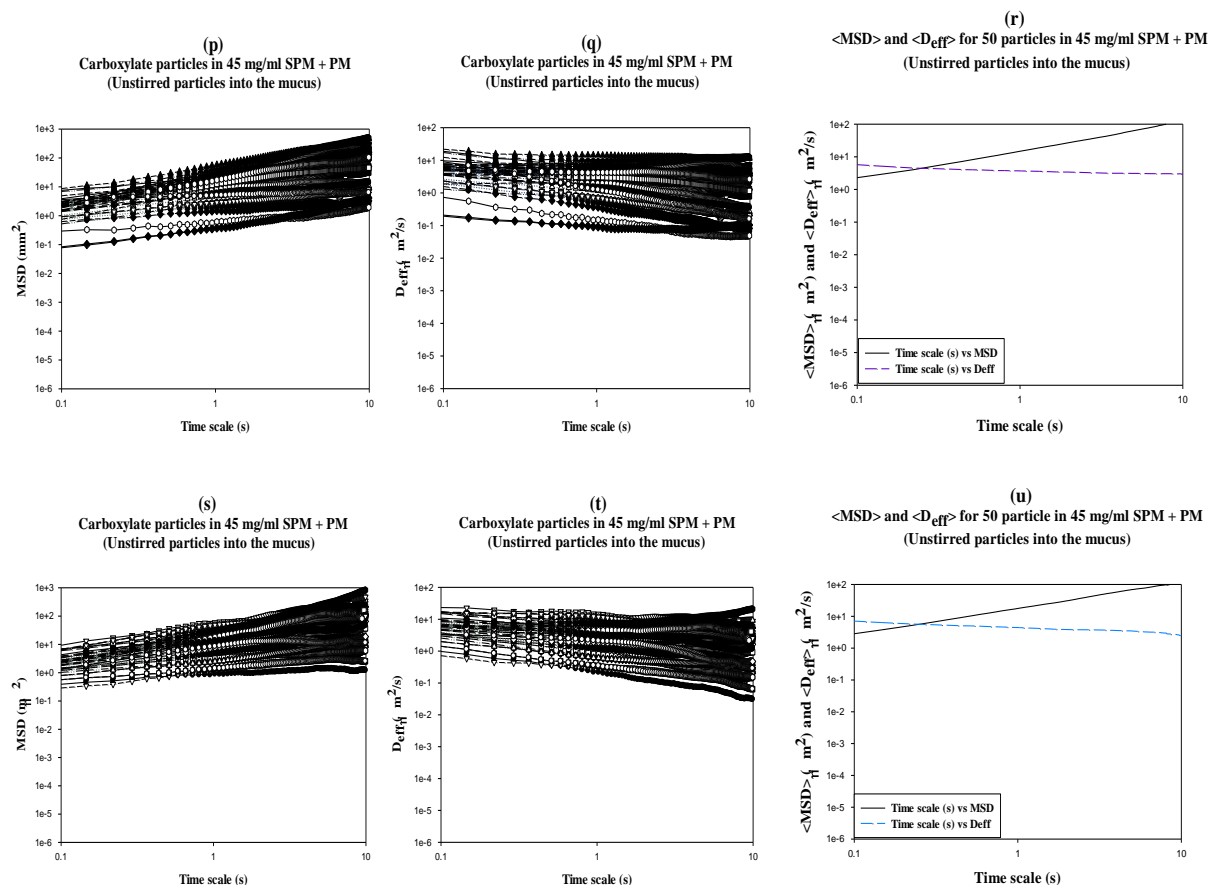


Figure 5.13: The motion of unstirred carboxylate nanoparticle in sigma pig mucus + polymeric mucus. Duplicate ensemble mean square displacement (MSD) (p, s), effective diffusivity (q, t), and mean MSD (MSD) (solid line) plus mean (D_{eff}) (dashed line) (r, u) for 50 COOH-modified nanoparticles in 45 mg/ml sigma pig mucus + polymeric mucus.

*SPM= Sigma pig mucus, *PM= Polymeric mucus



Mucus barrier components, challenges for nanoscale drug delivery

Figure 5.14 Provides duplicate mean MSD ($\langle \text{MSD} \rangle$) and mean Deff ($\langle \text{Deff} \rangle$) for 100 COOH-modified nanoparticles in 45 mg/ml sigma pig mucus + polymeric mucus + by combing r, and u panels from the Figure 5.13.

In order to determine if results were representative, a set of exclusion criteria was applied over all duplicate results to determine if they could be considered as one data set (refer to Chapter 3, section 3.2, Exclusion criteria).

**$\langle \text{MSD} \rangle$ and $\langle \text{Deff} \rangle$ for 100 COOH particles in 45 mg/ml SPM + PM
(Unstirred particles into the mucus)**

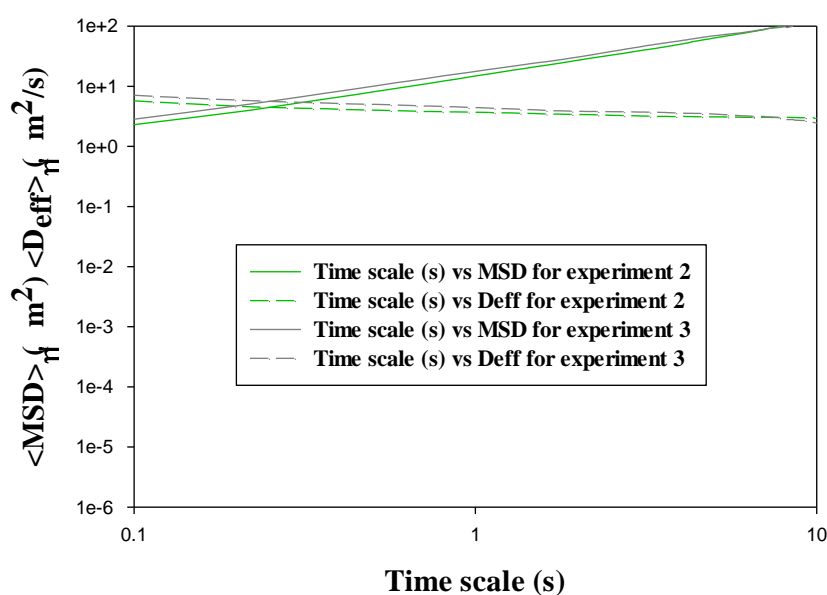


Figure 5.14: Duplicate combined MSD and Deff plots for unstirred carboxylate nanoparticle in sigma pig mucus + polymeric mucus. Ensemble-averaged mean square displacement $\langle \text{MSD} \rangle$ (solid lines) and mean effective diffusivities $\langle \text{Deff} \rangle$ (dashed lines) of 100 unstirred carboxylate-modified nanoparticles (200 nm in diameter) in 45 mg/ml sigma pig mucus + polymeric mucus provided by two replicated experiments (This Figure is combined plot of r, and u from Figure 5.13 as function of time scale).



Mucus barrier components, challenges for nanoscale drug delivery

To quantify whether these two repeats mean MSD ($\langle \text{MSD} \rangle$) and mean Deff ($\langle \text{Deff} \rangle$) values can be treated as same data set, we compared maximum and minimum MSD and Deff values of 100 unstirred carboxylate nanoparticles from the each duplicate experiments and are shown in Figure 5.15 A, B.

Considering points 1, 2, and 3 of defined exclusion criteria, results are representative, and therefore these two replicates satisfy the applied criteria and can be treated as a single data set (See applied exclusion criteria in Chapter 3, section 3.2, Exclusion criteria, page 47).

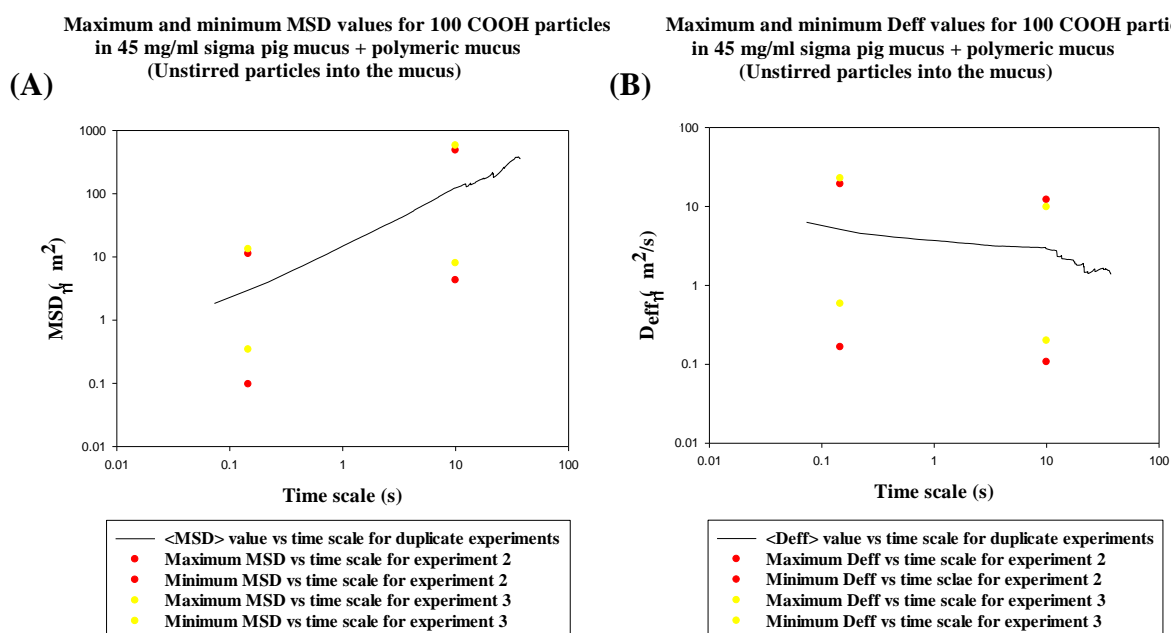


Figure 5.15: Maximum and minimum MSD and Deff values from duplicate experiments for unstirred carboxylate in sigma pig mucus + polymeric mucus. Panel A presents maximum and minimum MSD values for 100 unstirred carboxylate nanoparticles in 45 mg/ml sigma pig mucus + polymeric mucus between 0.1 to 10 second time scale, Panel B presents maximum and minimum Deff values for 100 unstirred carboxylate particles in 45 mg/ml sigma pig mucus + polymeric mucus between 0.1 to 10 second time scale.

*SPM= Sigma pig mucus, *PM= Polymeric mucus



5.7 The motion of carboxylate nanoparticle treated with G-blocks in sigma pig mucus + polymeric mucus

The motion of nanoparticles was investigated in sigma pig mucus + polymeric mucus in the presence of G-blocks using multiple particle tracking. Therefore, the following sample taken in account,

- Carboxylate nanoparticles treated with 0.04 mg/ml G-blocks and nanoparticle suspensions were gently stirred in 45 mg/ml sigma pig mucus + polymeric mucus (30 and 15 mg/ml respectively) (stirred → nanoparticle suspensions were mixed into mucus sample) (Data analysis is provided in Figure 5.10).

The mean square displacement (MSD) was calculated and used to calculate effective diffusivity (D_{eff}). The averaged-mean square displacement ($\langle D_{eff} \rangle$) and mean D_{eff} ($\langle D_{eff} \rangle$) values are shown in Figure 5.16. As can be seen from Figure 5.16, unstirred COOH nanoparticles which treated with 0.04 mg/ml G-blocks show sub-diffusive motion in 45 mg/ml sigma pig mucus + polymeric mucus.



Mucus barrier components, challenges for nanoscale drug delivery

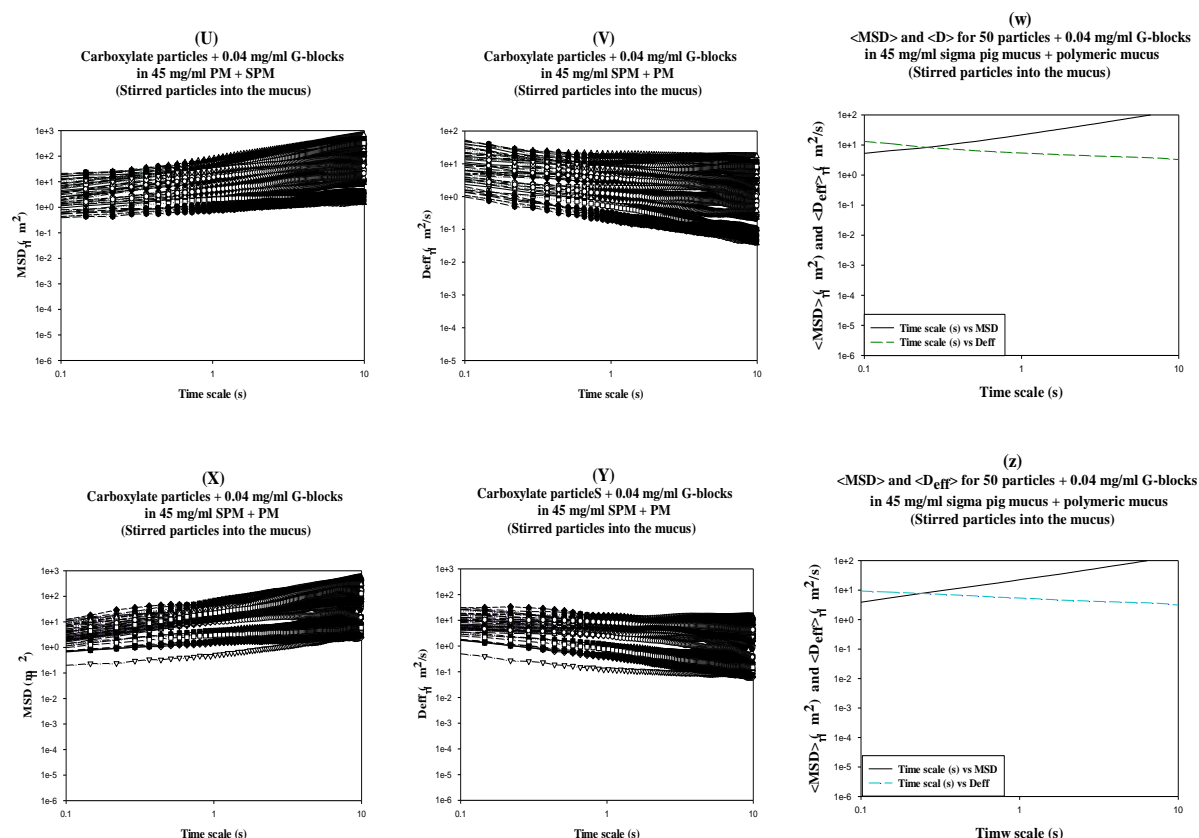


Figure 5.16: The motion of stirred carboxylate nanoparticle treated with G-blocks in sigma pig mucus + polymeric mucus. Duplicate ensemble mean square displacement (MSD) (U, X), effective diffusivity (V, Y), mean MSD (MSD) (solid line) and mean (Deff) (dashed line) (W, Z) for 50 stirred COOH-modified nanoparticles treated with 0.04 mg/ml G-blocks in 45 mg/ml sigma pig mucus + polymeric mucus.

*SPM= Sigma pig mucus, *PM= Polymeric mucus



Mucus barrier components, challenges for nanoscale drug delivery

Figure 5.17 provides duplicate mean MSD ($\langle \text{MSD} \rangle$) and mean Deff ($\langle \text{Deff} \rangle$) for 100 stirred COOH-modified nanoparticles treated with 0.04 mg/ml in 45 mg/ml sigma pig mucus + polymeric mucus by combining W, and Z panels from the Figure 5.16.

In order to quantify if results were representative, a set of exclusion criteria was applied over all triplicate results to determine if they could be considered as one data set (refer to Chapter 3, section 3.2, Exclusion criteria).

$\langle \text{MSD} \rangle$ $\langle \text{Deff} \rangle$ for 100 COOH particles + 0.04 mg/ml G-blocks in 45 mg/ml SPM + PM
(Stirred particles into the mucus)

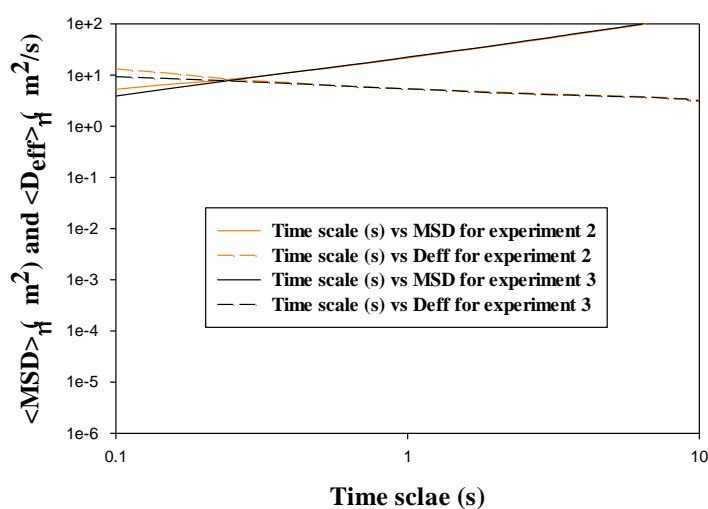


Figure 5.17: Duplicate combined MSD and Deff plots for stirred carboxylate nanoparticle treated with G-blocks in sigma pig mucus + polymeric mucus. Ensemble-averaged mean square displacement $\langle \text{MSD} \rangle$ (solid lines) and mean effective diffusivities $\langle \text{Deff} \rangle$ (dashed lines) of 100 stirred carboxylate particles (200 nm in diameter) in 45 mg/ml sigma pig mucus + polymeric mucus provided by two replicated experiments (This Figure is combined plot of W, and Z from Figure 5.16 as function of time scale).



Mucus barrier components, challenges for nanoscale drug delivery

To quantify whether these two repeats mean MSD ($\langle \text{MSD} \rangle$) and mean Deff ($\langle \text{Deff} \rangle$) values can be treated as same data set, we compared maximum and minimum MSD and Deff values of 50 COOH-modified nanoparticles from the each triplicate experiment and are shown in Figure 5.18 A and B.

Considering points 1, 2, and 3 of defined exclusion criteria, results are representative, and therefore these two replicates satisfy the applied criteria and can be treated as a single data set (See applied exclusion criteria in Chapter 3, section 3.2, Exclusion criteria, page 47).

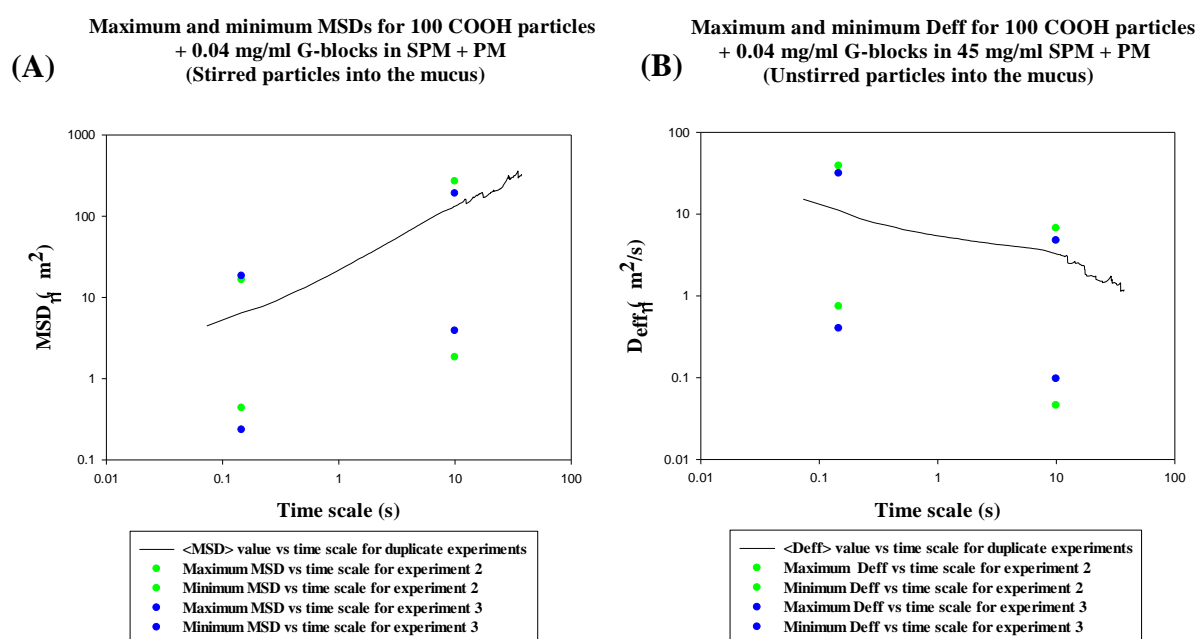


Figure 5.18: Maximum and minimum MSD and Deff values from duplicate experiments for stirred carboxylate treated with G-blocks in sigma pig mucus + polymeric mucus. Panel A presents maximum and minimum MSD values for 100 stirred carboxylate-modified nanoparticles in 45 mg/ml sigma pig mucus + polymeric mucus between 0.1 to 10 second time scales, (A), and panel B presents maximum and minimum Deff values for 100 stirred carboxylate-modified nanoparticles treated with 0.04 mg/ml G-blocks in 45 mg/ml sigma pig mucus + polymeric mucus between 0.1 to 10 second time scales.

*SPM= Sigma pig mucus, *PM= Polymeric mucus



Mucus barrier components, challenges for nanoscale drug delivery

The motion of nanoparticles was investigated in sigma pig mucus + polymeric mucus using multiple particle tracking. Therefore, the following sample taken in account,

- Carboxylate nanoparticles were treated with 0.04 mg/ml G-blocks and were added on top left side of chamber contains 45 mg/ml sigma pig mucus + polymeric mucus (30 and 15 mg/ml respectively) (unstirred) (Data analysis is provided in Figure 5.19).

The mean square displacement (MSD) was calculated and used to calculate effective diffusivity (Deff). The averaged-mean square displacement ($\langle \text{Deff} \rangle$) and mean Deff ($\langle \text{Deff} \rangle$) values are shown in Figure 5.19. As can be seen from Figure 5.19, unstirred COOH nanoparticles treated with 0.04 mg/ml G-blocks which show sub-diffusive motion in 45 mg/ml sigma pig mucus + polymeric mucus.

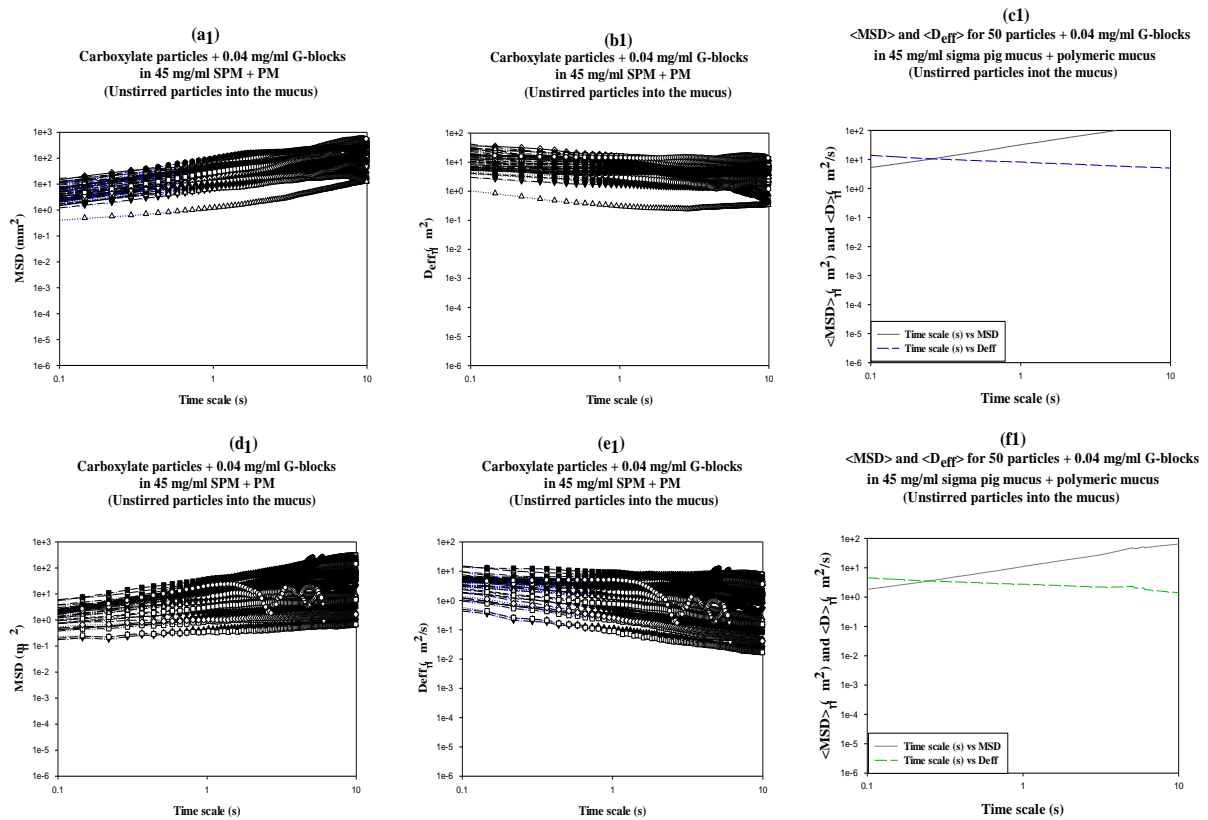


Figure 5.19: The motion of unstirred carboxylate nanoparticle treated with G-blocks in sigma pig mucus + polymeric mucus. Duplicate ensemble mean square displacement (MSD) (a1, d1), effective diffusivity (b1, e1), and mean MSD (MSD) (solid line) plus mean (Deff) (dashed line) (c1, f1) for 50 unstirred COOH-modified nanoparticles treated with 0.04 mg/ml G-blocks in 45 mg/ml sigma pig mucus + polymeric mucus.



Mucus barrier components, challenges for nanoscale drug delivery

Figure 5.20 provides duplicate mean MSD ($\langle \text{MSD} \rangle$) and mean Deff ($\langle \text{Deff} \rangle$) for 100 unstirred COOH-modified nanoparticles treated with 0.04 mg/ml G-blocks in 45 mg/ml sigma pig mucus + polymeric mucus by combining c1, and f1 panels from the Figure 5.19.

In order to quantify if results were representative, a set of exclusion criteria was applied over all triplicate results to determine if they could be considered as one data set (refer to Chapter 3, section 3.2, Exclusion criteria).

$\langle \text{MSD} \rangle$ and $\langle \text{Deff} \rangle$ for 100 COOH particles + 0.04 mg/ml G-blocks in 45 mg/ml SPM + PM
(Unstirred particles inot the mucus)

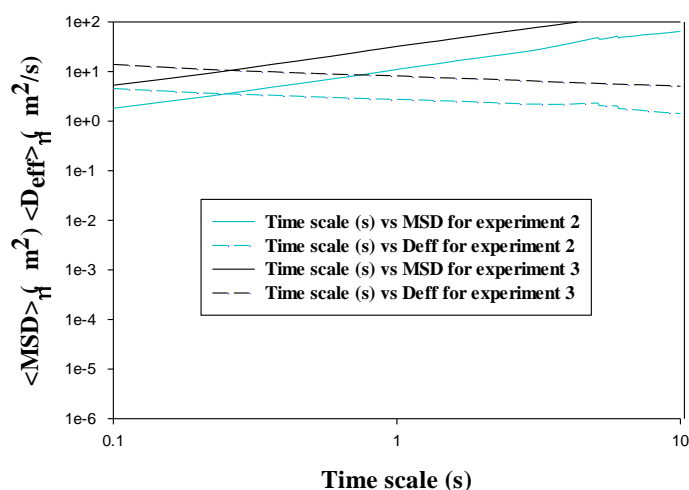


Figure 5.20: Duplicate combined MSD and Deff plots for unstirred carboxylate nanoparticle treated with G-blocks in sigma pig mucus + polymeric mucus .Ensemble-averaged mean square displacement $\langle \text{MSD} \rangle$ (solid lines) and mean effective diffusivities $\langle \text{Deff} \rangle$ (dashed lines) of 100 unstirred carboxylate nanoparticles (200 nm in diameter) treated with 0.04 mg/ml G-blocks in 45 mg/ml sigma pig mucus + polymeric mucus provided by two replicated experiments (This Figure is combined plot of c1, and f1 from Figure 5.19 as function of time scale).

*SPM= Sigma pig mucus, *PM= Polymeric mucus



Mucus barrier components, challenges for nanoscale drug delivery

To quantify whether these two repeats mean MSD ($\langle \text{MSD} \rangle$) and mean Deff ($\langle \text{Deff} \rangle$) values can be treated as same data set, we compared maximum and minimum MSD and Deff values of 100 unstirred COOH-modified nanoparticles from the each duplicate experiment and are shown in Figure 5.21 A and B.

Considering points 1, 2, and 3 of defined exclusion criteria, results are representative, and therefore these two replicates satisfy the applied criteria and can be treated as a single data set (See applied exclusion criteria in Chapter 3, section 3.2, Exclusion criteria, page 47).

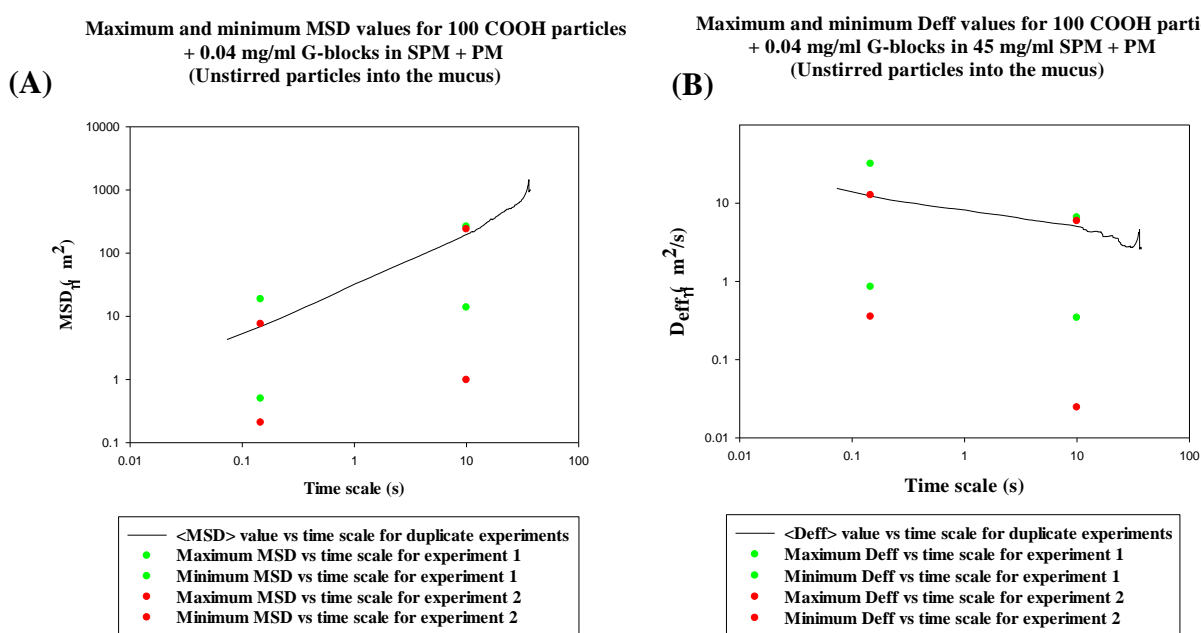


Figure 5.21: Maximum and minimum MSD and Deff values from duplicate experiments for unstirred carboxylate treated with G-blocks in sigma pig mucus + polymeric mucus. Panel A presents mean maximum and minimum MSD values for 100 unstirred carboxylate nanoparticles treated with 0.04 mg/ml G-blocks in 45 mg/ml sigma pig mucus + polymeric mucus between 0.1 to 10 second time scales, and panel B shows mean maximum and minimum Deffs values for 100 unstirred carboxylate-modified nanoparticles treated with 0.04 mg/ml G-blocks in 45 mg/ml sigma pig mucus + polymeric mucus between 0.1 to 10 second time scales.



5.8 Real-time dynamic motion of carboxylate-modified nanoparticles in sigma pig mucus contains G-blocks

The transport of carboxylate-modified nanoparticles was investigated in mucus samples using multiple particle tracking technique (MPT).

The following samples were studied,

- Carboxylate nanoparticles motion in 45 mg/ml sigma pig mucus without G-blocks treatment (Data analysis is provided in Chapter 5, Figure 5.23, panels M, N, and O)
- Carboxylate nanoparticles motion in 45 mg/ml sigma pig mucus mixed with 0.04 mg/ml G-blocks (Data analysis is provided in Chapter 5, Figure 5.22, panels A, B, and C)
- Carboxylate nanoparticles motion in 45 mg/ml sigma pig mucus mixed with 0.5 mg/ml G-blocks (Data analysis is provided in Chapter 5, Figure 5.22, panels D, E, and F).

For all three conditions above (1, 2, and 3), nanoparticle suspensions were gently stirred in mucus samples (Stirred → nanoparticle suspensions were mixed in mucus samples).

Figure 5.22 shows mean square displacements (MSD), and average mean square displacement ($\langle \text{MSD} \rangle$) of 100 COOH-modified particles in 45 mg/ml sigma pig mucus. The MSD values allowed us to determine effective diffusivity (D_{eff}) ($\text{MSD}/4 \cdot T$). (Note that all values are plotted as function of time scale).

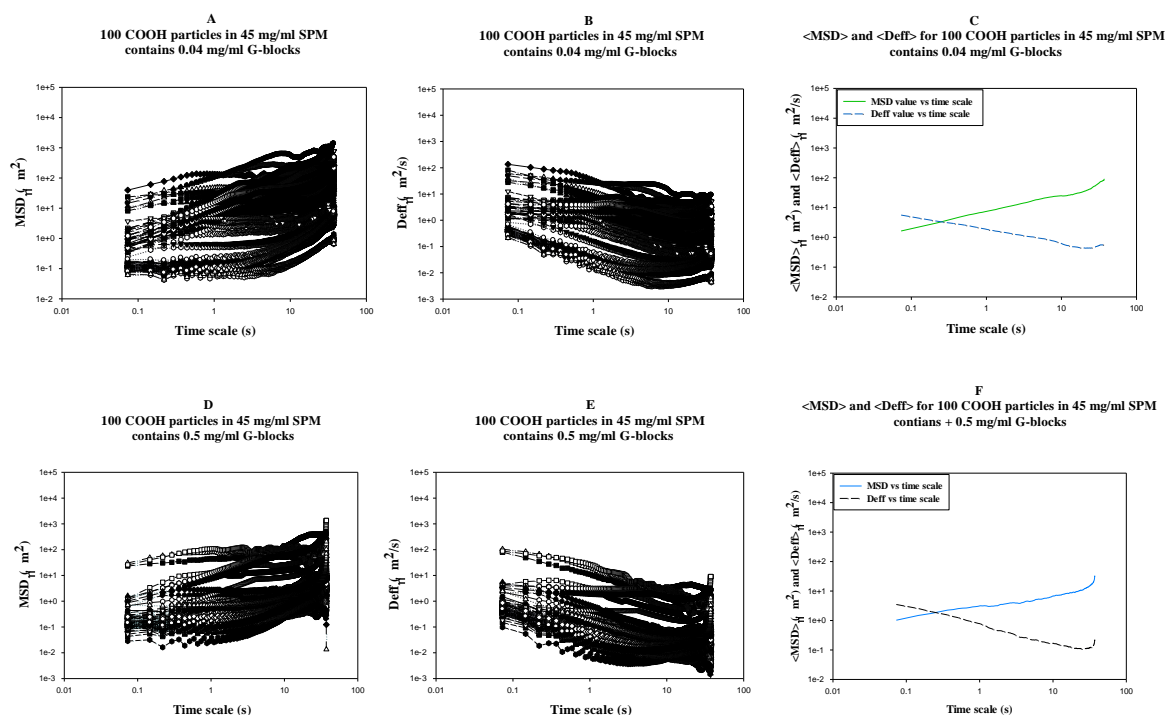


Figure 5.22: Real-time dynamic motion of carboxylate nanoparticle in sigma pig mucus contains G-blocks. Ensemble MSD, Deff, mean MSD (<MSD>), and mean Deff (<Deff>) (A, B, C) for 100 carboxylate-modified nanoparticles treated with 0.04 mg/ml G-blocks in 45 mg/ml sigma pig mucus, and The MSD, Deff, mean MSD (<MSD>), and mean Deff (<Deff>) (D, E, F) for 100 carboxylate-modified nanoparticles treated with 0.5 mg/ml G-blocks in 45 mg/ml sigma pig mucus.



5.9 Real-time dynamic motion of carboxylate nanoparticle treated with G-blocks in sigma pig mucus

The transport of carboxylate-modified nanoparticles was investigated in 45 mg/ml sigma pig mucus using multiple particle tracking (MPT).

The following samples were studied,

- Carboxylate nanoparticle suspensions without G-blocks treatment were gently stirred in 45 mg/ml sigma pig mucus (stirred → nanoparticle suspensions were mixed in mucus) (Data analysis is provided in Chapter 5, Figure 5.23, panels M, N, and O).
- Carboxylate nanoparticle suspensions were mixed with 0.04 mg/ml G-blocks and were stirred gently in 45 mg/ml sigma pig mucus (stirred → nanoparticle suspensions were mixed in mucus) (Data analysis is shown in Chapter 5, Figure 5.23, panels G, H, and I)
- Carboxylate nanoparticle suspensions were mixed with 0.5 mg/ml G-blocks and were stirred gently in 45 mg/ml sigma pig mucus (stirred → nanoparticle suspensions were mixed in mucus) (Data analysis is presented in Chapter 5, Figure 5.23, panels J, K, and L).

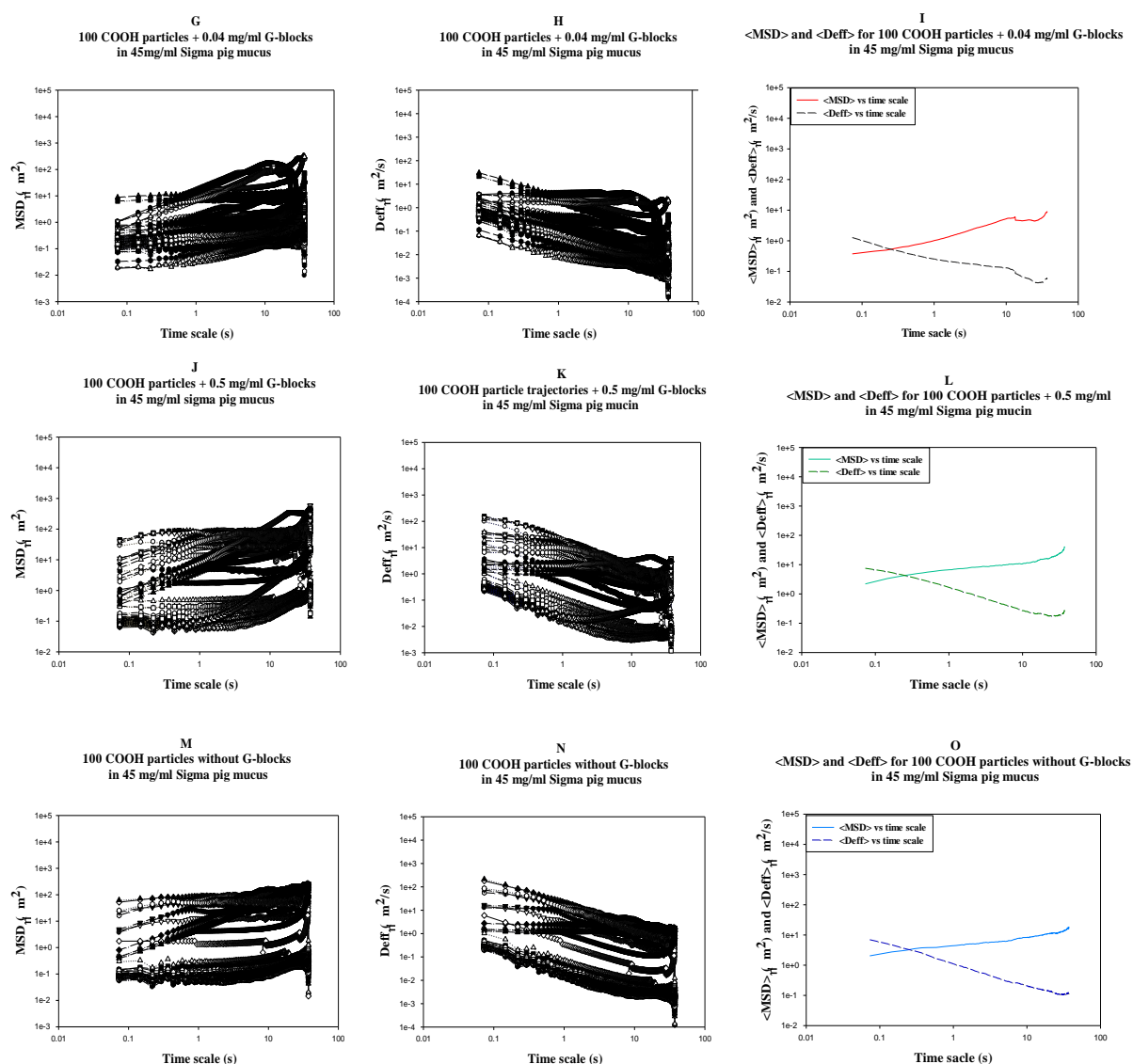


Figure 5.23: Real-time dynamic motion of carboxylate nanoparticle treated with G-blocks in sigma pig mucus. Ensemble MSD, Deff, $\langle \text{MSD} \rangle$, and $\langle \text{Deff} \rangle$ values of 100 COOH-modified nanoparticles in 45 mg/ml of sigma pig mucus. The MSD, Deff, mean MSD ($\langle \text{MSD} \rangle$), and mean Deff ($\langle \text{Deff} \rangle$) (G, H, I) in 45 mg/ml sigma pig mucus mixed with 0.04 mg/ml G-blocks, The MSD, Deff, mean MSD ($\langle \text{MSD} \rangle$), and mean Deff ($\langle \text{Deff} \rangle$) (J, K, L) in 45 mg/ml sigma pig mucus mixed with 0.5 mg/ml G-blocks, The MSD, Deff, mean MSD ($\langle \text{MSD} \rangle$), and mean Deff ($\langle \text{Deff} \rangle$) (M, N, O) for carboxylate nanoparticles with no G-blocks treatment in 45 mg/ml sigma pig mucus.



5.10 The movement of amine nanoparticles in sigma pig mucus contains G-blocks

To deepen our knowledge about the interaction between nanoparticles and mucus network, we used the amine-modified nanoparticles for our experiments as well. The mean square displacement (MSD), and effective diffusivity (D_{eff}) of 100 amine-modified nanoparticles calculated, and plotted versus time scale.

Therefore, the following studies were taken into account,

- Amine nanoparticles motion in 45 mg/ml sigma pig mucus without G-blocks treatment (Data analysis is provided in Chapter 5, Figure 5.25, panels B, C, and D)
- Amine nanoparticles motion in 45 mg/ml sigma pig mucus mixed with 0.04 mg/ml G-blocks (Data analysis is provided in Chapter 5, Figure 5.24, panels V, W, and X)
- Amine nanoparticles motion in 45 mg/ml sigma pig mucus mixed with 0.5 mg/ml G-blocks (Data analysis is provided in Chapter 5, Figure 5.24, panels Y, Z, and A).

Figure 5.24 presents mean square displacement (MSD), mean MSD ($\langle MSD \rangle$), effective diffusivity (D_{eff}), and mean D_{eff} ($\langle D_{eff} \rangle$) values of amine-modified nanoparticles in 45 mg/ml sigma pig mucus samples mixed with 0.04 mg/ml and 0.5 mg/ml G-blocks respectively.

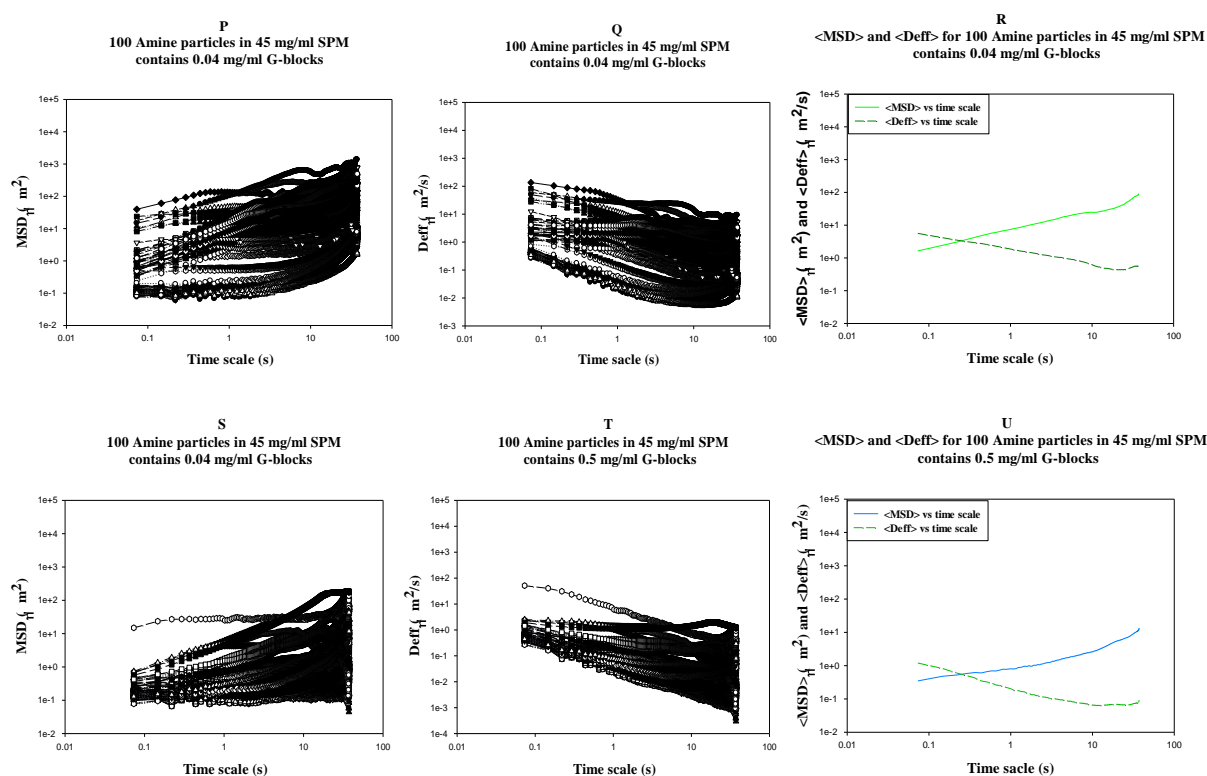


Figure 5.24: The movement of amine nanoparticle in sigma pig mucus contains G-blocks. Ensemble MSD, Deff, $\langle \text{MSD} \rangle$, and $\langle \text{Deff} \rangle$ values of 100 amine-modified nanoparticles in 45 mg/ml of Sigma pig mucus. The MSD, Deff, mean MSD ($\langle \text{MSD} \rangle$), and mean Deff ($\langle \text{Deff} \rangle$) (P, Q, R) in 45 mg/ml sigma pig mucus mixed with 0.04 mg/ml G-blocks, The MSD, Deff, mean MSD ($\langle \text{MSD} \rangle$), and mean Deff ($\langle \text{Deff} \rangle$) (S, T, U) in 45 mg/ml sigma pig mucus mixed with 0.5 mg/ml G-blocks.



5.11 The movement of amine nanoparticle treated with G-blocks in sigma pig mucus

The motion of carboxylate-modified nanoparticles (treated with G-blocks concentrations) was investigated in sigma pig mucus using MPT.

Therefore, the following samples were studied,

- Amine nanoparticle suspensions without G-blocks treatment were gently stirred in 45 mg/ml sigma pig mucus (stirred → nanoparticle suspensions were mixed in mucus) (Data analysis is provided in Chapter 5, Figure 5.25, panels B, C, and D).
- Amine nanoparticle suspensions were mixed with 0.04 mg/ml G-blocks and were stirred gently in 45 mg/ml sigma pig mucus (stirred → nanoparticle suspensions were mixed in mucus) (Data analysis is shown in Chapter 5, Figure 5.25, panels V, W, and X)
- Amine nanoparticle suspensions were mixed with 0.5 mg/ml G-blocks and were stirred gently in 45 mg/ml sigma pig mucus (stirred → nanoparticle suspensions were mixed in mucus) (Data analysis is presented in Chapter 5, Figure 5.25, panels Y, Z, and A).

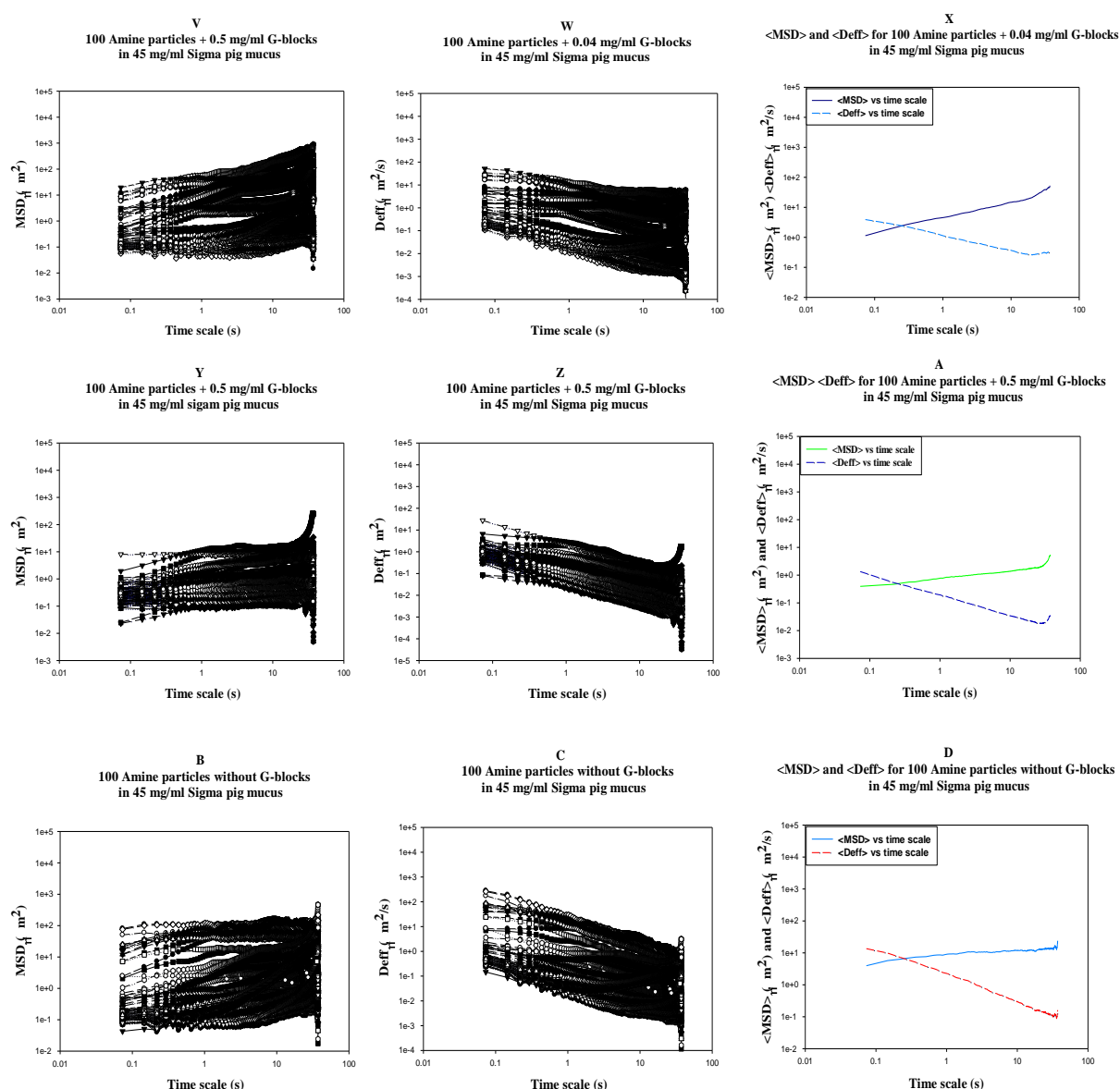


Figure 5.25: The movement of amine nanoparticle treated with G-blocks in sigma pig mucus. Ensemble MSD, Deff, <MSD>, and <Deff> values of 100 amine-modified particles in 45 mg/ml of Sigma pig mucus. The MSD, Deff, and mean MSD (<MSD>) mean Deff (<Deff>) (V, W, X) for amine nanoparticles treated with 0.04 mg/ml G-blocks in 45 mg/ml sigma pig mucus, The MSD, Deff, and mean MSD (<MSD>) mean Deff (<Deff>) (Y, Z, A) for amine nanoparticles treated with 0.5 mg/ml G-blocks in 45 mg/ml sigma pig mucus, The MSD, Deff, mean MSD (<MSD>), and mean Deff (<Deff>) (B, C, D) for amine nanoparticles with no G-blocks treatment in 45 mg/ml sigma pig mucus.



Bibliography

1. Ensign, L.M., et al., Mucus penetrating nanoparticles: biophysical tool and method of drug and gene delivery. *Adv Mater*, 2012. 24(28): p. 3887-94.
2. Cone, R.A., Barrier properties of mucus. *Adv Drug Deliv Rev*, 2009. 61(2): p. 75-85.
3. Wang, Y.Y., et al., Mucoadhesive nanoparticles may disrupt the protective human mucus barrier by altering its microstructure. *PLoS One*, 2011. 6(6): p. e21547.
4. Ashida, H., et al., Bacteria and host interactions in the gut epithelial barrier. *Nat Chem Biol*, 2012. 8(1): p. 36-45.
5. Lai, S.K., et al., Micro- and macrorheology of mucus. *Adv Drug Deliv Rev*, 2009. 61(2): p. 86-100.
6. Ensign, L.M., R. Cone, and J. Hanes, Oral drug delivery with polymeric nanoparticles: the gastrointestinal mucus barriers. *Adv Drug Deliv Rev*, 2012. 64(6): p. 557-70.
7. Sigurdsson, H.H., J. Kirch, and C.M. Lehr, Mucus as a barrier to lipophilic drugs. *Int J Pharm*, 2013.
8. Pepic, I., J. Lovric, and J. Filipovic-Grcic, How do polymeric micelles cross epithelial barriers? *Eur J Pharm Sci*, 2013.
9. Button, B., et al., A periciliary brush promotes the lung health by separating the mucus layer from airway epithelia. *Science*, 2012. 337(6097): p. 937-41.
10. Thornton, D.J., K. Rousseau, and M.A. McGuckin, Structure and function of the polymeric mucins in airways mucus. *Annu Rev Physiol*, 2008. 70: p. 459-86.
11. Occhipinti, P. and P.C. Griffiths, Quantifying diffusion in mucosal systems by pulsed-gradient spin-echo NMR. *Adv Drug Deliv Rev*, 2008. 60(15): p. 1570-82.
12. Silva, C.A., et al., Interaction of chitosan and mucin in a biomembrane model environment. *J Colloid Interface Sci*, 2012. 376(1): p. 289-95.
13. Dawson, M., et al., Transport of polymeric nanoparticle gene carriers in gastric mucus. *Biotechnol Prog*, 2004. 20(3): p. 851-7.

*SPM= Sigma pig mucus, *PM= Polymeric mucus



Mucus barrier components, challenges for nanoscale drug delivery

14. Teubl, B.J., et al., The oral cavity as a biological barrier system: Design of an advanced buccal in vitro permeability model. *Eur J Pharm Biopharm*, 2013. 84(2): p. 386-93.
15. Lavaud, M.C. and J. Trouillas, [The mucus: a medium of life]. *Gynecol Obstet Fertil*, 2012. 40(1): p. 19-23.
16. Lai, S.K., et al., Micro- and macrorheology of mucus. *Advanced drug delivery reviews*, 2009. 61(2): p. 86-100.
17. Nordgard, C.T. and K.I. Draget, Oligosaccharides as modulators of rheology in complex mucous systems. *Biomacromolecules*, 2011. 12(8): p. 3084-90.
18. Cone, R.A., Barrier properties of mucus. *Advanced drug delivery reviews*, 2009. 61(2): p. 75-85.
19. Lai, S.K., Y.Y. Wang, and J. Hanes, Mucus-penetrating nanoparticles for drug and gene delivery to mucosal tissues. *Adv Drug Deliv Rev*, 2009. 61(2): p. 158-71.
20. Huang, F., et al., Quantitative nanoparticle tracking: applications to nanomedicine. *Nanomedicine (Lond)*, 2011. 6(4): p. 693-700.
21. Ensign, L.M., et al., Mucus penetrating nanoparticles: biophysical tool and method of drug and gene delivery. *Advanced materials (Deerfield Beach, Fla.)*, 2012. 24(28): p. 3887-94.
22. Varela, J.A., et al., Quantifying size-dependent interactions between fluorescently labeled polystyrene nanoparticles and mammalian cells. *J Nanobiotechnology*, 2012. 10: p. 39.
23. Tong, S., et al., Engineering imaging probes and molecular machines for nanomedicine. *Science China. Life sciences*, 2012. 55(10): p. 843-61.
24. Pison, U., et al., Nanomedicine for respiratory diseases. *European journal of pharmacology*, 2006. 533(1-3): p. 341-50.
25. Kumar, A., X. Zhang, and X.J. Liang, Gold nanoparticles: Emerging paradigm for targeted drug delivery system. *Biotechnology advances*, 2012.
26. Laroui, H., S.V. Sitaraman, and D. Merlin, Gastrointestinal delivery of anti-inflammatory nanoparticles. *Methods Enzymol*, 2012. 509: p. 101-25.



Mucus barrier components, challenges for nanoscale drug delivery

27. Laroui, H., S.V. Sitaraman, and D. Merlin, Chapter six - Gastrointestinal Delivery of Anti-inflammatory Nanoparticles, in *Methods in Enzymology*, D. Nejat, Editor. 2012, Academic Press. p. 101-125.
28. Draget, K.I. and C. Taylor, Chemical, physical and biological properties of alginates and their biomedical implications. *Food Hydrocolloids*, 2011. 25(2): p. 251-256.
29. Borgogna, M., et al., On the Initial Binding of Alginate by Calcium Ions. The Tilted Egg-box Hypothesis. *J Phys Chem B*, 2013.
30. Jorgensen, T.E., et al., Influence of oligoguluronates on alginate gelation, kinetics, and polymer organization. *Biomacromolecules*, 2007. 8(8): p. 2388-97.
31. Sikorski, P., et al., Evidence for egg-box-compatible interactions in calcium-alginate gels from fiber X-ray diffraction. *Biomacromolecules*, 2007. 8(7): p. 2098-103.
32. Flume, P.A. and D.R. Van Devanter, State of progress in treating cystic fibrosis respiratory disease. *BMC Med*, 2012. 10: p. 88.
33. das Neves, J., et al., Interactions of microbicide nanoparticles with a simulated vaginal fluid. *Mol Pharm*, 2012. 9(11): p. 3347-56.
34. Monnier, N., et al., Bayesian approach to MSD-based analysis of particle motion in live cells. *Biophys J*, 2012. 103(3): p. 616-26.
35. Suh, J., M. Dawson, and J. Hanes, Real-time multiple-particle tracking: applications to drug and gene delivery. *Adv Drug Deliv Rev*, 2005. 57(1): p. 63-78.
36. Suh, J., D. Wirtz, and J. Hanes, Efficient active transport of gene nanocarriers to the cell nucleus. *Proc Natl Acad Sci U S A*, 2003. 100(7): p. 3878-82.
37. Suh, J., M. Dawson, and J. Hanes, Real-time multiple-particle tracking: applications to drug and gene delivery. *Advanced drug delivery reviews*, 2005. 57(1): p. 63-78.
38. Fogg, F.J., et al., Characterization of pig colonic mucins. *Biochem J*, 1996. 316 (Pt 3): p. 937-42.
39. Shotton, M., Confocal scanning microscopy and its applications for biological specimens. *Jornal of Cell Science* 94, 1989: p. 175-206.

*SPM= Sigma pig mucus, *PM= Polymeric mucus



Mucus barrier components, challenges for nanoscale drug delivery

40. WIKIPEDIA, http://en.wikipedia.org/wiki/Exclusion_criteria
41. Lai, S.K., et al., Rapid transport of large polymeric nanoparticles in fresh undiluted human mucus. *Proc Natl Acad Sci U S A*, 2007. 104(5): p. 1482-7.
42. Schuster, B.S., et al., Nanoparticle diffusion in respiratory mucus from humans without lung disease. *Biomaterials*, 2013. 34(13): p. 3439-46.
43. Ensign, L.M., et al., Ex vivo characterization of particle transport in mucus secretions coating freshly excised mucosal tissues. *Mol Pharm*, 2013. 10(6): p. 2176-82.
44. McGill, S.L. and H.D. Smyth, Disruption of the mucus barrier by topically applied exogenous particles. *Mol Pharm*, 2010. 7(6): p. 2280-8.
45. Mukhopadhyay, R., et al., Ordering of binary polymeric nanoparticles on hydrophobic surfaces assembled from low volume fraction dispersions. *J Am Chem Soc*, 2007. 129(44): p. 13390-1.



Appendixes

Appendix A: Nanoparticles showed active motion

As discussed earlier in result and discussion, chapter 3, the exclusion criteria applied in order to exclude any image series that showed apparent active transport, because nanoparticles must not exhibit active mobility in mucus matrix. Therefore, such a result would not be considered in this thesis and are given here,

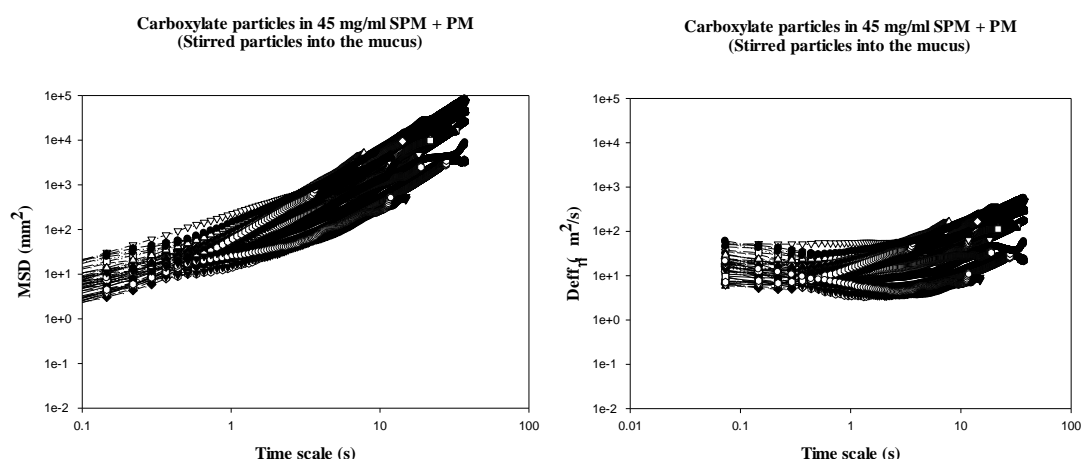


Figure A.1: Shows active mobility of carboxylate nanoparticles in 45 mg/ml sigma pig mucus + polymeric mucus. (A) Ensemble MSD value, and (B) Deff value obtained at 73-ms time intervals (Experiment 2, chamber 5).

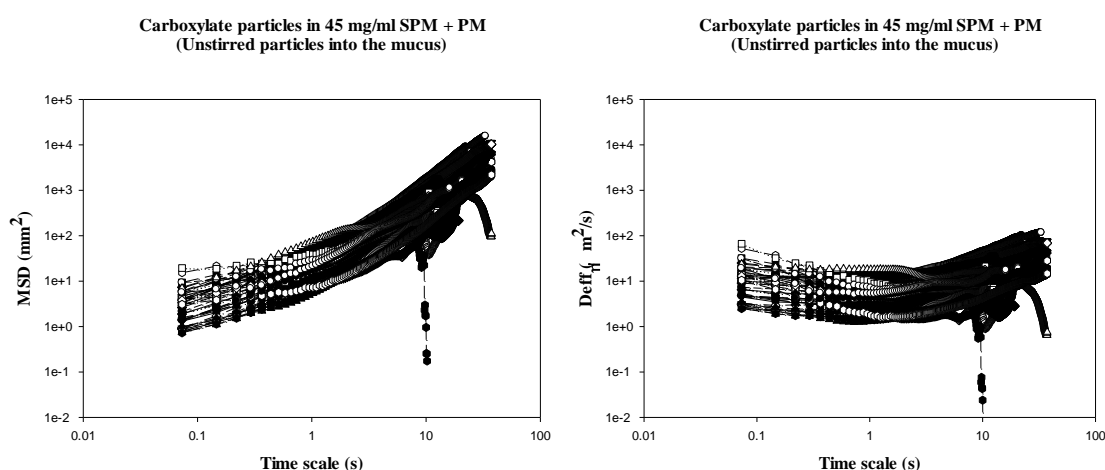


Figure A.2: Shows active mobility of carboxylate nanoparticles in 45 mg/ml sigma pig mucus + polymeric mucus. (A) Ensemble MSD value, and (B) Deff values obtained at 73-ms time intervals (Experiment 1, chamber 6).

*SPM= Sigma pig mucus, *PM= Polymeric mucus

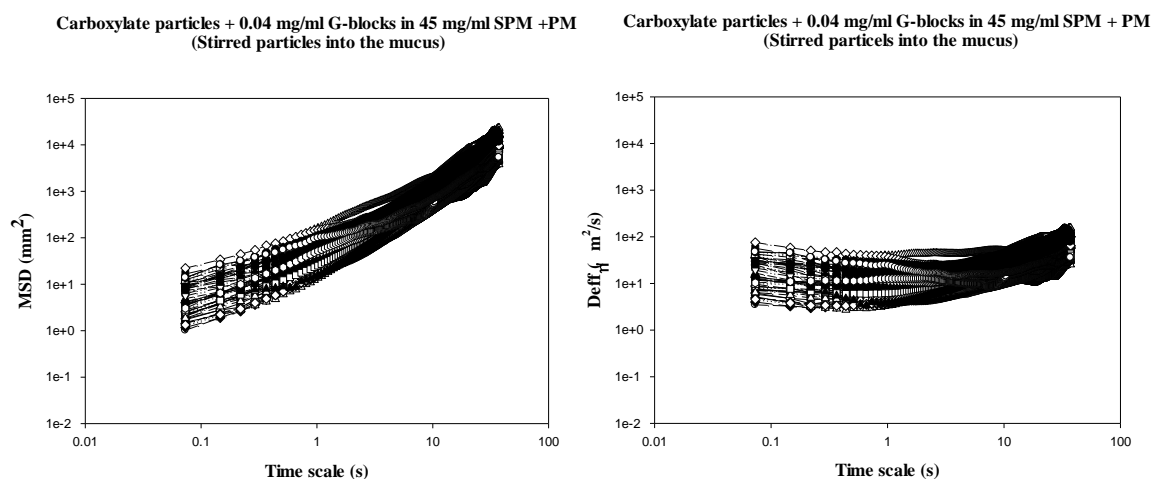


Figure A.3: Shows active mobility of carboxylate nanoparticles in 45 mg/ml sigma pig mucus + polymeric mucus. (A) Ensemble MSD value, and (B) Deff values obtained at 73-ms time intervals (Experiment 1, chamber 7).

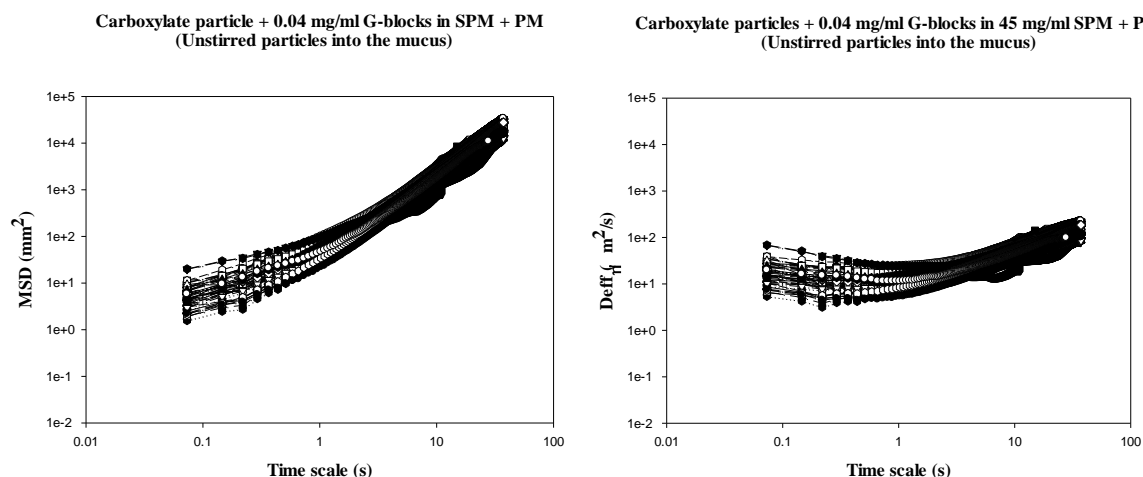


Figure A.4: Shows active mobility of carboxylate nanoparticles in 45 mg/ml sigma pig mucus + polymeric mucus. (A) Ensemble MSD value, and (B) Deff values obtained at 73-ms time intervals (Experiment 1, chamber 8).

*SPM= Sigma pig mucus, *PM= Polymeric mucus



Appendix B: Experimental design and protocols

Preparation of MES buffer

MES buffer solution prepared by dissolving dried powdered of MES buffer (4.88 gr) in 100ml milli-Q water (5ml). MES buffer solution was adjusted to pH=6 by pH meter and distilled water added to it to give the final volume of 500ml. MES buffer solution sealed and kept at 4°C in a cold room for this experiment.

Sigma pig mucus preparation

Sigma pig mucin dried powder weight out (0.045 gr) and solubilized in 1 ml of MES buffer (100 mM). The suspension left to stand on magnetic stirrer in a cold room (4 °C) for 24 hours.

Sigma pig mucus + polymeric mucus preparation

Sigma pig mucin (0.03 gr) + polymeric mucin (0.015) dried powder weight out and solubilized in 1 ml of MES buffer (100 mM). The suspension left to stand on magnetic stirrer in a cold room (4 °C) for 24 hours.

G-blocks preparation

G-blocks dried powder (0.025 gr) weight out and solubilized in 1 ml of MES buffer (100 mM). The suspension gently stirred for 5 minute and left in a cold room (4 °C).

*SPM= Sigma pig mucus, *PM= Polymeric mucus



Preparation of G-blocks concentrations

Method 1

G-blocks (0.04 mg/ml)

Beads stock: 2%

Concentration 0.4 % → 1/5 dilution

20 mg/ml G-blocks – 25 mg/ml G-blocks [MES buffer + 20 mg/ml G-blocks]

40 µl of G-blocks + 10 µl beads → 0.4 % beads in 20 mg/ml G-blocks → 5 µl into the mucus

205 µl in mucus → 200 µl of mucus (2 types of mucin) + 5 µl beads diluted in G-blocks

Method 2

G-blocks (0.04 mg/ml)

200 µl → 205 µl

150 µl of 60 mg/ml mucin + 50 µl of 2 mg/ml G-blocks + 5 µl of beads (0.41 %)

5 µl of beads (0.41 %) → 10 µl beads stock + 39 µl MES buffer

G-blocks (0.5 mg/ml)

200 µl → 205 µl

150 µl of 60 mg/ml mucin + 50 µl of 160 mg/ml G-blocks + 5 µl of beads (0.41 %)

5 µl of beads (0.41 %) → 10 µl beads stock + 39 µl MES buffer

0.04 mg/ml = 40 µg/ml

2 mg/ml → 160 µg/ml

2 mg/ml → 1 + 115 → 100 µl + 1150 µl (MES buffer) → 1250 µl of 160 µg/ml



Table B.1: Experimental design for phase 1 of experiments (Carboxylate modified-nanoparticle)

Cover glass slide chamber	Nanoparticle	Mucus sample	Method of beads addition	G-blocks
Eight chamber	2% w/w	45 mg/ml	Stirred/Unstirred	mg/ml
Chamber 1	Carboxylate	Sigma pig mucus (200 µl)	Stirred	-
Chamber 2	Carboxylate	Sigma pig mucus (200 µl)	Unstirred	-
Chamber 3	Carboxylate	Sigma pig mucus (200 µl)	Stirred	0.04
Chamber 4	Carboxylate	Sigma pig mucus (200 µl)	Unstirred	0.04
Chamber 5	Carboxylate	SPM + PM mucus (200 µl)	Stirred	-
Chamber 6	Carboxylate	SPM + PM mucus (200 µl)	Unstirred	-
Chamber 7	Carboxylate	SPM + PM mucus (200 µl)	Stirred	0.04
Chamber 8	Carboxylate	SPM + PM mucus (200 µl)	Unstirred	0.04

- In Chambers 1, and 5, 5 µl of a mixture of beads-MES buffer were gently stirred in sigma pig mucus and in sigma pig mucus + polymeric mucus respectively.
- In Chambers 2, and 6, 5 µl of a mixture of beads-MES buffer were added on top left side in sigma pig mucus and in sigma pig mucus + polymeric mucus respectively.
- In Chambers 3, and 7, 5 µl of a mixture of beads-G-blocks were gently stirred in sigma pig mucus and in sigma pig mucus + polymeric mucus.
- In Chambers 4, and 8, 5 µl of a mixture of beads-G-blocks were added on top left side in sigma pig mucus and in sigma pig mucus + polymeric mucus respectively.

*The experiment performed in triplicate repeats.

* G-blocks suspension made by method 1, (Preparation of G-blocks concentrations).

*SPM= Sigma pig mucus, *PM= Polymeric mucus



Phase 2 of experiments

Table B.2: Experimental design for phase 2 of experiments (Carboxylate-modified nanoparticle)

Cover glass slide chamber	Nanoparticle	Mucus sample	Method of beads addition	G-blocks
Eight chamber	2% w/w	45 mg/ml	Stirred/Unstirred	mg/ml
Chamber 1	Carboxylate	Sigma pig mucus (150 µl)	Stirred	0.04
Chamber 2	Carboxylate	Sigma pig mucus (150 µl)	Stirred	0.04
Chamber 3	Carboxylate	Sigma pig mucus (150 µl)	Stirred	0.04
Chamber 4	Carboxylate	Sigma pig mucus (150 µl)	Stirred	0.04
Chamber 5	Carboxylate	Sigma pig mucus (150 µl)	Stirred	0.04
Chamber 6	Carboxylate	Sigma pig mucus (150 µl)	Stirred	0.04
Chamber 7	Carboxylate	Sigma pig mucus (150 µl)	Stirred	0.04
Chamber 8	Carboxylate	Sigma pig mucus (150 µl)	Stirred	0.04

*In Chambers 1, 2, 3, and 4, sigma pig mucus subjected to treat with G-blocks and nanoparticle suspensions (55 µl of mixture of beads-MES buffer) were gently stirred into mucus.

*In Chambers 5, 6, 7, and 8, nanoparticles were treated with G-blocks (55 µl of mixture of beads-G-blocks) and were gently stirred in sigma pig mucus.

*G-blocks suspension was prepared by method 2, (Preparation of G-blocks concentrations).

*Note that same procedure was used and performed for amine nanoparticles (Table 3).



Mucus barrier components, challenges for nanoscale drug delivery

Table B.3: Experimental design for phase 2 of experiments (Amine modified-nanoparticle)

Cover glass slide chamber	Nanoparticle	Mucus sample	Method of beads addition	G-blocks
Eight chamber	2% w/w	45 mg/ml	Stirred/Unstirred	mg/ml
Chamber 1	Amine	Sigma pig mucus (150 µl)	Stirred	0.04
Chamber 2	Amine	Sigma pig mucus (150 µl)	Stirred	0.04
Chamber 3	Amine	Sigma pig mucus (150 µl)	Stirred	0.04
Chamber 4	Amine	Sigma pig mucus (150 µl)	Stirred	0.04
Chamber 5	Amine	Sigma pig mucus (150 µl)	Stirred	0.04
Chamber 6	Amine	Sigma pig mucus (150 µl)	Stirred	0.04
Chamber 7	Amine	Sigma pig mucus (150 µl)	Stirred	0.04
Chamber 8	Amine	Sigma pig mucus (150 µl)	Stirred	0.04

*In Chambers 1, 2, 3, and 4, sigma pig mucus subjected to treat with G-blocks and nanoparticle suspensions (55 µl of mixture of beads-MES buffer) were gently stirred into mucus.

*In Chambers 5, 6, 7, and 8, nanoparticles were treated with G-blocks (55 µl of mixture of beads-G-blocks) and were gently stirred in sigma pig mucus.

*G-blocks suspension was prepared by method 2, (Preparation of G-blocks concentrations).

*SPM= Sigma pig mucus, *PM= Polymeric mucus



Appendix C: Confocal microscope setting

The motion of amine and carboxylate modified nanoparticles were imaged with Leica microscope according to instruction given in Table D.1.

Table C.1: Confocal microscope operation set up.

Confocal laser scanning microscope	
Model: Leica TCS SP5	
Laser	Argon, 488
Power	20 %
Beam path setting	FITC
PMT	PMT1
Gain	572.2 v
Image resolution	512×512 pixels
Laser	Argon, 488
Power	20 %
Beam path setting	FITC
PMT	PMT1
Acquisition mode	XYT
Time interval	73-ms
Duration	2 min
Objective	HCXPLAPO CS 63.0x 1.20 WATER UV
Number of frame	512



Appendix D: Matlab pre difiend script

The code was made by Astrid Bjorkoy for Catherine T. Nordgard in 2011. This script is used to convert all trajectories into mean square displacement (MSD) value in Matlab. Input and output file to Matlab was .txt. Alteratons was made from the original code concerning file source and saving positions, only to match the computer used for the work.

Matlab R2009a was used at computer lab at NTNU.

Function ParticleTracker

```
% Prompt for lag time between frames
% Promt for name of resultfile!
prompt = {'Enter time interval:', 'Enter name of result file:'};
dlg_title = 'Input for Trajectory Calculations';
num_lines = 1;
def = {'1', 'results.txt'};
answer = inputdlg(prompt, dlg_title, num_lines, def);

timeinterval = str2double(answer{1});
filnavn = answer{2};

% Open the file with the trajectory data
[File, Path] = uigetfile('*.txt', 'Open Trajectory file', ...
    'M:\Mikroskopi\Catherine Taylor\', 'MultiSelect', 'Off')

s1 = char(strcat(Path, File));
fid = fopen(s1);

k = 1;
% Figure out what trajectories are in this file, put the names in
% Nr.Trajectory and the number of frames for particle k in Particles
while 1
    tline = fgetl(fid);
    if ~ischar(tline), break, end
    if ~isempty(tline)
        if tline(1) == '%'
            nr = 0;
            Nr(k).Trajectory = tline(4:end);
            k = k+1;
        else nr = nr+1;
        end
    else Particles(k-1) = nr;
    end
end
fclose(fid);

% Import the trajectory data and put data in newData1
rawData1 = importdata(s1);
*SPM= Sigma pig mucus, *PM= Polymeric mucus
```



Mucus barrier components, challenges for nanoscale drug delivery

```
% For some simple files (such as a CSV or JPEG files), IMPORTDATA might
% return a simple array. If so, generate a structure so that the output
% matches that from the Import Wizard.
[unused,name] = fileparts(s1); %#ok
newData1.(genvarname(name)) = rawData1;

% Create new variables in the base workspace from those fields.
vars = fieldnames(newData1);
for i = 1:length(vars)
    assignin('base', vars{i}, newData1.(vars{i}));
end

j = 1;
pend = 0;

% For each particle, calculate the msd's for each time step!
% The frame number and (x,y) for each particle are between pstart and pend
% in the data file newData1.
for particle = 1:length(Particles)
    pstart = pend + 1;
    pend = pstart + (Particles(particle)-1);
    % p is an array containing the frame numbers
    p = newData1.(genvarname(name))(pstart:pend,1);
    x = newData1.(genvarname(name))(pstart:pend,2);
    y = newData1.(genvarname(name))(pstart:pend,3);
    % maxstep is the maximum lag time possible for the particle
    maxstep = p(end)-p(1);
    for step = 1:maxstep
        ave = []; % vector of msd's
        i = p(1); % number of startframe
        while i+step <= p(end)
            % ignore frames missing!
            if ~ismember(i,p) || ~ismember((i+step),p)
            else
                % find the correct position in p, x and y for i and i+step
                i1 = find(p==i);
                i2 = find(p==(i+step));
                new = ((x(i1)-x(i2))^2 + (y(i1)-y(i2))^2);
                ave = [new ave];
            end
            i = i+1;
        end
        if ~isempty(ave)
            msd(particle, step) = mean(ave); %mean msd for this step/lag time
        end
    end
end

% Save the data to a file: lag time in first column, data for the
% particles in the other columns.
datafile = strcat(Path, filnavn);
fid = fopen(char(datafile),'a');
```



Mucus barrier components, challenges for nanoscale drug delivery

```
fprintf(fid,'%s', 'Step');
for i = 1:length(Particles)
    fprintf(fid,'\t %s',Nr(i).Trajectory);
end
fprintf(fid,'\n');

% size(msd,2) is the maximum number of frames for the particles
% in the data file newData1
for i = 1:size(msd,2)
    fprintf(fid,'%6.4f \t', i*timeinterval);
    for j = 1:length(Particles)
        % if there's data missing for this lag time, skip info!
        % else save the result
        if msd(j,i) == 0 fprintf(fid,'\t');
        else fprintf(fid,'%6.4f \t',msd(j,i));
        end
    end
    fprintf(fid,'\n');
end

end
```

*SPM= Sigma pig mucus, *PM= Polymeric mucus